SISSA **ISAS**

SCUOLA INTERNAZIONALE SUPERIORE DI STUDI AVANZATI

INTERNATIONAL SCHOOL FOR ADVANCED STUDIES

Semiclassical methods in 2D QFT: spectra and finite–size effects

Thesis submitted for the degree of
"Doctor Philosophiæ"

Candidate:
Valentina Riva

Supervisor:
Prof. Giuseppe Mussardo

External referee:
Prof. Germán Sierra

October 2004

Abstract

In this thesis, we describe some recent results obtained in the analysis of two–dimensional quantum field theories by means of semiclassical techniques. These achievements represent a natural development of the non–perturbative studies performed in the past years for conformally invariant and integrable theories, which have lead to analytical predictions for several measurable quantities in the universality classes of statistical systems. Here we propose a semiclassical method to control analytically the spectrum and the finite–size effects in both integrable and non–integrable theories. The techniques used are appropriate generalization of the ones introduced in seminal works during the Seventies by Dashen, Hasllacher and Neveu and by Goldstone and Jackiw. Their approaches, which do not require integrability and therefore can be applied to a large class of system, are best suited to deal with those quantum field theories characterized by a non–linear interaction potential with different degenerate minima. In fact, these systems display kink excitations which generally have a large mass in the small coupling regime. Under these circumstances, although the results obtained are based on a small coupling assumption, they are nevertheless non-perturbative, since the kink backgrounds around which the semiclassical expansion is performed are non-perturbative too.

Contents

Introduction

Non–perturbative methods in quantum field theory (QFT) play a central rôle in theoretical physics, with applications in many areas, from string theory to condensed matter. In the last years, a considerable progress has been registered in the study of two–dimensional systems. For these models, in fact, exact results have been obtained in the particular situations when the systems are conformally invariant or integrable.

Conformal invariance does not merely represent a restriction on the solvable problems. In fact, it provides a fruitful link between QFT and statistical mechanics, realized through the ideas of scaling and renormalization, which explain the basic features of phase transitions and are naturally encoded in the QFT framework. In fact, physical systems at a second order phase transition (called critical) are characterized by the divergence of the correlation length, which makes unimportant the fine details of their microscopic structure and leads to an organization of the critical behaviours in universality classes. As a consequence, the order parameter fluctuations can be described with the language of conformal field theories (CFT). The corresponding dynamics can be exactly solved in two-dimensions, since in this case conformal invariance permits to determine universal amplitudes and to extract as well the entire spectrum of the theory.

Furthermore, dynamics in the vicinity of a critical point can be described by perturbed CFT, obtained by adding to the action operators which break the conformal symmetry and introduce a mass scale in the system, inducing a renormalization group flow. Suitable choices of the perturbing operator make the off-critical massive field theory integrable, with consequent elasticity and factorization of the scattering. In two dimensions, this fact together with a simplified kinematics leads to the exact computation of the scattering amplitudes, which encode in their analytical structure the complete information about the spectrum. Moreover, the knowledge of the S–matrix permits to implement the so–called form factors approach, which makes the analysis of off–shell correlators possible.

Within this program, during the the last years measurable universal quantities for many statistical models have been computed. The studied systems include, for instance, the Ising model in a magnetic field, the tricritical Ising model, the q-state Potts model, percolation and self-avoiding walks. In all other cases, the understanding of two dimensional QFT has been reached up to now either by conformal perturbation theory or numerical methods.

A complete understanding of QFT also requires the control of finite–size effects, both for practical and theoretical reasons. In fact, the finite–volume energy spectrum contains a lot of information about the properties of the theory in infinite volume. On the one hand, this permits to control the systematic error induced by the finiteness of the samples in the extrapolation procedure of numerical simulations. On the other hand, scattering data can be extracted from the numerical analysis through this correspondence. Moreover, defining a theory in finite volume one can explicitly follow the renormalization group flow between its ultraviolet (UV) conformal

limit and the infrared (IR) massive behaviour, since these two limits correspond, respectively, to volumes much smaller or larger than the correlation length. Finally, QFT in finite volume are intimately related to another important subject, i.e. QFT at finite temperature.

At present, finite–size effects have been studied non–perturbatively only in the above mentioned cases of conformal or integrable QFT. At criticality, in fact, powerful analytical techniques are available to extract the entire spectrum of the transfer matrix. Furthermore, in integrable massive theories, the knowledge of the exact S–matrix permits to study the system at finite temperature, with the so–called Thermodynamic Bethe Ansatz. This technique provides integral equations, mostly solved numerically, for the ground state energy of the theory in finite volume. In all other cases, the control of finite–size effects has been reached either by perturbative or numerical methods.

A natural development of the above mentioned studies of two–dimensional QFT consists in looking for some techniques to control analytically non–integrable systems and finite–size effects, both for theoretical reasons and their application to several condensed–matter or statistical systems. My original contribution to this research stream has been presented in the papers [1-4] and will be described in this thesis. The basic tool used is an appropriate generalization and extension of semiclassical methods, which have proved to be efficient in analysing non-perturbative effects in QFT since their introduction in the seminal works [23, 24]. The semiclassical approach does not require integrability, therefore it can be applied on a large class of systems. At the same time, it permits to face problems which are not fully understood even in the integrable cases, such as the analytic study of QFT in finite volume. In particular, it has led to new non–perturbative results on form factors at a finite volume [1], spectra of non–integrable models [2] and energy levels of QFT on finite geometries [3, 4].

The semiclassical method is best suited to deal with those quantum field theories characterized by a non–linear interaction potential with different degenerate minima. In fact, these systems display kink excitations, associated to static classical backgrounds which interpolate between the degenerate vacua and generally have a large mass in the small coupling regime. Under these circumstances, although the results obtained are based on a small coupling assumption, they are nevertheless non-perturbative, since the kink backgrounds around which the semiclassical expansion is performed are non-perturbative too. In any case, the restriction on the variety of examinable theories imposed by the above requirements is rather mild, since non–linearity is the main feature of a wealth of relevant physical problems.

In the study of non–integrable spectra and finite–size effects, we have used two basic results. The first is the well–known semiclassical quantization technique, introduced by Dashen, Hasslacher and Neveu (DHN) in [23]. It consists in solving a Schrödinger–like problem, associated to the "stability equation" for the small quantum fluctuations around the classical backgrounds, and in building the energy levels of the system in terms of the classical energy and the stability frequencies. The second tool is a covariant refinement of a result due to Goldstone and Jackiw [24]. They have shown that the classical kink backgrounds can be interpreted at quantum level as the Fourier transform of the form factors between kink states. In [1], we have overcome the drawbacks of the original result, which was expressed non-covariantly in terms of the particles space momentum, using the so-called rapidity variable, which is Lorentz invariant. This refinement opened the way to the use of semiclassical form factors in the analysis of particle spectra and correlation functions, because it permits to go in the crossed channel and write the form

factor between the vacuum and a kink-antikink state. Since the analytical structure of these form factors encodes the information about the masses of all the kink-antikink bound states, in this way it is possible to explore non-perturbatively the complete spectrum of non–integrable theories, a purpose for which there are no other known analytical techniques. In [1], a prediction about the spectrum of the ϕ^4 field theory in the broken $\mathbb{Z}_2$ symmetry phase was made, in agreement with previous approximate results. In the following work [2], a detailed analysis of the spectrum was performed in the double Sine-Gordon model, which turns out to be a relevant description of many concrete physical systems and displays appealing features such as false vacuum decay and phase transition phenomena.

The study of finite–size effects can be tackled after having identified suitable classical solutions to describe the kinks in finite volume. With this respect, the key result of [1] is the construction of such backgrounds for the Sine-Gordon and the broken ϕ^4 theories on a cylindrical geometry with antiperiodic boundary conditions. The form factors are then expressed as a Fourier series expansion of the classical solutions, and they are used to obtain an estimate of the spectral representation of correlation functions in finite volume. This result adds to few others, which however strictly rely on specific integrable structures of the considered models, while it can be in principle extended to any theory displaying topologically non-trivial backgrounds. The complete DHN quantization has been then performed in [3] for static classical solutions on a finite geometry. In particular, the example of the Sine–Gordon model with periodic boundary conditions has been explicitly treated, reconstructing the scaling function and the excited energy levels in terms of the size of the system. Finally, the same theory, defined this time on a strip with Dirichlet boundary conditions, has been studied in [4]. The semiclassical achievements provide an explicit analytical control on the interpolation between the massive field theory and its UV limit, and can be compared with the numerical results obtained in the sine–Gordon model with different techniques. However, their application is more general, and permits to estimate the scaling functions also in non–integrable theories.

The thesis is organized as follows. In Chapter 1 we review the non–perturbative results available for conformal and integrable QFT in two dimensions, with particular emphasis on their applications to statistical mechanics. In Chapter 2 we introduce the semiclassical techniques established in the past for QFT in infinite volume, and we test the efficiency of the semiclassical approximation by comparing the results obtained in the sine–Gordon model with the exact ones provided by the integrability of the theory. Chapter 3 is devoted to the analysis of the spectra of excitations in the non–integrable systems defined by the ϕ^4 field theory in the broken $\mathbb{Z}_2$ symmetry phase and by the Double Sine–Gordon model. Finally, in Chapter 4 we present the study of finite–size effects. In particular, we describe the form factors in the sine–Gordon and broken ϕ^4 theories defined on a twisted cylinder, and the energy levels in the sine–Gordon model defined both on a periodic cylinder and on a strip with Dirichlet boundary conditions.

Chapter 1

Quantum field theories in 2D and statistical physics

One of the most fruitful applications that QFT has found in recent years is the analysis of the universality classes of two–dimensional statistical models near their critical points, which correspond to second order phase transitions. Critical systems, in fact, fall into universality classes which can be classified by conformally invariant field theories (CFT). The corresponding dynamics can be exactly solved in two-dimensions through a systematic computation of correlators, allowed by conformal invariance. Furthermore, dynamics in the vicinity of a critical point can be described by perturbed CFT, obtained by adding to the action operators which break the conformal symmetry and introduce a mass scale in the system. Suitable choices of the perturbing operator make the off-critical massive field theory integrable, with consequent elasticity and factorization of the scattering. In two dimensions, this fact together with the simplified kinematics leads to the possibility of computing exactly the scattering amplitudes, which encode in their analytical structure the complete information about the spectrum. Moreover, the knowledge of the S–matrix permits to implement the so–called form factors approach, which makes the analysis of off–shell correlators possible. Within this program, during the the last years measurable universal quantities for many statistical models have computed. The studied systems include, for instance, the Ising model in a magnetic field, the tricritical Ising model, the q-state Potts model, percolation and self-avoiding walks.

In this Chapter, we will introduce the basic concepts related to conformal invariance and integrability. Section 1.1 presents a brief overview of conformal field theories, with few examples which will be referred to in the following Chapters. In Section 1.2 we discuss the main features of massive scattering in integrable quantum field theories, exploiting the powerful consequences of the simplified two–dimensional kinematics. Finally, Section 1.3 describes a useful effective Lagrangian description of CFT.

1.1 Critical systems and conformal field theories

A statistical mechanical system is said to be critical when its correlation length ξ, defined as the typical distance over which the order parameters are statistically correlated, increases infinitely ($\xi \to \infty$). Correspondingly, length scales lose their relevance, and scale invariance emerges. This is peculiar of the continuous (or second order) phase transitions, which consist in a sudden change of the macroscopic properties of the system as some parameters (e.g. the temperature)

are varied, without finite jumps in the energy (characteristic of first order transitions). A remarkable property of these systems is that the fine details of their microscopic structure become unimportant, and the various possible critical behaviours are organized in universality classes, which depend only on the space dimensionality and on the underlying symmetry. This allows a description of the order parameter fluctuations in the language of a field theory, which is invariant under the global scale transformations

$$x^\mu \rightarrow x'^{\,\mu} = \lambda x^\mu \,,$$

provided that the fields transform as

$$\Phi(x) \rightarrow \Phi'(x') = \lambda^{-\Delta} \Phi(x) \,,$$

where Δ is called the scaling dimension of the field Φ.

The use of conformal invariance to describe statistical mechanical systems at criticality is motivated by a theorem, due to Polyakov, which states that local field theories which are scaling invariant are also conformally invariant [5]. Therefore, every universality class of critical behaviour can be identified with a conformal field theory (CFT), i.e. a quantum field theory that is invariant under conformal symmetry. This way of studying critical systems started with a pioneering paper by Belavin, Polyakov and Zamolodchikov [6], and is systematically presented in many review articles and text books (see for instance [7, 8, 9]). We will now concisely summarize the main properties of CFT.

An infinitesimal coordinate transformation $x^\mu \rightarrow x^\mu + \xi^\mu(x)$ is called conformal if it leaves the metric tensor $g_{\mu\nu}$ invariant up to a local scale factor, i.e.

$$g_{\mu\nu}(x) \rightarrow \varrho(x) g_{\mu\nu}(x).$$

These transformations, which include rotations, translations and dilatations, preserve the angle between two vectors and satisfy the condition

$$\partial_\mu \xi_\nu + \partial_\nu \xi_\mu = \frac{2}{d} \eta_{\mu\nu} (\partial \cdot \xi), \tag{1.1.1}$$

where d is the dimension of space-time. In two dimensions, since the conformal group enlarges to an infinite set of transformations, it is possible to solve exactly the dynamics of a critical system, assuming conformal invariance and a short-distance operator product expansion (OPE) for the fluctuating fields. In fact, if we describe euclidean two-dimensional space-time with complex coordinates

$$z = x^0 + ix^1 \,, \qquad \bar{z} = x^0 - ix^1 \,,$$

eq.(1.1.1) specializes to the Cauchy-Riemann equations for holomorphic functions. Therefore the solutions are holomorphic or anti-holomorphic transformations, $z \rightarrow f(z)$ and $\bar{z} \rightarrow \bar{f}(\bar{z})$, such that $\partial_{\bar{z}} f = \partial_z \bar{f} = 0$. These functions admit the Laurent expansion

$$f(z) = \sum_{n=-\infty}^{\infty} a_n \, z^{n+1} \,, \qquad \bar{f}(\bar{z}) = \sum_{n=-\infty}^{\infty} a'_n \, \bar{z}^{n+1} \,,$$

which has an infinite number of parameters. In this way, the conformal group enlarges to an infinite set of transformations.

Defining now a two–dimensional quantum field theory invariant under conformal transformation, we can associate to each field an holomorphic and an antiholomorphic comformal dimensions h and $\bar{h}$, defined in terms of the scaling dimension Δ and of the spin s as

$$h = \frac{1}{2}(\Delta + s) , \qquad \bar{h} = \frac{1}{2}(\Delta - s) . \qquad (1.1.2)$$

A field is called primary if it transforms under a local conformal transformation $z \to w = f(z)$ as

$$\phi'(w, \bar{w}) = \left(\frac{dw}{dz}\right)^{-h} \left(\frac{d\bar{w}}{d\bar{z}}\right)^{-\bar{h}} \phi(z, \bar{z}) . \qquad (1.1.3)$$

Conformal invariance fixes the form of the correlators of two and three primary fields up to a multiplicative constant:

$$\langle \phi_1(z_1, \bar{z}_1) \, \phi_2(z_2, \bar{z}_2) \rangle = \begin{cases} \dfrac{C_{12}}{z_{12}^{2h} \, \bar{z}_{12}^{2\bar{h}}} & \text{if } h_1 = h_2 = h \text{ and } \bar{h}_1 = \bar{h}_2 = \bar{h} \\ 0 & \text{otherwise} \end{cases} , \qquad (1.1.4)$$

$$\langle \phi_1(z_1, \bar{z}_1) \, \phi_2(z_2, \bar{z}_2) \, \phi_3(z_3, \bar{z}_3) \rangle = C_{123} \frac{1}{z_{12}^{h_1+h_2-h_3} \, z_{23}^{h_2+h_3-h_1} \, z_{13}^{h_3+h_1-h_2}} \qquad (1.1.5)$$

$$\times \frac{1}{\bar{z}_{12}^{\bar{h}_1+\bar{h}_2-\bar{h}_3} \, \bar{z}_{23}^{\bar{h}_2+\bar{h}_3-\bar{h}_1} \, \bar{z}_{13}^{\bar{h}_3+\bar{h}_1-\bar{h}_2}} ,$$

where $z_{ij} = z_i - z_j$ and $\bar{z}_{ij} = \bar{z}_i - \bar{z}_j$.

It is typical of correlation functions to have singularities when the positions of two or more fields coincide. The operator product expansion (OPE) is the representation of a product of operators (at positions x and y) by a sum of terms involving single operators multiplied by functions of x and y, possibly diverging as $x \to y$. This expansion has a weak sense, being valid within correlation functions, and leads to the construction of an algebra of scaling fields defined by

$$\phi_i(x)\phi_j(y) = \sum_k \hat{C}_{ij}^k(x, y)\phi_k(y), \qquad (1.1.6)$$

where $\hat{C}_{ij}^k(x, y)$ are the structure constants. Translation and scaling invariance forces these functions to have the following form:

$$\hat{C}_{ij}^k(x, y) = \frac{C_{ij}^j}{|x - y|^{\Delta_i+\Delta_j-\Delta_k}},$$

where C_{ij}^j are exactly the undetermined multiplicative constants of the tree-point correlators (1.1.5).

A particularly important operator is the stress–energy tensor $T^{\mu\nu}$, which expresses the variation of the action under a transformation of coordinates $x^\mu \to x^\mu + \xi^\mu(x)$:

$$\delta S = -\frac{1}{2\pi} \int d^2x \, T^{\mu\nu}(x)\partial_\mu \xi_\nu .$$

Conformal invariance is equivalent to the vanishing of δS under the condition (1.1.1), and it is guaranteed by the tracelessness of the stress-energy tensor. Together with translation and rotation invariance ($\partial_\mu T^{\mu\nu} = 0$), the condition $T^\mu_\mu = 0$ is expressed in complex coordinates as

$$\partial_{\bar{z}} T = 0 \qquad \text{and} \qquad \partial_z \bar{T} = 0,$$

where $T(z) = T_{11} - T_{22} + 2iT_{12}$ and $\bar{T}(\bar{z}) = T_{11} - T_{22} - 2iT_{12}$. Therefore the stress-energy tensor splits into a holomorphic and an antiholomorphic part. In two dimensions, it is possible to deduce the following OPE for the stress-energy tensor and a primary field of dimension $(h, \bar{h})$:

$$T(z)\,\phi(w,\bar{w}) = \frac{h}{(z-w)^2}\,\phi(w,\bar{w}) + \frac{1}{z-w}\,\partial_w\phi(w,\bar{w}) + \text{regular terms} , \qquad (1.1.7)$$

$$\bar{T}(\bar{z})\,\phi(w,\bar{w}) = \frac{\bar{h}}{(\bar{z}-\bar{w})^2}\,\phi(w,\bar{w}) + \frac{1}{\bar{z}-\bar{w}}\,\partial_{\bar{w}}\phi(w,\bar{w}) + \text{regular terms} .$$

Furthermore, it is possible to show that the OPE of the stress-energy tensor with itself has the form:

$$T(z)T(w) = \frac{c/2}{(z-w)^4} + \frac{2}{(z-w)^2}\,T(w) + \frac{1}{z-w}\,\partial T(w) + \text{regular terms} , \qquad (1.1.8)$$

where the constant c, called central charge, depends on the specific model. A similar expression holds for the antiholomorphic component. The holomorphic and antiholomorphic components of the stress-energy tensor can be expanded in Laurent series respectively on modes L_n and $\bar{L}_n$, which are the quantum generators of the local conformal transformations

$$T(z) = \sum_{n=-\infty}^{\infty} \frac{L_n}{z^{n+2}} , \qquad \bar{T}(\bar{z}) = \sum_{n=-\infty}^{\infty} \frac{\bar{L}_n}{\bar{z}^{n+2}} , \qquad (1.1.9)$$

and obey the Virasoro algebra

$$[L_n, L_m] = (n-m)\,L_{n+m} + \frac{c}{12}\,n(n^2-1)\,\delta_{n+m,0} ,$$

$$[\bar{L}_n, \bar{L}_m] = (n-m)\,\bar{L}_{n+m} + \frac{c}{12}\,n(n^2-1)\,\delta_{n+m,0} , \qquad (1.1.10)$$

$$[L_n, \bar{L}_m] = 0 .$$

In virtue of the decomposition of (1.1.10) in the direct sum of two algebras, one in the holomorphic and the other in the antiholomorphic sector, the general properties of CFT have the same form in the two sectors, and from now on we will only restrict to the holomorphic part.

Comparing definition (1.1.9) with the OPE (1.1.7), we can deduce the action of some generators on a primary field:

$$
\begin{aligned}
(L_0\phi)(z) &= h\,\phi(z) \\
(L_{-1}\phi)(z) &= \partial\phi(z) \\
(L_n\phi)(z) &= 0 \quad \text{if} \quad n \geq 1
\end{aligned}
\qquad (1.1.11)
$$

The relation $[L_0, L_n] = -nL_n$ leads to the interpretation of generators L_n with $n > 0$ as destruction operators and with $n < 0$ as creation operators. Hence primary fields define highest weight representations of the Virasoro algebra, being annihilated by all destruction operators. The action of creation operators on these fields is encoded in the regular part of the OPE (1.1.7), and defines the so-called descendant fields

$$\phi^{(n_1,n_2,...,n_k)} = (L_{-n_1}L_{-n_2}...L_{-n_k})\,\phi ,$$

which are again eigenvectors of L_0:

$$L_0\left[\phi^{(n_1,n_2,...,n_k)}\right] = \left(h + \sum_{i=1}^{k} n_i\right)\phi^{(n_1,n_2,...,n_k)} .$$

The number $N = \sum_{i=1}^{k} n_i$ is called level of the descendant. As an example, the stress-energy tensor is a level two descendant of the identity $(T = L_{-2}\mathbb{I})$. The set $[\phi]$ constituted by all the descendant fields of a primary operator ϕ is called conformal family. It is possible to show that every correlation function involving descendant fields can be computed by applying a linear differential operator to the correlation function of the corresponding primary fields.

The Hilbert space of states of a CFT is built by acting on the vacuum with the operators evaluated at $z = 0$. Therefore, the primary states are given by

$$| h \rangle \equiv \phi(0)| 0 \rangle \,,$$

and the descendent states can be obtained from them as $L_{-n_1} L_{-n_2}...L_{-n_k}| h \rangle$.

In concluding this section, it is worth mentioning how the central charge c has the physical meaning of measuring the response of the system to the introduction of a macroscopic scale [10, 11, 12]. In fact, the complex plane can be conformally mapped to an infinite cylinder of circumference R by the transformation (see Fig. 1.1)

$$z \to w(z) = \frac{R}{2\pi} \ln z \,. \tag{1.1.12}$$

Implementing the above transformation on the stress–energy tensor one gets

$$T_{cyl.}(w) = \left(\frac{2\pi}{R} \right)^2 \left[T_{pl.}(z)z^2 - \frac{c}{24} \right].$$

If we assume that the vacuum energy density $\langle T_{pl.} \rangle$ vanishes on the plane, we see that it is non–zero on the cylinder:

$$\langle T_{cyl.} \rangle = -\frac{c\pi^2}{6R^2}.$$

The central charge is then proportional to the Casimir energy, which naturally goes to zero as the macroscopic scale R goes to infinity. In particular, the hamiltonian and the momentum are expressed on the cylinder in terms of the Virasoro generators as

$$H = \frac{2\pi}{R} \left(L_0 + \bar{L}_0 - \frac{c}{12} \right) \qquad P = \frac{2\pi i}{R} \left(L_0 - \bar{L}_0 \right) \tag{1.1.13}$$
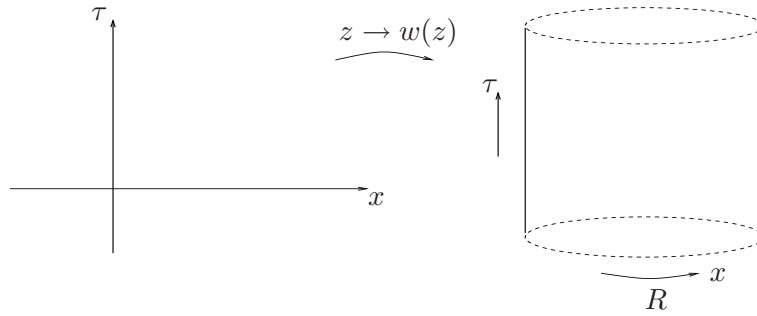

Figure 1.1: Conformal map (1.1.12) from plane to cylinder.

1.1.1 Examples

We will now describe few examples of CFT, which will be further discussed in the thesis. We limit ourselves to the statement of the main results, whose proofs can be found in the literature.

Gaussian CFT

An interesting CFT, only apparently trivial, is given by the gaussian action which describes a free bosonic field

$$\mathcal{A}_{\mathrm{G}} = \frac{1}{2}g \int d^2x \; \partial_\mu \phi \, \partial^\mu \phi \; , \tag{1.1.14}$$

where g is a normalization parameter. The two–point function of the field ϕ is expressed as

$$\langle \phi(z)\phi(w) \rangle = -\frac{1}{4\pi g} \log(z-w) + \mathrm{const.} \; .$$

Using Wick's theorem, one can easily show that the OPE between the energy–momentum tensor $T(z) \equiv -2\pi g : \partial\phi \, \partial\phi :$ and the operator $\partial\phi$ is given by

$$T(z)\partial\phi(w) = \frac{\partial\phi(w)}{(z-w)^2} + \frac{\partial^2\phi(w)}{(z-w)} + \mathrm{regular\ terms} \; ,$$

from which it follows that $\partial\phi$ is a primary field with conformal dimensions $h = \bar{h} = 1$. Furthermore, the OPE of T with itself

$$T(z)T(w) = \frac{1/2}{(z-w)^4} + \frac{2T(w)}{(z-w)^2} + \frac{\partial T(w)}{(z-w)} + \mathrm{regular\ terms}$$

shows that the theory is characterized by a central charge $c = 1$. Besides $\partial\phi$, other primary operators can be built by normal ordering the exponentials of ϕ:

$$V_\alpha(z,\bar{z}) =: e^{i\alpha\phi(z,\bar{z})} : \; .$$

These fields, called vertex operators, have conformal dimensions $h = \bar{h} = \frac{\alpha^2}{8\pi g}$.

A generalization of the above theory is obtained compactifying the bosonic field, i.e. making it an angular variable on a circle of radius $\mathcal{R}$. This can be done by defining the theory on a cylinder of circumference R with boundary conditions

$$\phi(x+R,t) = \phi(x,t) + 2\pi n \, \mathcal{R} \; . \tag{1.1.15}$$

The index n, called winding number, labels the various sectors of this CFT, together with an index s related to the discrete eigenvalues $\frac{2\pi s}{\mathcal{R}}$ of the momentum operator on the circle. In each sector, the states $|s,n\rangle$ with lowest anomalous dimension are created by the vertex operators

$$V_{s,n}(z,\bar{z}) =: \exp\left[i\alpha^+_{s,n}\varphi(z) + i\alpha^-_{s,n}\bar{\varphi}(\bar{z})\right] : \; , \tag{1.1.16}$$

i.e.

$$|s,n\rangle = V_{s,n}(0,0) \, |\,\mathrm{vac}\rangle \; ,$$

where

$$\begin{aligned}
\alpha^\pm_{s,n} &= \frac{s}{\mathcal{R}} \pm 2\pi g \, n\mathcal{R} \; ; \\
\phi(x,t) &= \varphi(z) + \bar{\varphi}(\bar{z}) \; .
\end{aligned}$$

Their conformal dimensions are given by

$$h_{s,n} = 2\pi g\left(\frac{s}{4\pi g \, \mathcal{R}} + \frac{1}{2}n\mathcal{R}\right)^2 \; , \qquad \bar{h}_{s,n} = 2\pi g\left(\frac{s}{4\pi g \, \mathcal{R}} - \frac{1}{2}n\mathcal{R}\right)^2 \; . \tag{1.1.17}$$

Minimal models

Virasoro minimal models are particular CFT characterized by a finite set of conformal families, in virtue of a truncation of the operator algebra. These theories can be labelled as $\mathcal{M}(p, p')$ with two integers p and p', in terms of which the central charge and the conformal dimensions of primary fields are expressed as

$$c = 1 - 6\frac{(p - p')^2}{p\, p'} \; , \tag{1.1.18}$$

$$h_{r,s} = \frac{(p\, r - p'\, s)^2 - (p - p')^2}{4p\, p'} \; , \tag{1.1.19}$$

with

$$1 \leq r < p' \qquad \text{and} \qquad 1 \leq s < p \; .$$

The conformal dimensions are organized in a rectangle in the (r, s) plane, called Kac table. The number of distinct fields is $(p - 1)(p' - 1)/2$, since there is a symmetry $h_{r,s} = h_{p'-r,p-s}$ which makes half of the Kac rectangle redundant. It can be shown that minimal models are unitary only if $|p - p'| = 1$, and in this case they are usually labelled with $p' = m$ and $p = m + 1$.

The simplest unitary minimal model is $\mathcal{M}(4, 3)$, which has central charge $c = \frac{1}{2}$ and the Kac table shown in Fig. 1.2.
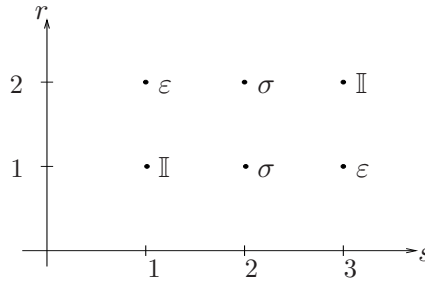
Figure 1.2: Kac table of the minimal model $\mathcal{M}(4, 3)$

This field theory is in the same universality class as the lattice Ising model [6], defined by the usual configuration energy

$$E[\sigma] = -J\sum_{\langle i,j \rangle} \sigma_i \sigma_j - h\sum_i \sigma_i \; , \qquad \sigma_i \in \{-1, 1\} \; .$$

Besides the identity operator $\phi_{1,1} = \mathbb{I}$, the theory contains the operator $\phi_{1,2} = \sigma$ with conformal dimension $h_\sigma = \frac{1}{16}$, which is the continuum version of the lattice spin σ_i, and $\phi_{1,3} = \varepsilon$, with $h_\varepsilon = \frac{1}{2}$, which corresponds to the interaction energy $\sigma_i \sigma_{i+1}$. The algebra defined by the OPE (1.1.6) can be schematically represented in this model by the fusion rules

$$\sigma \times \sigma \sim \mathbb{I} + \varepsilon \; ,$$
$$\sigma \times \varepsilon \sim \sigma \; ,$$
$$\varepsilon \times \varepsilon \sim \mathbb{I} \; .$$

This notation means, for instance, that the OPE of σ with σ (or fields belonging to their families) may contain terms belonging only to the conformal families of $\mathbb{I}$ and ε.
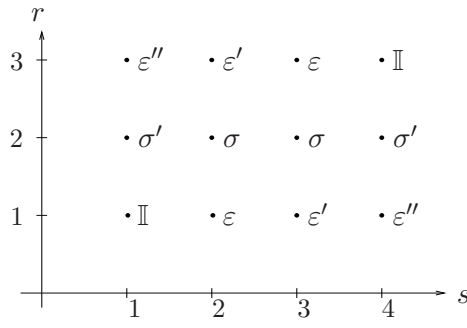
Figure 1.3: Kac table of the minimal model $\mathcal{M}(5,4)$

The next unitary model, $\mathcal{M}(5,4)$, displays a richer structure. The Kac table of this model, which has central charge $c = \frac{7}{10}$, is shown in Fig. 1.3.

It was recognized in [13] that the lattice model associated with this conformal field theory is the dilute Ising model at its tricritical fixed point (TIM), defined by

$$E[\sigma, t] = -J \sum_{\langle i,j \rangle} \sigma_i \sigma_j t_i t_j - \mu \sum_i (t_i - 1) , \qquad \sigma_i \in \{-1, 1\}, \ t_i \in \{0, 1\} ,$$

where μ is the chemical potential and t_i is the vacancy variable. The corresponding phase diagrams is drawn in Figure 1.4, where I and II denote respectively a first and second order phase transition, and the point $(J_I, 0)$ represents the Ising model, with all lattice's site occupied.
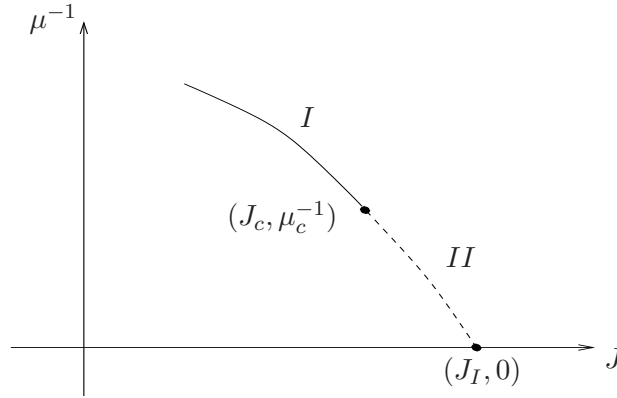
Figure 1.4: Phase diagram of the TIM.

The field $\phi_{1,2} = \varepsilon$, with $h_\varepsilon = \frac{1}{10}$, corresponds to the energy density, while $\phi_{1,3} = \varepsilon'$, with $h_{\varepsilon'} = \frac{6}{10}$, is the vacancy (or subleading energy) operator. The leading and subleading magnetization fields are respectively $\phi_{2,2} = \sigma$ and $\phi_{2,1} = \sigma'$, with $h_\sigma = \frac{3}{80}$ and $h_{\sigma'} = \frac{7}{16}$. The remaining field $\phi_{1,4} = \varepsilon''$ has conformal dimension $h_{\varepsilon''} = \frac{3}{2}$. Dividing the operators in even and odd with respect to the $\mathbb{Z}_2$ symmetry of the model under $\sigma_i \to -\sigma_i$, we can list the fusion rules in the following way:

even × even	even × odd	odd × odd
$\varepsilon \times \varepsilon = \mathbb{I} + \varepsilon'$	$\varepsilon \times \sigma = \sigma + \sigma'$	$\sigma \times \sigma = \mathbb{I} + \varepsilon + \varepsilon' + \varepsilon''$
$\varepsilon \times \varepsilon' = \varepsilon + \varepsilon''$	$\varepsilon \times \sigma' = \sigma$	$\sigma \times \sigma' = \varepsilon + \varepsilon'$
$\varepsilon \times \varepsilon'' = \varepsilon'$	$\varepsilon' \times \sigma = \sigma + \sigma'$	$\sigma' \times \sigma' = \mathbb{I} + \varepsilon''$
$\varepsilon' \times \varepsilon' = \mathbb{I} + \varepsilon'$	$\varepsilon' \times \sigma' = \sigma$	
$\varepsilon' \times \varepsilon'' = \varepsilon$	$\varepsilon'' \times \sigma = \sigma$	
$\varepsilon'' \times \varepsilon'' = \mathbb{I}$	$\varepsilon'' \times \sigma' = \sigma'$	

1.2 Integrable quantum field theories

The scaling region in the vicinity of second order phase transitions can be described by a given CFT perturbed by its relevant operators Φ_i (characterized by an anomalous dimension $\Delta_i < 2$), with the action

$$\mathcal{A} = \mathcal{A}_{CFT} + \sum_i \lambda_i \int d^2 x \, \Phi_i(x) \,, \tag{1.2.1}$$

where the couplings have mass dimension $\lambda_i \sim [m]^{2-\Delta_i}$. The relevant operators, being super-renormalizable with respect to UV divergencies, do not affect the behaviour of the system at short distances, but they change it at large scales. Any combination of the relevant fields defines a Renormalization Group (RG) trajectory which starts from the given CFT and can reach another critical point (defined by a different CFT) or a non–critical fixed point, corresponding to a massive QFT. From now on, we will only consider this second case. It was shown in [14] that, depending on the choice of the perturbing operator, the off-critical massive field theory can be integrable, with consequent elasticity and factorization of the scattering. Obviously, this kind of theories covers only a class of the statistical systems of interest, however this class includes relevant physical problems. For instance, integrable QFT correspond to the Ising model with thermal or magnetic perturbation separately, described respectively by

$$\mathcal{A}_{\mathcal{M}(4,3)} + \lambda_\varepsilon \int d^2 x \, \phi_{1,3}(x) \qquad \text{and} \qquad \mathcal{A}_{\mathcal{M}(4,3)} + \lambda_\sigma \int d^2 x \, \phi_{1,2}(x) \,,$$

or to the tricritical Ising model perturbed by the leading energy operator

$$\mathcal{A}_{\mathcal{M}(5,4)} + \lambda_\varepsilon \int d^2 x \, \phi_{1,2}(x) \,.$$

We will now present a brief overview of integrable massive quantum field theories, underlying their basic features (for an exhaustive review, see [15]). This will also give us the opportunity of introducing the most important kinematical quantities used in the following.

An integrable QFT is characterized by the presence of an infinite set of conserved charges, which make the corresponding scattering theory purely elastic and factorized [16]. This implies that an arbitrary n-particle collision process can be described by the product of $n(n-1)/2$ elastic pair collisions. Hence the determination of the complete S matrix reduces to that of the two-particle amplitudes, which are defined as

$$|A_i(p_1) A_j(p_2)\rangle_{in} = S_{ij}^{kl} |A_k(p_3) A_l(p_4)\rangle_{out} \,, \tag{1.2.2}$$

where $A_i(p_1)$ and $A_j(p_2)$ denote the incoming particles (with 2-momenta p_1^μ and p_2^μ), and $A_k(p_3)$ and $A_l(p_4)$ the outgoing states (see Fig. 1.5).
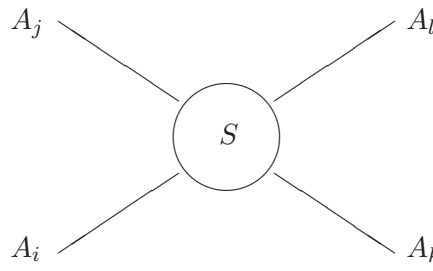
Figure 1.5: Two-particle S-matrix

Lorentz invariance fixes the two body S-matrix to be a function of the Mandelstam variables $s = (p_1 + p_2)^2$, $t = (p_1 - p_3)^2$ and $u = (p_1 - p_4)^2$, which satisfy the relation $s + t + u = \sum_{i=1}^{4} m_i^2$. Since in (1+1) dimensions and for elastic scattering only one of these variables is independent, it is convenient to introduce a parameterization of the momenta in terms of the so-called rapidity variable θ:

$$p_i^0 = m_i \cosh \theta_i , \qquad p_i^1 = m_i \sinh \theta_i , \qquad (1.2.3)$$

which corresponds to the following expression for the Mandelstam variable s:

$$s = (p_1 + p_2)_\mu (p_1 + p_2)^\mu = m_i^2 + m_j^2 + 2 m_i m_j \cosh \theta_{ij} , \qquad (1.2.4)$$

with $\theta_{ij} = \theta_i - \theta_j$. The functions S_{ij}^{kl} will then depend only on the rapidity difference of the involved particles:

$$|A_i (\theta_1) A_j (\theta_2)\rangle_{in} = S_{ij}^{kl} (\theta_{12}) |A_k (\theta_2) A_l (\theta_1)\rangle_{out} .$$

Elasticity of the scattering processes implies a drastic simplification in the analytic structure of the S–matrix, which can be extended to be an analytic function in the complex s–plane [17]. In fact, contrary to the generic case, where many branch cuts are present, in the elastic case the two–particle S-matrix only displays two square root branching points at the two–particle thresholds $(m_i - m_j)^2$ and $(m_i + m_j)^2$, and is real valued on the interval of the real axis between them. From (1.2.4) it follows that the functions $S_{ij}^{kl} (\theta)$ are meromorphic in θ, and real at $\mathrm{Re}(\theta) = 0$. The two cuts in the s variable, in fact, are unfolded by the transformation (1.2.4): for instance, the upper side of the cut along $[(m_i + m_j)^2 , \infty]$ is mapped into the positive semiaxis $0 < \theta < \infty$, while the lower side is mapped into the negative semiaxis $-\infty < \theta < 0$. The physical sheet of the s–plane goes into the strip $0 \leq \mathrm{Im}(\theta) \leq \pi$, while the second Riemann sheet is mapped into $-\pi \leq \mathrm{Im}(\theta) \leq 0$. The structure in the θ plane repeats then with periodicity $2\pi i$. See Fig. 1.6 for a representation of the analytic structure of the S–matrix in the two variables s and θ.

The two-particle S-matrices satisfy the usual requirements of unitarity, expressed as

$$\sum_{n,m} S_{ij}^{nm} (\theta) S_{nm}^{kl} (-\theta) = \delta_i^k \delta_j^l , \qquad (1.2.5)$$

and crossing symmetry, given by

$$S_{ik}^{lj} (\theta) = S_{ij}^{kl} (i\pi - \theta) , \qquad (1.2.6)$$

since the analytic continuation $s \to t$ from the s-channel to the t-channel corresponds to the change of variable $\theta \to i\pi - \theta$. Furthermore, the amplitudes are restricted by the star-triangle (or Yang-Baxter) equations

$$S_{i_1 i_2}^{k_1 k_2} (\theta_{12}) S_{k_1 k_3}^{j_1 j_3} (\theta_{13}) S_{k_2 i_3}^{j_2 k_3} (\theta_{23}) = S_{i_1 i_3}^{k_1 k_3} (\theta_{13}) S_{k_1 k_2}^{j_1 j_2} (\theta_{12}) S_{i_2 k_3}^{k_2 j_3} (\theta_{23}) , \qquad (1.2.7)$$
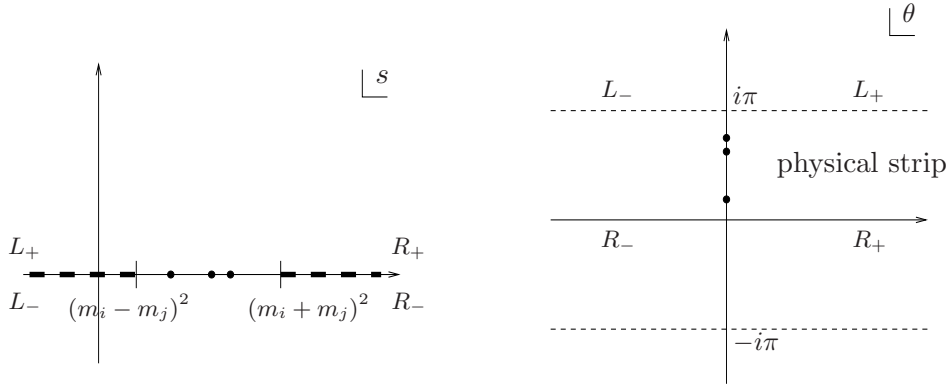
Figure 1.6: Analytic structure of the elastic S–matrix in the variables s and θ.

where a sum over the intermediate indices is understood. The system of equations (1.2.5), (1.2.6) and (1.2.7) is in many cases sufficient to solve the kinematics of the problem, determining a consistent solution for the two-particle S-matrix, up to a so-called CDD ambiguity, which consists in multiplying the solution by factors that alone satisfy the same equations.

Since the bound states of a theory correspond to singularities of the S-matrix, its analytic structure encodes the spectrum of the system. Stable bound states are usually associated to simple poles in the s variable located in the real interval $(m_i - m_j)^2 < s < (m_i + m_j)^2$. These are mapped by (1.2.4) onto the imaginary θ–axis of the physical strip (see Fig. 1.6). If a two–particle amplitude with initial states A_i and A_j has a simple pole in the s-channel at $\theta = iu_{ij}^n$ (A_n is the associated intermediate bound state), in the vicinity of this singularity we have

$$S_{ij}^{kl}(\theta) \sim \frac{iR_{ij}^n}{\left(\theta - iu_{ij}^n\right)} , \qquad \text{with} \qquad R_{ij}^n = \Gamma_{ij}^n \Gamma_n^{kl} \tag{1.2.8}$$

where Γ_{ij}^n are the on-shell three–particle coupling constants of the underlying quantum field theory (see Fig. 1.7). Remembering that the corresponding singularity in the s variable is of the form $(s - m_n^2)^{-1}$ and using relation (1.2.4), we get the following expression for the mass of the bound state:

$$m_n^2 = m_i^2 + m_j^2 + 2\,m_i\,m_j\,\cos u_{ij}^n. \tag{1.2.9}$$
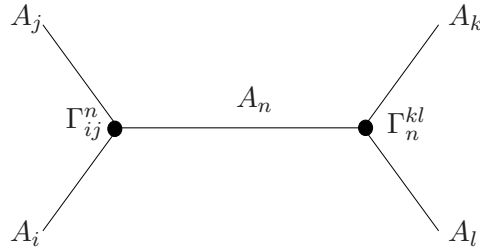
Figure 1.7: First-order pole in the S–matrix

The dynamics of the system can be determined by implementing the so–called "bootstrap principle", which consists in identifying the bound states with some of the particles appearing as asymptotic states. This leads to further equations which permit to fix the CDD ambiguities mentioned above and to identify the particle content of the theory.

Finally, it is worth recalling that unstable bound states (resonances) are associated to $s-$ variable poles in the second Riemann sheet at $s = \left(m_k - i\frac{\Gamma_k}{2}\right)^2$, where Γ_k is the inverse life–time of the particle. These correspond to poles in θ located in the strip $-\pi \le \text{Im}(\theta) \le 0$ at positions $\theta = -iu_{ij}^k + \alpha_{ij}^k$ satisfying

$$
\begin{aligned}
m_k^2 - \frac{\Gamma_k^2}{4} &= m_i^2 + m_j^2 + 2\,m_i\,m_j\,\cos u_{ij}^k\,\cosh \alpha_{ij}^k\,, \\
m_k\,\Gamma_k &= 2\,m_i\,m_j\,\sin u_{ij}^k\,\sinh \alpha_{ij}^k\,.
\end{aligned}
\tag{1.2.10}
$$

The knowledge of the exact S-matrix further permits to extract non–perturbative information on the correlation functions of the theory. In fact, the spectral function $\rho^{(\Phi)}$ associated to a given operator Φ, defined as

$$
\langle\,0\,|\,\Phi(x)\Phi(0)|\,0\,\rangle \equiv \int \frac{d^2p}{(2\pi)^2}\,\rho^{(\Phi)}(p^2)\,e^{ip\cdot x}\,,
$$

can be expanded as a sum over complete sets of particle states

$$
\rho^{(\Phi)}(p^2) = 2\pi \sum_n \frac{1}{n!} \int\; d\Omega_1...d\Omega_n \quad \delta(p^0 - p_1^0... - p_n^0)\,\delta(p^1 - p_1^1... - p_n^1)\,\times
$$
$$
\times\,\left|\,F_{a_1...a_n}^{\Phi}(\theta_1,\ldots,\theta_n)\,\right|^2\,,
\tag{1.2.11}
$$

where $d\Omega \equiv \frac{dp}{2\pi\,2E} = \frac{d\theta}{4\pi}$ and

$$
F_{a_1...a_n}^{\Phi}(\theta_1,\ldots,\theta_n) = \langle\,0\,|\,\Phi(0)\,|\,A_{a_1}(\theta_1)\ldots A_{a_n}(\theta_n)\,\rangle\,.
\tag{1.2.12}
$$

The matrix elements (1.2.12), called "form factors" and pictorially depicted in Fig. 1.8, are subject to the Watson equations, which relate them to the scattering amplitudes. In the case of integrable theories these equations take a simplified form [18, 19, 20], which permit the determination of form factors once the S-matrix is known. Furthermore, it has been shown in a series of works (see, for instance [21]) that the spectral representation has a fast convergent behaviour, therefore accurate estimates of correlators and other related physical quantities can be obtained by just using few exact terms in the series (1.2.11), having consequently a great simplification of the problem.
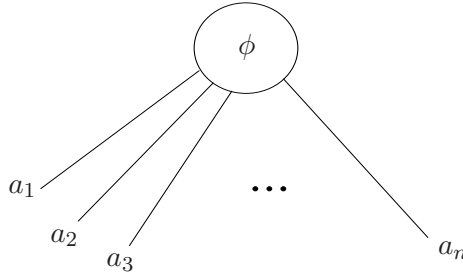

Figure 1.8: Form factor (1.2.12)

Here we limit ourselves to the description of the main equations ruling the simplest non–trivial form factors, i.e. the two–particle ones, that we will use and discuss in the following. The

discontinuity of the matrix elements across the unitarity cut leads to the following relation with the two–particle scattering amplitudes:

$$F_{ab}^{\Phi}(\theta) = S_{ab}^{cd}(\theta) F_{cd}^{\Phi}(-\theta) \ , \tag{1.2.13}$$

where $\theta = \theta_1 - \theta_2$. The crossing symmetry of the form factor is expressed as

$$F_{a\bar{a}}^{\Phi}(\theta + 2i\pi) = e^{-2i\pi\gamma_{\Phi,a}} F_{\bar{a}a}^{\Phi}(-\theta) \ , \tag{1.2.14}$$

where the phase factor $e^{-2i\pi\gamma_{\Phi,a}}$ is inserted to take into account a possible semi-locality of the operator which interpolates the particle a (i.e. any operator φ_a such that $\langle 0|\varphi_a|a\rangle \neq 0$) with respect to the operator $\Phi(x)$. When $\gamma_{\Phi,a} = 0$, there is no crossing symmetric counterpart to the unitarity cut but when $\gamma_{\Phi,a} \neq 0$, there is instead a non-locality discontinuity in the plane of the Mandelstam variable s defined in (1.2.4), with $s = 0$ as branch point. In the rapidity parameterization there is however no cut because the different Riemann sheets of the s-plane are mapped onto different sections of the θ-plane; the branch point $s = 0$ is mapped onto the points $\theta = \pm i\pi$ which become therefore the locations of simple annihilation poles. The residues at these poles are given by

$$\mathrm{Res}_{\theta=\pm i\pi} F_{ab}^{\Phi}(\theta) = i\delta_{\bar{a}b}(1 - e^{\mp 2i\pi\gamma_{\Phi,a}})\langle 0|\Phi|0\rangle \ . \tag{1.2.15}$$

Finally, the two–particle form factors inherit the s–channel bound state poles of the S–matrix, and the corresponding residua are given by

$$\mathrm{Res}_{\theta=iu_{ab}^c} F_{ab}^{\Phi}(\theta) = i\Gamma_{ab}^c F_c^{\Phi} \ . \tag{1.2.16}$$

where the couplings Γ_{ab}^c coincide with the ones in (1.2.8). This relation, pictorially represented in Fig. 1.9, is the property of form factors that we will mostly exploit in the following.
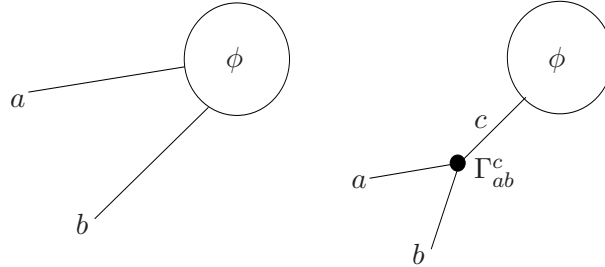
Figure 1.9: Dynamical pole (1.2.16) in the two–particle form factor $F_{ab}^{\Phi}(\theta)$

1.3 Landau–Ginzburg theory

As we have seen in Sect. 1.1, statistical models at the critical point can be described by conformal field theories (CFT), and many systems of physical relevance have been identified with the Virasoro minimal models. The operators of these theories can be organized in a finite number of families, and this simplifies the dynamics allowing in principle for a complete solution. The only disadvantage of this kind of theories is that they have no Lagrangian formulation, therefore they cannot be studied by a path–integral approach and the underlying physics is not always

transparent. However, for a class of minimal theories, the unitary ones $\mathcal{M}(m+1, m)$, there is a simple effective Lagrangian description, suggested in [22], which is realized by a self–interacting field ϕ subjected to a power–like potential. The field ϕ stands for the order parameter of the statistical system, and the potential $V(\phi)$, whose extrema correspond to the various critical phases of the system, is usually chosen to be invariant under the reflection $\phi \to -\phi$. For a potential of degree $2(m-1)$, this ensures the existence of $m-1$ minima separated by $m-2$ maxima. Several critical phases of the system can coexist if the corresponding extrema coincide. The most critical potential is therefore a monomial of the form

$$V_m(\phi) = \phi^{2(m-1)} .$$

Starting from the field ϕ, one can construct composite fields $: \phi^k :$ by normal ordering its powers. These have been shown in [22] to display the same fusion properties as the operators present in the minimal model $\mathcal{M}(m+1, m)$, supporting in this way the correspondence. In particular, the field ϕ is always associated to the primary operator $\phi_{2,2}$.

One of the nicest features of the Landau–Ginzburg description is that it provides a very intuitive picture of the perturbation of CFT away from the critical points, since this simply corresponds to adding opportune powers of ϕ to V_m.

For instance, the universality class of the Ising model is described by $m = 3$, the spin operator corresponds to $\sigma \sim \phi$ and the energy operator to $\varepsilon \sim: \phi^2 :$. Therefore the thermal perturbation of the critical point is described by the Landau–Ginzburg theory

$$V(\phi) = A\phi^4 + B\phi^2 + C ,$$

where the sign of B refers to high or low temperature, respectively (see Fig. 1.10).
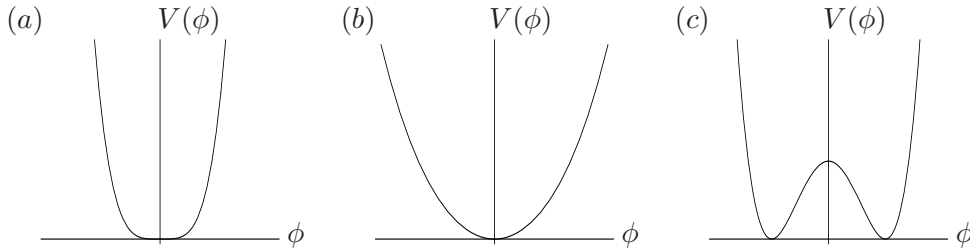
Figure 1.10: Landau–Ginzburg potential for the Ising model (a) at the critical point, (b) at high temperature, (c) at low temperature.

Another very interesting example is given by the case $m = 4$, which corresponds to the tricritical Ising model. The operator content of the theory is in this case identified as

$$\begin{cases} \sigma \sim \phi \\ \varepsilon \sim: \phi^2 : \\ \sigma' \sim: \phi^3 : \\ \varepsilon' \sim: \phi^4 : \\ \varepsilon'' \sim: \phi^6 : \end{cases}$$

Hence, for instance, the perturbation of the tricritical point by leading and subleading energy densities is described as

$$V(\phi) = A\phi^6 + B\phi^4 + C\phi^2 + D \,,$$

and some of the resulting potentials are shown in Fig. 1.11.
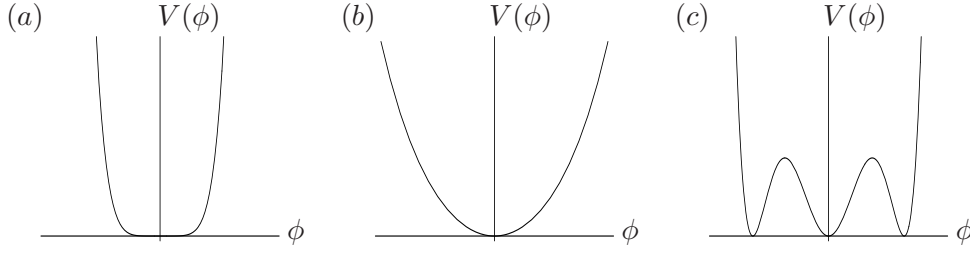
Figure 1.11: Landau–Ginzburg potential for the tricritical Ising model (a) at the tricritical point, (b) with positive leading and subleading energy perturbations, (c) with positive leading and negative subleading energy perturbations.

In concluding this Section it is worth to remark how the above mentioned correspondence between Lagrangians and minimal models is based on euristic arguments which are not rigorously proven. Furthermore, quantum corrections can be very strong, hence a quantitative analysis of statistical system is generally not possible starting from the Lagrangian formulation. However, the qualitative picture offered by the Landau–Ginzburg theory, being essentially based on the symmetries of the model, remains valid also at quantum level. In particular, this description nicely illustrates the underlying physics in cases when the potential displays degenerate minima, since the classical solutions interpolating between the minima have a direct meaning of quantum particles, as we are going to show in the next Chapter.

Chapter 2

Semiclassical Quantization

In this Chapter we will describe the two basic technical tools used in the following to investigate non–integrable spectra and finite–size effects. The first is represented by the semiclassical quantization technique introduced for relativistic field theories in a series of papers by Dashen, Hasslacher and Neveu (DHN) [23] by using an appropriate generalization of the WKB approximation in quantum mechanics. The second is a result due to Goldstone and Jackiw [24], which relates the form factors of the basic field between kink states to the Fourier transform of the classical solution describing the kink.

Here we only focus on the description of these two results, that we will fully exploit in the following. However, it should be mentioned that the semiclassical study of QFT was developed during the Seventies by few independent groups and with complementary techniques, such as the path–integral approach, the inclusion of fermions and the analysis of higher order corrections in the semiclassical expansion. It is worth mentioning, for instance, the work of Callan and Gross [25], Gervais, Jevicki and Sakita [26], Faddeev and Korepin [27]. A complete review of these beautiful achievements can be found in [28].

We will restrict to the study of two–dimensional theories, in virtue of their simplified kinematics that allows for a powerful applications of the semiclassical techniques. However, it is well known that the semiclassical methods are naturally formulated for QFT in any dimension $(d + 1)$, and have provided, for instance, relevant insight in the study of four–dimensional gauge theories. In fact, the main feature that makes interesting their use is the presence of non–linear interaction, which gives rise to topologically non–trivial classical solutions. Classical non–linear equations have been always recognized to play a crucial role in the description of physical phenomena, in virtue of their intriguing complex features (see for instance [30, 31]). The expectation of finding interesting properties also in the associated quantum field theories, first acquired by Skyrme [32], opened the way to the non–perturbative semiclassical studies that we are going to describe.

The Chapter is organized as follows. In Section 2.1 we introduce the DHN quantization technique for static non–perturbative backgrounds. In Section 2.2 we describe the Goldstone and Jackiw's result and its relativistic formulation, proposed in [1], which is the basic tool used in the following to study the spectrum of non–integrable QFT. Finally, in Section 2.3 we apply the above techniques to the sine–Gordon model, where, in virtue of the integrability of the theory, exact result to be compared with the semiclassical ones are available.

2.1 DHN method

The semiclassical quantization of a field theory defined by a Lagrangian

$$\mathcal{L} = \frac{1}{2} \left(\partial_\mu \phi \right) \left(\partial^\mu \phi \right) - V(\phi) \tag{2.1.1}$$

is based on the identification of a classical background $\phi_{cl}(x,t)$ which satisfies the Euler–Lagrange equation of motion

$$\partial_\mu \partial^\mu \phi_{cl} + V'(\phi_{cl}) = 0 . \tag{2.1.2}$$

The procedure is particularly simple and interesting if one considers finite–energy static classical solutions $\phi_{cl}(x)$ in 1+1 dimensions, usually called "kinks" or "solitons". Their presence is one of the main features of a large class of 1+1–dimensional field theories defined by a non–linear interaction $V(\phi)$ displaying discrete degenerate minima ϕ_i, which are constant solutions of the equation of motion and are called "vacua". The (anti)kinks interpolate between two next neighbouring minima of the potential, and consequently they carry topological charges $Q = \pm 1$, where

$$Q \equiv \frac{1}{\phi_{i+1} - \phi_i} \int\limits_{-\infty}^{\infty} dx \, \frac{d\phi(x,t)}{dx} . \tag{2.1.3}$$

The conservation of this quantity, which can be easily deduced from the associated conserved current

$$j^\mu = \epsilon^{\mu\nu} \partial_\nu \phi , \qquad Q = \frac{1}{\phi_{i+1} - \phi_i} \int\limits_{-\infty}^{\infty} dx \, j^0 ,$$

will play a crucial role in the following.

Being static solutions of the equation of motion, i.e. time independent in their rest frame, the kinks can be simply obtained by integrating the first order differential equation related to (2.1.2)

$$\frac{1}{2} \left(\frac{\partial \phi_{cl}}{\partial x} \right)^2 = V(\phi_{cl}) + A , \tag{2.1.4}$$

further imposing that $\phi_{cl}(x)$ reaches two different minima of the potential at $x \to \pm\infty$. These boundary conditions, which describe the infinite volume case, require the vanishing of the integration constant A. As we will see in the following, the kink solutions in a finite volume correspond instead to a non–zero value of A, related to the size of the system.

For definiteness in the illustration of the method, we will focus on the example of the ϕ^4 theory in the broken $\mathbb{Z}_2$ symmetry phase, defined by the potential

$$V(\phi) = \frac{\lambda}{4} \phi^4 - \frac{m^2}{2} \phi^2 + \frac{m^4}{4\lambda} . \tag{2.1.5}$$

This theory displays two degenerate minima at $\phi_\pm = \pm \frac{m}{\sqrt{\lambda}}$, and a static (anti)kink interpolating between them

$$\phi_{cl}(x) = (\pm) \frac{m}{\sqrt{\lambda}} \tanh \frac{m}{\sqrt{2}} (x - x_0) , \tag{2.1.6}$$

where the arbitrariness of the center of mass position x_0 is due to the translational invariance of the theory. The corresponding classical energy is obtained by integrating the energy density

$\varepsilon_{cl}(x) \equiv \frac{1}{2} \left(\frac{d\phi_{cl}}{dx} \right)^2 + V(\phi_{cl})$:

$$\mathcal{E}_{cl} \equiv \int_{-\infty}^{\infty} dx \, \varepsilon_{cl}(x) = \frac{2\sqrt{2}}{3} \frac{m^3}{\lambda} \ . \tag{2.1.7}$$

Fig. 2.1 shows the potential, the classical kink and its energy density.
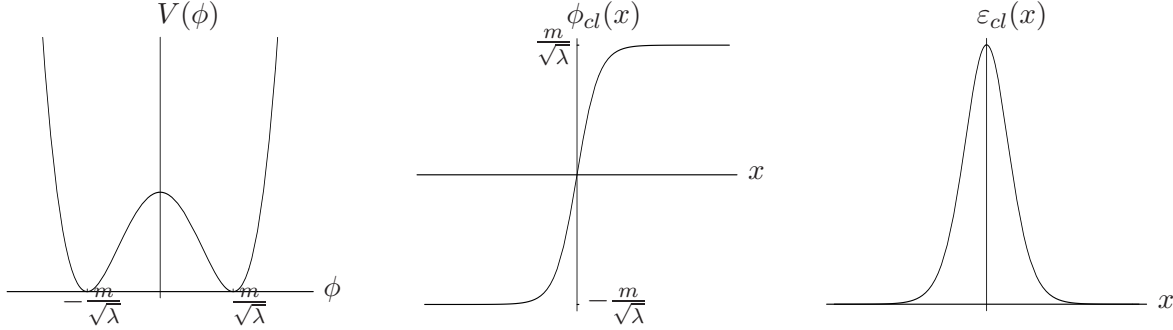
Figure 2.1: Potential $V(\phi)$, kink $\phi_{cl}(x)$ and energy density $\varepsilon_{cl}(x)$.

The kinks exhibit certain particle properties. For instance, they are localized and topologically stable objects, since the conservation of topological charge forbids their decay into mesons with $Q = 0$. Moreover, in integrable theories their scattering is dispersionless and, in the collision processes, they preserve their form simply passing through each other. All the above properties are an indication that the kinks can survive the quantization, giving rise to the quantum states in one–particle sector of the corresponding QFT. As it is well known, one cannot apply directly to them the standard perturbative methods of quantization around the free field theory since the kinks are entirely non–perturbative solutions of the interacting theory. Their classical mass, for instance, is usually inversely proportional to the coupling constant (see (2.1.7) in the broken ϕ^4 example). In infinite volume, an effective method for the semiclassical quantization of such solutions (as well as of the vacua ones) has been developed in a series of papers by Dashen, Hasslacher and Neveu (DHN) [23] by using an appropriate generalization of the WKB approximation in quantum mechanics.

The DHN method consists in initially splitting the field $\phi(x, t)$ in terms of the static classical solution (which can be either one of the vacua or the kink configuration) and its quantum fluctuations, i.e.

$$\phi(x, t) = \phi_{cl}(x) + \eta(x, t) \quad , \quad \eta(x, t) = \sum_k e^{i\omega_k t} \, \eta_k(x) \ ,$$

and in further expanding the action of the theory in powers of η, obtaining for instance, in the example (2.1.5), the expansion in λ

$$S(\phi) = \int dx \, dt \, \mathcal{L}(\phi_{cl}) + \int dx \, dt \, \frac{1}{2} \, \eta(x, t) \left(\frac{d^2}{dt^2} - \frac{d^2}{dx^2} - m^2 + 3\lambda\phi_{cl}^2 \right) \eta(x, t) + \lambda \int dx \, dt \left(\phi_{cl} \, \eta^3 + \frac{1}{4}\eta^4 \right) \ . \tag{2.1.8}$$

The semiclassical approximation is realized by keeping only the quadratic terms, and as a result of this procedure, $\eta_k(x)$ satisfies the so called "stability equation"

$$\left[-\frac{d^2}{dx^2} + V''(\phi_{cl}) \right] \eta_k(x) = \omega_k^2 \, \eta_k(x) \ , \tag{2.1.9}$$

together with certain boundary conditions. The semiclassical energy levels in each sector are then built in terms of the energy of the corresponding classical solution and the eigenvalues ω_i of the Scrödinger–like equation (2.1.9), i.e.

$$E_{\{n_i\}} = \mathcal{E}_{cl} + \hbar \sum_k \left(n_k + \frac{1}{2}\right) \omega_k + O(\hbar^2) \,, \qquad (2.1.10)$$

where n_k are non–negative integers. In particular the ground state energy in each sector is obtained by choosing all $n_k = 0$ and it is therefore given by[1]

$$E_0 = \mathcal{E}_{cl} + \frac{\hbar}{2} \sum_k \omega_k + O(\hbar^2) \,. \qquad (2.1.11)$$

The semiclassical quantization technique was applied in [23] to the kink background (2.1.6), in order to compute the first quantum corrections to its mass, given at leading order by the classical energy. The stability equation (2.1.9) can be cast in the hypergeometric form in the variable $z = \frac{1}{2}(1 + \tanh \frac{mx}{\sqrt{2}})$, and the solution is

$$\eta(x) = z^{\sqrt{1-\frac{\omega^2}{2m^2}}}(1-z)^{-\sqrt{1-\frac{\omega^2}{2m^2}}} F\left(3, -2, 1 + 2\sqrt{1 - \frac{\omega^2}{2m^2}}; z\right) \,.$$

The corresponding spectrum is given by the two discrete eigenvalues

$$\omega_0^2 = 0 \,, \qquad \text{with} \qquad \eta_0(x) = \frac{1}{\cosh^2 \frac{mx}{\sqrt{2}}} \,, \qquad (2.1.12)$$

and

$$\omega_1^2 = \frac{3}{2} m^2 \,, \qquad \text{with} \qquad \eta_1(x) = \frac{\sinh \frac{mx}{\sqrt{2}}}{\cosh^2 \frac{mx}{\sqrt{2}}} \,, \qquad (2.1.13)$$

plus the continuous part, labelled by $q \in \mathbb{R}$,

$$\omega_q^2 = m^2\left(2 + \frac{1}{2}q^2\right) \,, \qquad \text{with} \qquad \eta_q(x) = e^{iqmx/\sqrt{2}}\left(3\tanh^2 \frac{mx}{\sqrt{2}} - 1 - q^2 - 3iq\tanh \frac{mx}{\sqrt{2}}\right) \,. \qquad (2.1.14)$$

The presence of the zero mode ω_0 is due to the arbitrary position of the center of mass x_0 in (2.1.6), while ω_1 and ω_q represent, respectively, an internal excitation of the kink particle and the scattering of the kink with mesons[2] of mass $\sqrt{2}\,m$ and momentum $mq/\sqrt{2}$. This interpretation will find a clear explanation in Sect. 2.2.

The semiclassical correction to the kink mass can be now computed as the difference between the ground state energy in the kink sector and the one of the vacuum sector, plus a mass counterterm due to normal ordering (see Fig. 2.2):

$$M = \mathcal{E}_{cl} + \frac{1}{2}m\sqrt{\frac{3}{2}} + \frac{1}{2}\sum_n \left[m\sqrt{2 + \frac{1}{2}q_n^2} - \sqrt{k_n^2 + 2m^2}\right] - \frac{1}{2}\delta m^2 \int\limits_{-\infty}^{\infty} dx \left[\phi_{cl}^2(x) - \frac{m^2}{\lambda}\right] \,,$$

with

$$\delta m^2 = \frac{3\lambda}{4\pi} \int\limits_{-\infty}^{\infty} \frac{dk}{\sqrt{k^2 + 2m^2}} \,.$$
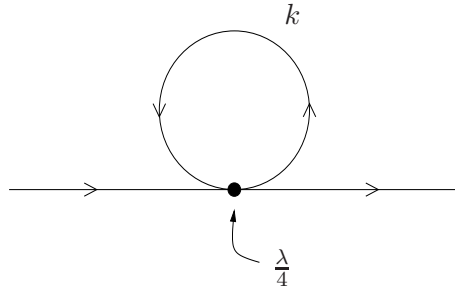
Figure 2.2: Tadpole diagram giving rise to δm^2.

The discrete values q_n and k_n are obtained putting the system in a big finite volume of size R with periodic boundary conditions:

$$2n\pi = k_n R = q_n \frac{mR}{\sqrt{2}} + \delta(q_n) \; ,$$

where the phase shift $\delta(q)$ is extracted from $\eta_q(x)$ in (2.1.14) as

$$\eta_q(x) \xrightarrow[x \to \pm\infty]{} e^{i\left[q \frac{mx}{\sqrt{2}} \pm \frac{1}{2}\delta(q)\right]} \; , \qquad\qquad \delta(q) = -2\arctan\left(\frac{3q}{2 - q^2}\right) \; .$$

Sending $R \to \infty$ and computing the integrals we finally have

$$M = \frac{2\sqrt{2}}{3}\frac{m^3}{\lambda} + m\left(\frac{1}{6}\sqrt{\frac{3}{2}} - \frac{3}{\pi\sqrt{2}}\right) \; . \tag{2.1.15}$$

In concluding this section, it is worth mentioning that the construction of the complete Hilbert space requires to consider time–dependent multi–kink solutions with finite energy. Their semiclassical quantization can be performed with an appropriate modification of the DHN method [23] to include the time–dependence. Moreover, the semiclassical computations can be extended at higher order in the small–coupling expansion, keeping cubic (and higher) powers of η in (2.1.8). This procedure is highly non–trivial, especially due to the presence of the zero mode $\omega_0 = 0$, which causes some divergencies at higher order in λ. However, effective methods for solving problem have been developed and applied in [25, 26], in the context of a path integral technique.

2.2 Classical solutions and form factors

2.2.1 Goldstone and Jackiw's result

A direct relation between the kink states and the corresponding classical solutions has been established by Goldstone and Jackiw [24], who have shown that the matrix element of the field ϕ between kink states is given, at leading order in the semiclassical limit, by the Fourier transform of the kink background. A detailed explanation of this result can be found in [28], and a similar achievement in a non–relativistic context is presented in [29].

---

[1]From now on we will fix $\hbar = 1$, since the semiclassical expansion in $\hbar$ is equivalent to the expansion in the interaction coupling λ.

[2]The mesons represent the excitations over the vacua, i.e. the constant backgrounds $\phi_\pm = \pm\frac{m}{\sqrt{\lambda}}$, therefore their square mass is given by $V''(\phi_\pm) = 2\,m^2$.

The technique to derive this result relies on the following assumptions, which consolidate the basic ideas already exposed in Sect. 2.1, and that we illustrate here in the case of the broken ϕ^4 theory (2.1.5):

1. The Hilbert space of the theory contains, in addition to the 'vacuum sector' (i.e. the vacuum and multi–meson states), the so–called kink sector. This is spanned by the states $|p\rangle$ and $|p^*\rangle$, representing the kink particle of momentum p in its ground state and excited state, respectively, and the states $|p, k_1, ..., k_m\rangle$ and $|p^*, k_1, ..., k_m\rangle$, representing the scattering states of the kink particle and m mesons.

2. The kink sector is orthogonal to the vacuum sector, hence the kink is stable against decay into mesons. In fact, although the states in the kink sector have higher energy than the vacuum sector ones, they are prevented from decaying by the conservation of the topological charge, which holds also in the quantum theory.

3. The mass of the quantum kink behaves as $M \sim \frac{1}{\lambda}$ in the weak coupling limit (see (2.1.7)).

4. The matrix elements of $\phi(x, t)$ between the above states behave in the weak coupling limit as

$$\langle p' | \phi | p \rangle \sim O\left(1/\sqrt{\lambda}\right)$$
$$\langle p' | \phi | p, k \rangle \text{ and } \langle p' | \phi | p^* \rangle \sim O(1)$$
$$\langle p', k_1', ..., k_l' | \phi | p, k_1, ..., k_m \rangle \sim O\left(\lambda^{(l+m-1)/2}\right)$$

This assumption, which will find confirmation *a posteriori*, relies on the fact that the kink classical background itself is of order $1/\sqrt{\lambda}$, and that the emission or absorption of every additional meson and the internal excitation of the kink carry a factor $\sqrt{\lambda}$. This can be intuitively understood by noticing that, in the expansion (2.1.8) of the interaction $V(\phi)$, the leading perturbative term is of order $\lambda \phi_{cl}$, i.e. of order $\sqrt{\lambda}$.

Let's now define the matrix element of the basic field $\phi(x, t)$ between in and out one–kink states, with momenta p_1 and p_2, as the Fourier transform of a function $\hat{f}(a)$, to be determined:

$$\langle p_2 | \phi(0) | p_1 \rangle = \int da\, e^{i(p_1 - p_2)a}\, \hat{f}(a) . \tag{2.2.1}$$

Next we consider the Heisenberg equation of motion for the quantum field $\phi(x, t)$

$$\left(\partial_t^2 - \partial_x^2\right) \phi(x, t) = m^2 \phi(x, t) - \lambda \phi^3(x, t) , \tag{2.2.2}$$

we take the matrix elements of both sides[3]

$$[-(p_1 - p_2)_\mu (p_1 - p_2)^\mu]\, e^{-i(p_1 - p_2)_\mu x^\mu} \langle p_2 | \phi(0) | p_1 \rangle =$$

$$= e^{-i(p_1 - p_2)_\mu x^\mu} \left\{ m^2 \langle p_2 | \phi(0) | p_1 \rangle - \lambda \langle p_2 | \phi^3(0) | p_1 \rangle \right\} , \tag{2.2.3}$$

---

[3]Lorentz invariance imposes the relation $\langle p_2 | \phi(x, t) | p_1 \rangle = e^{-i(p_1 - p_2)_\mu x^\mu} \langle p_2 | \phi(0) | p_1 \rangle$

and we equate them to leading order $1/\sqrt{\lambda}$. Assumption 3 implies that the kink momentum is very small compared to its mass, therefore in the left hand side of (2.2.3) we can neglect the energy difference

$$(E_1 - E_2)^2 = \left(\frac{p_1^2 - p_2^2}{2M} + ... \right)^2 = O(\lambda^2) .$$

Hence the left hand side gives, at leading order,

$$\int da \; e^{i(p_1 - p_2)a} \left(-\frac{d^2}{da^2} \hat{f}(a) \right) .$$

In the last term of the right hand side of (2.2.3), the cubic power of ϕ can be expanded over a complete set of states in the kink sector; in virtue of assumption 4, the leading term is obtained when the intermediate states are one–kink states:

$$-\lambda \sum_{p,q} \langle p_2 \,|\, \phi(0) \,|\, p \,\rangle \langle p \,|\, \phi(0) \,|\, q \,\rangle \langle q \,|\, \phi(0) \,|\, p_1 \,\rangle = -\lambda \int da \; e^{i(p_1 - p_2)a} \, [\, \hat{f}(a)\,]^3 . \qquad (2.2.4)$$

Hence, at leading order in λ, the function $\hat{f}(a)$ obeys the same differential equation satisfied by the kink solution, i.e.

$$\frac{d^2}{da^2} \hat{f}(a) = \lambda[\, \hat{f}(a)\,]^3 - m^2 \hat{f}(a) . \qquad (2.2.5)$$

This means that we can take $\hat{f}(a) = \phi_{cl}(a)$, adjusting its boundary conditions by an appropriate choice for the value of the constant A in eq. (2.1.4).

Therefore, we finally obtain

$$\langle p_2 \,|\, \phi(0) \,|\, p_1 \,\rangle = \int da \; e^{i(p_1 - p_2)a} \; \phi_{cl}(a) \; + \; \text{higher order terms} . \qquad (2.2.6)$$

Along the same lines, it is easy to prove that the form factor of an operator expressible as a function of ϕ is given by the Fourier transform of the same function of ϕ_{cl}. For instance, the form factor of the energy density operator ε can be computed performing the Fourier transform of $\varepsilon_{cl}(x) = \frac{1}{2} \left(\frac{d\phi_{cl}}{dx} \right)^2 + V(\phi_{cl})$.

Eq. (2.2.6) is the crucial achievement that opens the way to our study of non–integrable theories. However, it is worth to mention a further result obtained in [24], which confirms the interpretation of the stability frequencies ω_1 and ω_q described in the previous Section. Let's consider the form factor of ϕ between two states containing one kink and one kink plus one meson, respectively, and define a function $\hat{f}_k(a)$ as

$$\langle p_2, k \,|\, \phi(0) \,|\, p_1 \,\rangle = \int da \; e^{i(p_1 - p_2 - k)a} \; \hat{f}_k(a) . \qquad (2.2.7)$$

Calling ω_k the energy of the meson with momentum k, and equating again at leading order the two sides of the Heisenberg equation of motion evaluated between the above asymptotic states, we obtain the equation

$$\left[-\frac{d^2}{da^2} + V''(\phi_{cl}) \right] \hat{f}_k(a) = \omega_k^2 \, \hat{f}_k(a) , \qquad (2.2.8)$$

and consequently we can choose $\hat{f}_k(a) = \eta_k(a)/\sqrt{2\omega_k}$, where $\eta_k(a)$ is one of the eigenfunctions of (2.1.9) and the constant $1/\sqrt{2\omega_k}$ is chosen to realize a familiar boson normalization. This completely justifies the identification of the eigenvalues of (2.1.9) with the mesons energies.

Similarly, if we define the form factor of ϕ between a kink in the ground state and one in the internal excited state as

$$\langle p_2^* | \phi(0) | p_1 \rangle = \int da\, e^{i(p_1 - p_2)a}\, \hat{f}^*(a)\,, \qquad (2.2.9)$$

and we call ω_1 the energy of the internal excitation, we obtain

$$\left[-\frac{d^2}{da^2} + V''(\phi_{cl}) \right] \hat{f}^*(a) = \omega_1^2\, \hat{f}^*(a)\,, \qquad (2.2.10)$$

which leads to $\hat{f}^*(a) = \eta_1(a)/\sqrt{2\omega_1}$.

2.2.2 Relativistic formulation of Goldstone and Jackiw's result

The remarkable Goldstone and Jackiw's result has, unfortunately, two serious drawbacks: expressing the form factor as a function of the difference of momenta, Lorentz covariance is lost and moreover, the antisymmetry under the interchange of momenta makes problematic any attempt to go in the crossed channel and obtain the matrix element between the vacuum and a kink–antikink state.

In order to overcome these problems, in [1] we have refined the method proposed in [24]. This was done by using, instead of the space–momenta of the kinks, their rapidity variable θ, defined in (1.2.3). The approximation of large kink mass used by Goldstone and Jackiw can be realized considering the rapidity as very small. For example, in the ϕ^4 theory (2.1.5), where the kink mass M is of order $1/\lambda$, we work under the hypothesis that θ is of order λ. In this way we get consistently

$$E \equiv M \cosh\theta \simeq M\,, \qquad p \equiv M \sinh\theta \simeq M\,\theta \ll M\,. \qquad (2.2.11)$$

It is easy to see that the proof of (2.2.6) outlined in Sect. 2.2.1 still holds, if we define the form factor between kink states as the Fourier transform with respect to the rapidity difference:

$$\langle p_1 | \phi(0) | p_2 \rangle \equiv f(\theta) \equiv M \int da\, e^{i\,M\theta a}\phi_{cl}(a)\,, \qquad (2.2.12)$$

with the inverse Fourier transform defined as

$$\phi_{cl}(a) \equiv \int \frac{d\theta}{2\pi}\, e^{-i\,M\theta a} f(\theta)\,. \qquad (2.2.13)$$

In fact, the analysis of the r.h.s. of (2.2.3) remains unchanged, while the one of the l.h.s. is even improved, since we can exploit the approximation (2.2.11) directly on the covariant expression

$$-(p_1 - p_2)_\mu (p_1 - p_2)^\mu = -2M^2\,(1 - \cosh\theta) \simeq M^2\theta^2\,.$$

Our formalism only displays a small inessential difference with respect to [24], in the orders in λ of the various form factors (see assumption 4 in Sect. 2.2.1). In fact, the M factor in front of (2.2.12), which is a natural consequence of considering the rapidity as the basic variable, increases by $1/\lambda$ the order of all form factors, without however altering any conclusion.

With the above considerations, it is now possible to express the crossed channel form factor through the variable transformation $\theta \to i\pi - \theta$. We then have

$$F_2(\theta) \equiv \langle 0 | \phi(0) | p_1, \bar{p}_2 \rangle = f(i\pi - \theta)\,. \qquad (2.2.14)$$
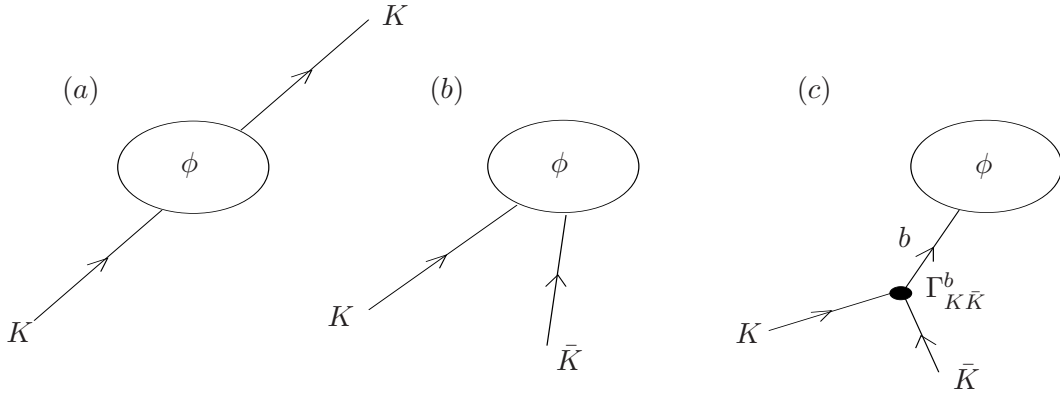
Figure 2.3: Pictorial representation of (a) the form factor $f(\theta)$, (b) the crossed channel form factor $F_2(\theta)$, (c) the form factor $F_2(\theta^*)$ at the dynamical pole θ^*.

The analysis of this quantity allows us, in particular, to get information about the spectrum of the theory. As we have shown in (1.2.16), in fact, its dynamical poles located at $\theta^* = i(\pi - u)$, with $0 < u < \pi$, correspond to kink–antikink bound states with masses given by (1.2.9), which in this case specializes to

$$m_{(b)} = 2M \sin \frac{u}{2} \ . \tag{2.2.15}$$

(see Fig. 2.3). It is worth noticing that this procedure for extracting the semiclassical bound states masses is remarkably simpler than the standard DHN method of quantizing the corresponding classical backgrounds, because in general these solutions depend also on time and have a much more complicated structure than the kink ones. Moreover, in non–integrable theories these backgrounds could even not exist as exact solutions of the field equations: this happens for example in the ϕ^4 theory, where the DHN quantization has been performed on some approximate backgrounds [23].

Once the matrix elements (2.2.14) are known, one can estimate the leading behaviour in λ of the spectral function $\rho^{(\phi)}$ in a regime of the momenta dictated by our assumption of small kink rapidity. The delta functions in (1.2.11) make meaningful the use of our form factors, derived in the small θ approximation, only if we consider a regime in which $p^0 \simeq M$ and $p^1 \ll M$ and, from now on, we will always understand this restriction. The leading $O(1/\lambda)$ contribution to the spectral function, denoted in the following by $\hat{\rho}^{(\phi)}(p^2)$, is given by the trivial vacuum term plus the kink-antikink contribution:

$$\hat{\rho}^{(\phi)}(p^2) = 2\pi\delta(p^0)\delta(p^1)|\langle 0|\phi(0)|0\rangle|^2 + \frac{\pi}{4} \frac{\delta\left(\frac{p^0}{M} - 2\right)}{M^2} \int \frac{d\theta_1}{2\pi} \left|F_2\left(2\theta_1 + i\pi - \frac{p^1}{M}\right)\right|^2 \ , \tag{2.2.16}$$

where the range of integration of the above quantity is of order p^1/M (note that, being $p^1/M \ll 1$, the integral can be roughly estimated by evaluating $|F_2|^2$ at $\theta_1 = 0$: this is what we will do in the following).

2.3   The Sine–Gordon model in infinite volume

The Sine–Gordon model, defined by the potential

$$V(\phi) = \frac{m^2}{\beta^2} \left(1 - \cos \beta\phi\right) \ , \tag{2.3.1}$$

gives us the chance of testing the validity of the semiclassical approximation. In fact, the integrability of this model has led to the exact computation of its spectrum and form factors [16, 18, 19, 20], which can be evaluated in the small-β limit to verify the semiclassical results.

This model has been object of intensive research efforts, since it plays a relevant role in several physical contexts, either as a classical non–linear system or as a quantum field theory. For instance, its non–linear equation of motion appears in the study of propagation of dislocations in crystals, self–induced transparency effects in non–linear optics and spin wave propagation in liquid ^{3}He (see [31] for a review). As a quantum field theory, it plays a crucial role in the description of quantum spin chains, in virtue of the bosonization procedure, which permits to express fermionic fields as exponentials of bosonic ones. In particular, an exact correspondence has been established in [33] between the sine–Gordon and the Thirring model, which describes massive fermions interacting through a four–fermion coupling.

The exact solution of the model shows that the spectrum of fundamental excitations is constituted by a soliton, an antisoliton and a given number of neutral particles, called "breathers" and obtained as soliton–antisoliton bound states [16]. The number of breathers depend on β as the integer part of $\frac{8\pi}{\gamma}$, where

$$\gamma = \frac{\beta^2}{1 - \beta^2/8\pi} \tag{2.3.2}$$

is the renormalized coupling constant. In particular, $\beta^2 = 4\pi$ represent a free point, above which no bound states exist and the theory is in a repulsive regime, while the regime of small β, that we will explore semiclassically, is deeply attractive.

The potential (2.3.1) displays infinite degenerate minima, and the soliton solutions of the equations of motion are given by configurations which interpolate between two neighbouring vacua. Focusing on the two minima at $\phi = 0$ and $\phi = \frac{2\pi}{\beta}$, these are connected by the classical soliton

$$\phi_{cl}(x) = \frac{4}{\beta} \arctan\left(e^{m(x-x_0)}\right) , \tag{2.3.3}$$

which is solution of eq. (2.1.4) with $A = 0$ and has classical mass $M_{cl} = 8\frac{m}{\beta^2}$. The semiclassical quantization of this background has been performed in [23]: eq. (2.1.9) can be cast in the hypergeometric form by using the variable $z = \frac{1}{2}(1 + \tanh mx)$, and its solution is expressed as

$$\eta(x) = \frac{1}{\beta} z^{\frac{1}{2}\sqrt{1-\frac{\omega^2}{m^2}}} (1-z)^{-\frac{1}{2}\sqrt{1-\frac{\omega^2}{m^2}}} F\left(2, -1, 1 + \sqrt{1 - \frac{\omega^2}{m^2}}, z\right) .$$

The corresponding spectrum is given by the discrete zero mode

$$\omega_0^2 = 0 , \qquad \text{with} \qquad \eta_0(x) = \frac{1}{2\cosh mx} ,$$

and by the continuous part

$$\omega_q^2 = m^2(1 + q^2) , \qquad \text{with} \qquad \eta_q(x) = e^{imqx} \frac{iq - \tanh mx}{1 + iq} .$$

For this integrable theory we can easily verify the interpretation of the continuous spectrum as representing the scattering states of the kink with neutral particles. In fact, the semiclassical phase shift $\delta(q)$, defined as

$$\eta_q(x) \xrightarrow[x\to\pm\infty]{} e^{i\left[qmx \pm \frac{1}{2}\delta(q)\right]} , \qquad \text{with} \qquad \delta(q) = 2\arctan\frac{1}{q} = -i\log\frac{q+i}{q-i} , \tag{2.3.4}$$

correctly reproduces the small-β limit of the exact one

$$\delta_{\text{exact}}(\theta) = -i \log S_{kb}(\theta) ,$$

where the kink–breather scattering amplitude [16]

$$S_{kb} = \frac{\sinh\theta + i\cos\frac{\gamma}{16}}{\sinh\theta - i\cos\frac{\gamma}{16}}$$

is evaluated in the kink rest frame, in which the breather momentum can be expressed as $mq = m\sinh\theta$.

Similarly to the broken ϕ^4 case discussed in Sect. 2.1, the semiclassical correction to the kink mass is given by

$$M - M_{cl} = \frac{1}{2}\sum_n \left[m\sqrt{1+q_n^2} - \sqrt{k_n^2 + m^2} \right] - \frac{\delta\mu^2}{\beta^2} \int_{-\infty}^{\infty} dx\, [1 - \cos\beta\phi_{cl}(x)] , \qquad (2.3.5)$$

with

$$\delta\mu^2 = -\frac{m^2\beta^2}{8\pi} \int_{-\infty}^{\infty} \frac{dk}{\sqrt{k^2+m^2}} . \qquad (2.3.6)$$

Determining the discrete values q_n and k_n in a large finite volume of size R with periodic boundary conditions and sending $R \to \infty$, one finally obtains the semiclassical quantum correction to the mass of the kink

$$M = \frac{8m}{\beta^2} - \frac{m}{\pi} . \qquad (2.3.7)$$

As we have already mentioned, it is known that the coupling constant renormalises as $\beta^2 \to \gamma$, and the exact quantum mass of the soliton is given by $M = \frac{8m}{\gamma}$, which coincides with the above expression (2.3.7). The equality of the semiclassical and the exact results for the masses is a remarkable property of the SG model.

In [1] we have derived and discussed the semiclassical form factor (2.2.12) relative to the kink background (2.3.3). Since the first quantum corrections to $M_{cl} = 8\frac{m}{\beta^2}$ are of higher order in β^2, we consistently approximate the kink mass M with this value and we assume that the (anti)soliton rapidity is of order β^2. The semi–classical form factor (2.2.12) is explicitly given by

$$f(\theta) = \frac{2\pi i}{\beta} \frac{1}{\theta \cosh\left[\frac{4\pi}{\beta^2}\theta\right]} + \frac{2\pi^2}{\beta^3}\delta\left(\frac{\theta}{\beta^2}\right) . \qquad (2.3.8)$$

In order to compare the corresponding $F_2(\theta)$ given by (2.2.14) with the semiclassical limit of the exact one, the only thing to take into account is that, in the definition of the exact form factor of the fundamental field $\phi(x)$, the asymptotic two–particle state is actually given by the antisymmetric combination of soliton and antisoliton. Since at our level the form factor between antisoliton states is simply

$$< \bar{p}_1 | \phi(0) | \bar{p}_2 > = \frac{4M}{\beta} \int_{-\infty}^{\infty} da\, e^{i(M\theta)\,a} \arctan\left(e^{-ma}\right) = f(-\theta) ,$$

we finally obtain

$$F_2(\theta) = \frac{4\pi i}{\beta} \frac{1}{(i\pi - \theta)\cosh\left[\frac{4\pi}{\beta^2}(i\pi - \theta)\right]} . \qquad (2.3.9)$$

In the regime $i\pi - \theta \simeq O(\beta^2)$, this function indeed agrees with the exact result [18]

$$F_2^{exact}(\theta) = \frac{2\pi i}{\beta} \frac{1}{\sinh \frac{i\pi-\theta}{2}} \frac{\cosh \frac{i\pi-\theta}{2}}{\cosh \left[\frac{1}{2\xi}(i\pi - \theta)\right]} G(i\pi - \theta) , \qquad (2.3.10)$$

where $\xi = \gamma/8\pi$ and

$$G(\theta) = \exp \left[\int_0^\infty \frac{dt}{t} \frac{\sinh \frac{t}{2}(1-\xi)}{\sinh \frac{t}{2}\xi} \frac{\sin^2 \frac{\theta t}{2\pi}}{\cosh \frac{t}{2}} \frac{}{\sinh t} \right] . \qquad (2.3.11)$$

Furthermore, we can also check that the dynamical poles of (2.3.9), located at

$$\theta_n = i\pi \left[1 - \frac{\beta^2}{8\pi}(2n + 1)\right] , \qquad -\frac{1}{2} < n < -\frac{1}{2} + \frac{4\pi}{\beta^2} ,$$

consistently reproduce the odd part of the well-known semiclassical breathers spectrum [23]

$$m_b^{(2n+1)} = 2M \sin \left[\frac{\beta^2}{16}(2n + 1)\right] = (2n + 1) m \left[1 - \frac{(2n + 1)^2}{3 \times 8^3}\beta^4 + ...\right] \qquad (2.3.12)$$

Since in the vacuum sector $\langle 0|\phi|0\rangle = 0$, in this model the $1/\beta^2$ leading contribution to the spectral function takes the form:

$$\hat{\rho}(p^2) = 4\pi^3 \delta \left(\frac{p^0}{M} - 2\right) \frac{1}{\beta^2(p^1)^2 \cosh^2 \left[\frac{\pi}{2}\frac{p^1}{m}\right]} . \qquad (2.3.13)$$

Furthermore, in [3] we have presented a more quantitative comparison which permits to conclude that formula (2.2.12), though proven under the semiclassical assumption of small coupling and small rapidities, remarkably extends its validity to finite values of the coupling and to a large range of the rapidities. Consider, for instance, the form factor of the energy operator (up to a normalization N) $g(\theta) = N\langle \theta_2|\epsilon(0)|\theta_1\rangle$, whose semiclassical and exact expressions are given, respectively, by

$$g_{\text{semicl.}}(\theta) = \frac{\theta}{2} \frac{1}{\sinh \left[\frac{4\pi}{\beta^2}\theta\right]} \qquad (2.3.14)$$

$$g_{\text{exact}}(\theta) = \sinh \frac{\theta}{2} \frac{1}{\sinh \frac{\theta}{2\xi}} G(\theta) \qquad (2.3.15)$$

with $G(\theta)$ defined in (2.3.11). Fig. 2.4 shows how, for small values of the coupling, the agreement between the two functions is very precise for the whole range of the rapidity. Furthermore, the discrepancy between exact and semiclassical formulas at larger values of β can be simply cured, in our example, by substituting the bare coupling β^2 with its renormalized expression γ into the semiclassical result (2.3.14), as shown in Fig. 2.5. Hence we can conclude that the monodromy factor (2.3.11), which is the relevant quantity missing in our approximation, does not play a significant role in the quantitative evaluation of the form factor even for certain finite values of the coupling[4].

---

[4]It is easy to understand the reason of this conclusion in the above example: at small values of θ we have $G(\theta) \simeq 1$, whereas for $\theta \to \infty$, when $G(\theta)$ may contribute, the whole form factor goes anyway to zero. Similar conclusion can be reached for all other form factors which vanish at $\theta \to \infty$.

Figure 2.4: Comparison between the exact function F given by (2.3.15) (continuous line) and its semiclassical approximation (2.3.14) (dotted line), at $\beta = 0.1$ and $\beta = 0.5$.

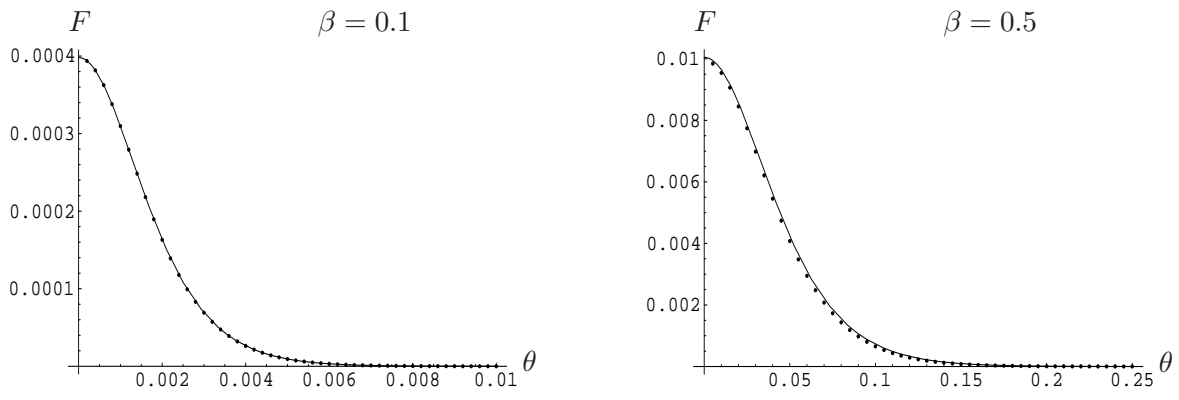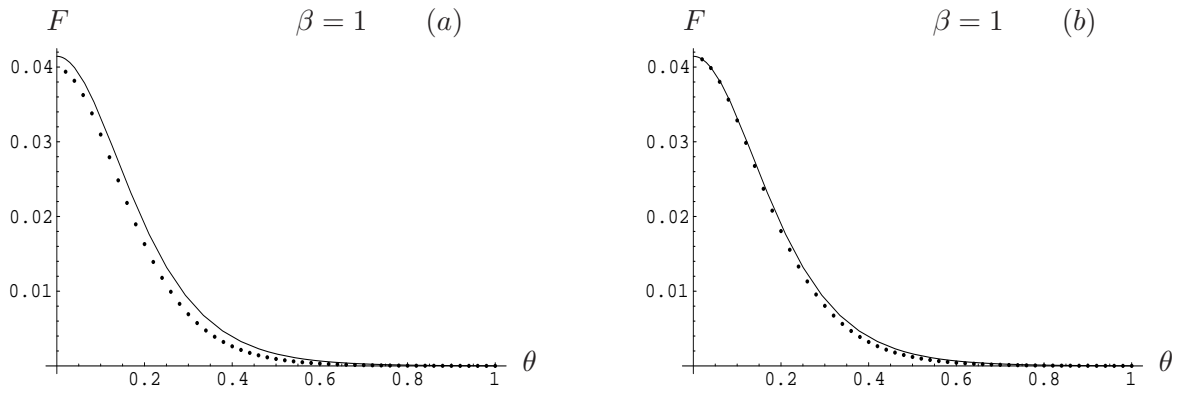Figure 2.5: Comparison, at $\beta = 1$, between (a) the exact function g given by (2.3.15) (continuous line) and its semiclassical approximation (2.3.14) (dotted line), (b) the exact function g given by (2.3.15) (continuous line) and its semiclassical approximation (2.3.14) with the substitution $\beta^2 \to \gamma$ (dotted line).

Chapter 3

Non-integrable quantum field theories

As a natural development of the studies on integrable quantum field theories, there has been recently an increasing interest in studying the properties of non–integrable quantum field theories in $(1 + 1)$ dimensions, both for theoretical reasons and their application to several condensed–matter or statistical systems. However, contrary to the integrable models, many features of these quantum field theories are still poorly understood: in most of the cases, in fact, their analysis is only qualitative and even some of their basic data, such as the mass spectrum, are often not easily available. Although one could always rely on numerical methods to shed some light on their properties, it is obviously important to develop and apply some theoretical tools to control them analytically. In this respect, there has been recently some progress, thanks to two different and complementary approaches.

The first approach, called the Form Factor Perturbation Theory (FFPT) [34], is best suited to deal with those non–integrable theories close to the integrable ones. The second approach, given by the semiclassical method introduced in Chapter 2, is on the other hand best suited to deal with those quantum field theories having kink excitations of large mass in their semiclassical limit. Although this method is restricted to work in a semiclassical regime, it permits however to analyse non–integrable theories in the whole coupling–constants space, even far from the integrable points.

In this Chapter, after illustrating the FFPT technique (Sect. 3.1), we describe the original results obtained with the semiclassical method for the ϕ^4 field theory in the broken symmetry phase (Sect. 3.2) and for the Double Sine–Gordon model (Sect. 3.3). The Appendices are devoted to some technical results obtained in the study of the Double Sine–Gordon theory.

3.1 Form Factor Perturbation Theory

The Form Factor Perturbation Theory technique (FFPT), introduced in [34], permits to obtain quantitative predictions on the mass spectrum, scattering amplitudes and other physical quantities in non–integrable theories which can be seen as a perturbation of integrable ones. As any other perturbation scheme, it works finely as far as the non–integrable theory is an adiabatic deformation of the original integrable model, i.e. when the two theories are isospectral. This happens when the field which breaks the integrability is *local* with respect to the operator which creates the particles. If, on the contrary, the field which moves the theory away from integra-

bility is *non–local* with respect to the particles, the resulting non–integrable model generally displays confinement phenomena and, in this case, some caution has to be taken in interpreting these perturbative results.

The method can be applied when the action $\mathcal{A}$ of the theory in exam is represented by a deformation of an integrable one $\mathcal{A}_0$ through a given operator Ψ:

$$\mathcal{A} = \mathcal{A}_0 + g \int d^2x \, \Psi(x) \,. \tag{3.1.1}$$

One of the first consequences of moving away from integrability is a change in the spectrum of the theory: the first order corrections to the mass of the particle a belonging to the spectrum of the unperturbed theory is in fact given by

$$\delta m_a^2 = 2g F_{a\bar{a}}^{\Psi}(i\pi) + O(g^2) \,, \tag{3.1.2}$$

where the particle–antiparticle form factor of the operator $\Psi(x)$, defined by the matrix element

$$F_{a\bar{a}}^{\Psi}(\theta_1 - \theta_2) = \langle 0 \mid \Psi(0) \mid a(\theta_1)\bar{a}(\theta_2)\rangle \,,$$

is introduced as function of the difference of the rapidity variables, defined in (1.2.3). The mass correction (3.1.2) may be finite or divergent, depending on the locality properties of the operator $\Psi(x)$ with respect to the particle a. The situation was clarified in [36] and it is worth recalling the main conclusion of that analysis.

As we have seen in (1.2.14), (1.2.15), if the operator which interpolate particle a is non–local with respect to the perturbing operator Ψ, the form factor $F_{a\bar{a}}^{\Psi}(\theta)$ displays an annihilation pole at $\theta = i\pi$, which is exactly the value at which the form factor is evaluated in (3.1.2). Therefore, in this case the mass correction received by particle a under the perturbation Ψ is formally infinite, unless the residue in (1.2.15) vanishes.

Let's consider as an example the case in which the unperturbed theory is the sine–Gordon model (2.3.1) with frequency β, and the perturbing operator is the exponential $\Psi_\alpha = e^{i\alpha\varphi}$. This vertex operator is semi–local with respect to the soliton particle s, with the index $\gamma_{\alpha,s}$ entering (1.2.14) given by $\gamma_{\alpha,s} = \alpha/\beta$, whereas it is local with respect to the breather particles b (i.e. $\gamma_{\alpha,b} = 0$). This implies that formula (3.1.2) can be safely applied to compute the first order correction to the mass of the breathers, whereas a divergence may appear in an analogous computation of the mass correction of the solitons. This divergence has to be seen as the mathematical signal that the solitons of the original integrable model no longer survive as asymptotic particles of the perturbed theory, i.e. they are confined.

3.2 Broken ϕ^4 theory

In this Section, we will describe the original results obtained in [1] and [2] about the spectrum of the ϕ^4 field theory in the $\mathbb{Z}_2$ broken symmetry phase. This non–integrable theory, defined by the potential (2.1.5)

$$V(\phi) = \frac{\lambda}{4}\phi^4 - \frac{m^2}{2}\phi^2 + \frac{m^4}{4\lambda} \,,$$

is invariably referred to as a paradigm for a wealth of physical phenomena. Just to mention a relevant example, in the Landau–Ginzburg language discussed in Sect. 1.3, it describes the universality class of the Ising model at low temperature. In spite of this deep interest, however, its non–perturbative features are still poorly understood.

3.2.1 Semiclassical spectrum

The main properties of the potential (2.1.5) and its kink background (2.1.6) have been already discussed in Sect. 2.1, where the semiclassical quantization of the kink has been described. Here we directly move to the computation of the kink–antikink form factors, in order to extract from their analytical structure information about the complete spectrum of the theory.

With our formulation in terms of the rapidity, we can write an unambiguous[1] Lorentz covariant expression for the form factor (2.2.12)

$$\langle p_2|\,\phi(0)|\,p_1\,\rangle \;=\; M\frac{m}{\sqrt{\lambda}}\int_{-\infty}^{\infty} da\,e^{iM\theta a}\,\tanh\left(\frac{ma}{\sqrt{2}}\right) =$$
$$= \frac{4}{3}i\pi\left(\frac{m}{\sqrt{\lambda}}\right)^3 \frac{1}{\sinh\left(\frac{2}{3}\pi\frac{m^2}{\lambda}\theta\right)}\;, \tag{3.2.1}$$

where the kink mass is approximated at leading order by the classical energy $M = \frac{2\sqrt{2}}{3}\frac{m^3}{\lambda}$.

It is of great interest to analyse in this case the dynamical poles of $F_2(\theta)$ for extracting information about the spectrum. They are located at

$$\theta_n = i\pi\left[1 - \frac{3}{2\pi}\frac{\lambda}{m^2}\,n\right]\;, \qquad 0 < n < \frac{2\pi}{3}\frac{m^2}{\lambda}\;, \tag{3.2.2}$$

and the corresponding bound states masses are given by

$$m_b^{(n)} = 2M\sin\left[\frac{3}{4}\frac{\lambda}{m^2}\,n\right] = n\,\sqrt{2}\,m\left[1 - \frac{3}{32}\frac{\lambda^2}{m^4}\,n^2 + ...\right]\;. \tag{3.2.3}$$

Note that the leading term is consistently given by multiples of $\sqrt{2}m$, which is the known mass of the elementary boson of this theory[2]. Contrary to the Sine-Gordon model, we now have all integer multiples of this mass and not only the odd ones: this is because we are in the broken phase of the theory, where the invariance under $\phi \to -\phi$ is lost. Furthermore, this spectrum exactly coincides with the one derived in [23] by building approximate classical solutions to represent the "breathers".

Another important information can be extracted from the residue of $F_2(\theta)$ on the pole corresponding to the lightest bound state $b^{(1)}$. This quantity, indeed, has to be proportional to the one-particle form factor $\langle 0|\,\phi|\,b^{(1)}\,\rangle$ through the semiclassical 3-particle on-shell coupling of kink, antikink and elementary boson $\Gamma_{k\bar{k}b}$, as shown in (1.2.16). Since in our normalization the one-particle form factor takes the constant value $1/\sqrt{2}$, at leading order in the coupling we get

$$\Gamma_{k\bar{k}b} = 2\sqrt{2}\,\frac{m}{\sqrt{\lambda}}\;, \tag{3.2.4}$$

a quantity so far unknown in the non–integrable ϕ^4 theory.

Finally, the $1/\lambda$ leading contribution of the spectral function is given in this case by

$$\hat{\rho}(p^2) = \frac{2\pi}{\lambda}\,\delta\left(p^0/m\right)\delta\left(p^1/m\right) + \frac{\pi^3}{2\lambda}\,\delta\left(\frac{p^0}{M}-2\right)\frac{1}{\sinh^2\left[\frac{\pi}{\sqrt{2}}\frac{p^1}{m}\right]}\;. \tag{3.2.5}$$

---

[1]This has to be contrasted with the tentative covariant extrapolation discussed in [24].

[2]The elementary bosons represent the excitations over the vacua, i.e. the constant backgrounds $\phi_\pm = \pm\frac{m}{\sqrt{\lambda}}$, therefore their square mass is given by $V''(\phi_\pm) = 2\,m^2$.

3.2.2 Resonances

The appearance of resonances in the classical kink–antikink scattering has been studied for this theory with numerical techniques in [35]. In this work, the key ingredient for the presence of resonances was identified in the presence of the so–called "shape mode", which is the discrete eigenvalue ω_1 of the small oscillations around the kink background, given in (2.1.13), corresponding to the internal excitation of the kink. We have shown in [2] how this mechanism can be analytically explained in our formalism. In fact, Goldstone and Jackiw's result on the form factor of the field ϕ between asymptotic states containing a simple and an excited kink, described by formulas (2.2.9) and (2.2.10), can be also refined in terms of the rapidity variable. In our case, where the fluctuation η_1 is given in (2.1.13), the covariant form factor, analytically continued in the crossed channel, is expressed as

$$\langle 0 | \phi(0) | \bar{p}_2 \, p_1^* \rangle \ = \ -i \, \frac{M \, \pi}{6^{1/4} \, m^{5/2}} \, \frac{M \, (i\pi - \theta)}{\cosh \left[\frac{\pi}{\sqrt{2} \, m} M \, (i\pi - \theta) \right]} \ . \tag{3.2.6}$$

The dynamical poles of this object correspond to bound states with masses

$$\left(m_{b^*}^{(n)} \right)^2 \ = \ 4M(M + \omega_1) \sin^2 \left[\frac{3}{8} \frac{\lambda}{m^2} (2n + 1) \right] + \omega_1^2 \ . \tag{3.2.7}$$

The states with

$$\frac{8}{3} \frac{m^2}{\lambda} \arcsin \sqrt{\frac{4M^2 - \omega_1^2}{4M(M + \omega_1)}} < 2n + 1 < \frac{4}{3} \frac{m^2}{\lambda} \pi \tag{3.2.8}$$

have masses in the range

$$2M < m_{b^*}^{(n)} < 2M + \omega_1 \ , \tag{3.2.9}$$

and, therefore, they can be seen as resonances in the kink-antikink scattering.

Since the numerical analysis done in [35] is independent of the coupling constant[3], a quantitative comparison with our semiclassical result is rather difficult, due to the dependence on λ of (3.2.8). However, the presence of many resonance states seen at classical level is qualitatively confirmed to persist also in the quantum field theory at small λ, i.e. in its semiclassical regime, according to (3.2.8).

3.3 Double Sine–Gordon model

An interesting non–integrable model where both FFPT and Semiclassical Method can be used is the so–called Double Sine–Gordon Model (DSG). It is defined by the potential

$$V(\varphi) \ = \ -\frac{\mu}{\beta^2} \cos \beta \, \varphi - \frac{\lambda}{\beta^2} \cos \left(\frac{\beta}{2} \varphi + \delta \right) + C \ , \tag{3.3.1}$$

where C is a constant that has be chosen such that to have a vanishing potential energy of the vacuum state. The classical dynamics of this model has been extensively studied in the past by means of both analytical and numerical techniques (see [37] for a complete list of the results), while its thermodynamics has been studied in [38] by using the transfer integral method [39], and with the path integral technique (see for instance [40]).

---

[3]Classically, in fact, one can always rescale the field and eliminate the coupling constant λ.

With λ or μ equal to zero, the DSG reduces to the ordinary integrable Sine–Gordon (SG) model with frequency β or $\beta/2$ respectively. Hence the DSG model with a small value of one of the couplings can be regarded as a deformation of the corresponding SG model and studied, therefore, by means of the FFPT [36]. On the other hand, for $\beta \to 0$, irrespectively of the value of the coupling constants λ and μ, the DSG model reduces to its semiclassical limit. Despite the non–integrable nature of the DSG model, its classical kink solutions are – remarkably enough – explicitly known [37, 38] and therefore the Semiclassical Method can be successfully applied to recover the (semi–classical) spectrum of the theory. As we will see in the following, the two approaches turn out to be complementary in certain regions of the coupling constants, i.e. both are needed in order to get the whole mass spectrum of the theory, whereas in other regions they provide the same picture about the spectrum of the excitations.

Apart from the theoretical interest in testing the efficiency of the two methods on this specific model where both are applicable, the study of the DSG is particularly important since this model plays a relevant role in several physical contexts, either as a classical non–linear system or as a quantum field theory. At the classical level, its non–linear equation of motion can be used in fact to study ultra–short optical pulses in resonant degenerate medium or texture dynamics in He^3 (see, for instance, [41] and references therein). As a quantum field theory, depending on the values of the parameters $\lambda, \mu, \beta, \delta$ in its Lagrangian, it displays a variety of physical effects, such as the decay of a false vacuum or the occurrence of a phase transition, the confinement of the kinks or the presence of resonances due to unstable bound states of excited kink–antikink states. Moreover, it finds interesting applications in the study of several systems, such as the massive Schwinger field theory or the Ashkin–Teller model [36], as well as in the analysis of the O(3) non–linear sigma model with θ term [42], i.e. the quantum field theory relevant for understanding the dynamics of quantum spin chains [43, 44]. The DSG model also matters in the investigation of other interesting condensed matter phenomena, such as the soliton confinement of spin–Peierls antiferromagnets [45], the dynamics of the spin chains in a staggered external field or the electron interaction in a staggered potential [46].

Motivated by the above combined theoretical and physical interests, we have performed in [2] a thorough study of the spectrum of the DSG model. In some regions of the coupling constants, the obtained original semiclassical results have revealed to be necessary to complete the spectrum analysis, while in other regions they have been compared with the analogous ones produced by FFPT. Here we present the main result of the semiclassical analysis of the spectrum of the DSG model and its comparison with the results coming from FFPT (Sect. 3.3.1). Furthermore, the phenomenon of false vacuum decay will be also discussed (Sect. 3.3.2). Finally, this Chapter's appendices are devoted to some technical results obtained in this study. In particular, Appendix 3.A presents the computation of the kink mass corrections by using the FFPT, Appendix 3.B lists the relevant expressions of the semiclassical form factors in DSG model, Appendix 3.C discusses the analysis of neutral states in comparison with the Sine–Gordon model, and Appendix 3.D describes the basic results in a closely related model, i.e. the Double Sinh–Gordon model.

3.3.1 Semiclassical spectrum

We will study the theory defined by (3.3.1) in a regime of small β, where the semiclassical results are expected to give a valuable approximation of the spectrum[4]. At the quantum level, the

---

[4]By applying the stability conditions found in [36] to this model, they reduce to the condition $\beta^2 < 8\pi$. Hence, for these values of β and, in particular in the semiclassical limit $\beta \to 0$, the potential (3.3.1) is stable under

different Renormalization Group trajectories originating from the gaussian fixed point described by the kinetic term $\frac{1}{2}(\partial_\mu\varphi)^2$ of the lagrangian are labelled by the dimensionless scaling variable $\eta = \lambda\mu^{-(8\pi-\beta^2/4)/(8\pi-\beta^2)}$ which simply reduces to the ratio $\eta = \frac{\lambda}{\mu}$ in the semiclassical limit. When λ or μ are equal to zero, the DSG model coincides with an ordinary Sine-Gordon model with coupling β or $\beta/2$, and mass scale $\sqrt{\mu}$ or $\sqrt{\lambda/4}$, respectively.

Since for general values of the couplings the potential (3.3.1) presents a $\frac{4\pi}{\beta}$-periodicity, it was noticed in [47] that one has an adiabatic perturbation of an integrable model only if the $\lambda = 0$ theory is regarded as a two–folded Sine-Gordon model. This theory is a modification of the standard Sine-Gordon model, where the period of the field ϕ is defined to be $\frac{4\pi}{\beta}$, instead of $\frac{2\pi}{\beta}$ [48]. As a consequence of this new periodicity assignment, such a theory has two different degenerate vacua $|k\rangle$, with $k = 0,1$ and $|k + 2\rangle \equiv |k\rangle$, which are defined by $\langle k|\phi|k\rangle = \frac{2\pi}{\beta}k$. Hence it has two different kinks, related to the classical backgrounds by the formula

$$K^{cl}_{k,k+1}(x) = \frac{2k\pi}{\beta} + \frac{4}{\beta}\arctan e^{mx} \qquad k = 0,1 ,\qquad (3.3.2)$$

and two corresponding antikinks, related to the classical solutions by the expression

$$\begin{aligned}
K^{cl}_{k+1,k}(x) &= \frac{2k\pi}{\beta} + \frac{4}{\beta}\arctan e^{-mx} \\
&= \frac{2(k+1)\pi}{\beta} - \frac{4}{\beta}\arctan e^{mx} \qquad k = 0,1 .
\end{aligned} \qquad (3.3.3)$$

Finally, in the spectrum there are also two sets of kink-antikink bound states $b_n^{(l)}$, with $l = 0,1$ and $n = 1, ..., \left[\frac{8\pi}{\xi}\right]$.

The flow between the two limiting Sine-Gordon models (with frequency β or $\beta/2$, respectively) displays a variety of different qualitative features, including confinement and phase transition phenomena, depending on the signs of λ and μ, and on the value of the relative phase δ. However, it was observed in [36] that the only values of δ which lead to inequivalent theories are those given by $|\delta| \leq \frac{\pi}{2}$. Furthermore, in virtue of the relations

$$\begin{aligned}
V_\delta\left(\phi + \tfrac{\pi}{\beta}, \lambda, \mu\right) &= V_{\delta+\pi/2}(\phi, \lambda, -\mu) , \\
V_\delta(-\phi, \lambda, \mu) &= V_{-\delta}(\phi, \lambda, \mu) ,
\end{aligned}$$

we can describe all the inequivalent possibilities keeping μ positive and the relative phase in the range $0 \leq \delta \leq \frac{\pi}{2}$. The sign of the coupling λ, instead, simply corresponds to a shift or a reflection of the potential, without changing its qualitative features. As we are going to show in the following, the case $\delta = \frac{\pi}{2}$ displays peculiar features, while a common description is possible for any other value of δ in the range $0 \leq \delta < \frac{\pi}{2}$.

It is worth mentioning that the possibility of writing exact classical solutions for all the different kinds of topological objects in this model finds a deep explanation in the relation between the trigonometric potential (3.3.1) and power-like potentials. In fact, defining

$$\varphi = \frac{n\pi}{\beta} \pm \frac{4}{\beta}\arctan Y , \qquad n = 0,1,2,3 , \qquad (3.3.4)$$

one can easily see that the first order equation which determines the kink solution

$$\frac{1}{2}\left(\frac{d\varphi}{dx}\right)^2 = -\frac{\mu}{\beta^2}\cos\beta\,\varphi - \frac{\lambda}{\beta^2}\cos\left(\frac{\beta}{2}\varphi + \delta\right) + C$$

renormalization and no countertems have to be added.

is mapped into the equation for Y

$$\frac{1}{2}\left(\frac{dY}{dx}\right)^2 = U(Y) \,, \tag{3.3.5}$$

where $U(Y)$ describes various kinds of algebraic potentials, depending on the values of n, δ and C. The $\delta = 0$ case was analysed in [49] and its classical solutions are very simple because $U(Y)$ only contains quartic and quadratic powers of Y. It is easy to see that a similar situation also occurs in the $\delta = \frac{\pi}{2}$ case; for instance, choosing $n = 1$ and $C = -\frac{1}{\beta^2}\left(\mu + \frac{\lambda^2}{8\mu}\right)$, one obtains the quartic potential

$$U(Y) = \frac{(4\mu + \lambda)^2}{128\mu}\left(\frac{4\mu - \lambda}{4\mu + \lambda}Y^2 - 1\right)^2 \,, \tag{3.3.6}$$

which has the well known classical background

$$Y(x) = \sqrt{\frac{4\mu + \lambda}{4\mu - \lambda}}\tanh\left(\sqrt{\mu - \frac{\lambda^2}{16\,\mu}}\frac{x}{2}\right) \,. \tag{3.3.7}$$

For generic δ, instead, also cubic and linear powers of Y appear, making more complicated the analysis of the classical solutions.

$\delta = 0$ case

It is convenient to start our discussion with the case $\delta = 0$. This case, in fact, displays those topological features which are common to all other models with $0 < \delta < \frac{\pi}{2}$, but it admits a simpler technical analysis, due to the fact that parity invariance survives the deformation of the original SG model. As we will see explicitly, in this case the results of the FFPT and the Semiclassical Method are complementary, since they describe different kinds of excitations present in the theory.
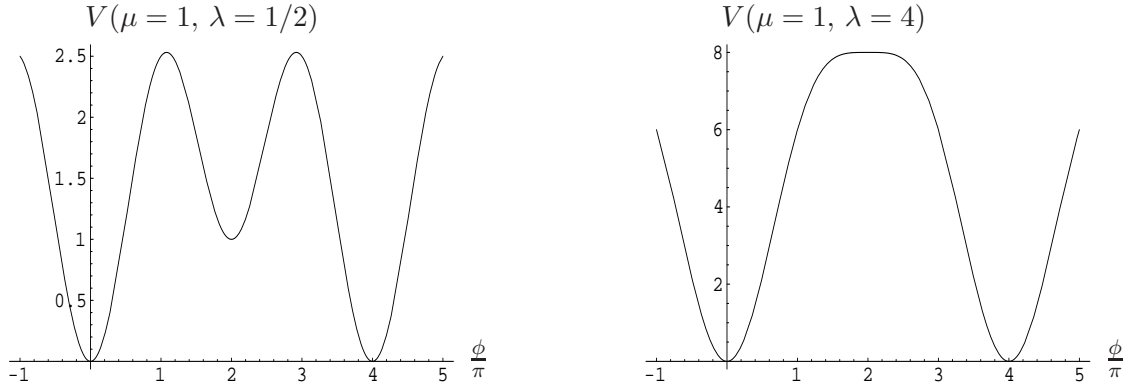
Figure 3.1: DSG potential in the case $\delta = 0$.

Fig.3.1 shows the shape of this DSG potential in the two different regimes, i.e. (i) $0 < \lambda < 4\mu$ and (ii) $\lambda > 4\mu$. The absolute minimum persists in the position $0 \pmod{\frac{4\pi}{\beta}}$ for any values of the couplings, while the other minimum at $\frac{2\pi}{\beta} \pmod{\frac{4\pi}{\beta}}$ becomes relative and disappears at the point $\lambda = 4\mu$. The breaking of the degeneration between the two initial vacua in the two–folded SG causes the confinement of the original SG solitons, as it can be explicitly checked by applying the FFPT. The linearly rising potential, responsible for the confinement of the SG solitons, gives

rise then to a discrete spectrum of bound states whose mass is beyond $2M_{SG}$, where M_{SG} is the mass of the SG solitons [36, 45].

The disappearing of the initial solitons represents, of course, a drastic change in the topological features of the spectrum. At the same time, however, a stable new static kink solution appears for $\lambda \neq 0$, interpolating between the new vacua at 0 and $\frac{4\pi}{\beta}$. The existence of this new topological solution is at the origin of the complementarity between the FFPT and the Semiclassical Method. By the first technique, in fact, one can follow adiabatically the deformation of the SG breathers masses: these are neutral objects that persist in the theory although the confinement of the original kinks has taken place. It is of course impossible to see these particle states by using the Semiclassical Method, since the corresponding solitons, which originate these breathers as their bound states, have disappeared. Semiclassical Method can instead estimate the masses of other neutral particles, i.e. those which appear as bound states of the new stable kink present in the deformed theory.

This new kink solution, interpolating between 0 and $\frac{4\pi}{\beta}$, is given explicitly by

$$\varphi_K(x) = \frac{2\pi}{\beta} + \frac{4}{\beta} \arctan \left[\sqrt{\frac{\lambda}{\lambda + 4\mu}} \sinh(m\,x) \right] , \qquad (3.3.8)$$

where

$$m^2 = \mu + \frac{\lambda}{4} \qquad (3.3.9)$$

is the curvature of the absolute minimum. Interestingly enough [37], this background admits an equivalent expression in terms of the superposition of two solitons of the unperturbed Sine-Gordon model, centered at the fixed points $\pm R$

$$\varphi_K(x) = \varphi_{SG}(x + R) + \varphi_{SG}(x - R) ,$$

where $\varphi_{SG}(x) = \frac{4}{\beta} \arctan [e^{m\,x}]$ are the usual Sine-Gordon solitons with the deformed mass parameter (3.3.9) whereas their distance $2R$ is expressed in terms of the couplings by

$$R = \frac{1}{m} \operatorname{arccosh} \sqrt{\frac{4\mu}{\lambda} + 1} .$$

By looking at Fig.3.2, it is clear that this background, in the small λ limit, describes the two confined solitons of SG, which become free in the $\lambda = 0$ point, i.e. where $R \to \infty$.
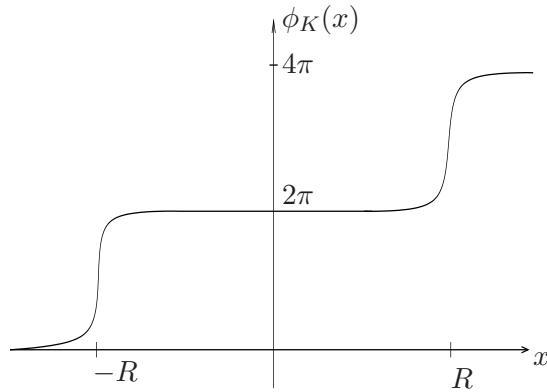

Figure 3.2: Kink solution (3.3.8)

The classical energy of this kink is given by

$$M_K = \frac{16\,m}{\beta^2} \left\{ 1 + \frac{\lambda}{\sqrt{4\mu(\lambda + 4\mu)}} \operatorname{arctanh}\sqrt{\frac{4\mu}{\lambda + 4\mu}} \right\} , \tag{3.3.10}$$

and in the $\lambda \to 0$ limit it tends to twice the classical energy of the Sine-Gordon soliton, i.e.

$$M_K \xrightarrow[\lambda \to 0]{} \frac{16\sqrt{\mu}}{\beta^2} ,$$

therefore confirming the above picture. In the $\mu \to 0$ limit, the asymptotic value of the above expression is instead the mass of the soliton in the Sine-Gordon model with coupling $\beta/2$. The expansion for small μ

$$M_K \xrightarrow[\mu \to 0]{} \frac{8\sqrt{\lambda/4}}{(\beta/2)^2} + \frac{\mu}{\beta^2} \frac{32}{3\sqrt{\lambda}} + O(\mu^2) , \tag{3.3.11}$$

gives the first order correction which is in agreement with the result of the FFPT in the semi-classical limit (see Appendix 3.A).

The bound states created by the kink (3.3.8) and its antikink can be obtained by looking at the poles of the semiclassical form factors of the fields $\varphi(x)$ and $\varepsilon(x)$, reported in Appendix 3.B, and their mass are given by[5]

$$m_{(K)}^{(n)} = 2M_K \sin\left(n\, \frac{m}{2M_K} \right) \quad , \quad 0 < n < \pi \frac{M_K}{m} . \tag{3.3.12}$$

For small μ we easily recognize the perturbation of the standard breathers in Sine-Gordon with $\beta/2$:

$$m_{(K)}^{(n)} \xrightarrow[\mu \to 0]{} \frac{64}{\beta^2} \sqrt{\frac{\lambda}{4}} \sin\left(n\, \frac{\beta^2}{64} \right) + \frac{2}{3} \frac{\mu}{\sqrt{\lambda}} \left[\frac{32}{\beta^2} \sin\left(n\, \frac{\beta^2}{64} \right) + n\, \cos\left(n\, \frac{\beta^2}{64} \right) \right] + O(\mu^2) , \tag{3.3.13}$$

while the expansion of the bound states masses for small λ

$$m_{(K)}^{(n)} \xrightarrow[\lambda \to 0]{} \frac{32\sqrt{\mu}}{\beta^2} \sin\left(n\, \frac{\beta^2}{32} \right) +$$
$$+ \frac{1}{8} \frac{\lambda}{\sqrt{\mu}} \left[\left(1 - \ln\frac{\lambda}{16\mu} \right) \frac{32}{\beta^2} \sin\left(n\, \frac{\beta^2}{32} \right) + n\, \ln\frac{\lambda}{16\mu} \cos\left(n\, \frac{\beta^2}{32} \right) \right] + O(\lambda^2)$$

deserves further comments: in fact, although the above masses have well-defined asymptotic values, they do not correspond however to any state of the unperturbed SG theory. The reason is that the classical background (3.3.8) in the $\lambda \to 0$ limit does not describe any longer a localized single particle. This implies that its Fourier transform cannot be interpreted as the two-particle form factor and, consequently, its poles cannot be associated to any bound states.

A technical signal of the disappearing of the above mentioned bound states in the $\lambda \to 0$ limit can be found by computing the three particle coupling among the kink, the antikink and the lightest bound state, given by (1.2.16). At leading order in β we get

$$\Gamma_{K\bar{K}b} = \frac{16\sqrt{2}}{\beta} \frac{m}{\sqrt{\lambda}} .$$

---

[5]Due to parity invariance, the dynamical poles of the form factor of φ between kink states only give the bound states with n odd. The even states can be obtained from the form factor of the energy operator $\epsilon(x)$.

The divergence of the coupling as $\lambda \to 0$ indicates that the considered scattering processes cannot be seen anymore as a bound state creation, i.e. the corresponding bound state disappears from the theory. A general discussion of the same qualitative phenomenon for the ordinary Sine-Gordon model can be found in [50], where the disappearing from the theory of a heavy breather at specific values of β is explicitly related to the divergence or to the imaginary nature of the three particle coupling among this breather and two lightest ones.

Summarizing, in this model we have three kinds of neutral objects, i.e. meson particles. The first kind (a) is given by the bound states originating from the confinement potential of the original solitons. These discrete states have masses above the threshold $2M_{SG}$, where M_{SG} is the mass of the SG solitons, and merge in the continuum spectrum of the non-confined solitons in the $\lambda \to 0$ limit [36, 45]. The second kind (b) is represented by the deformations of SG breathers, that can be followed by means of the FFPT and have masses, for small λ, in the range $[0, 2M_{SG}]$. Finally, the third kind (c) is given by the bound states (3.3.12) of the stable kink of the DSG theory and they have masses in the range $[0, 4M_{SG}]$. All these mass spectra are drawn in Fig. 3.3.
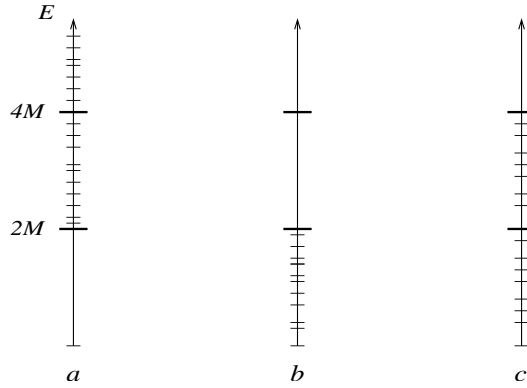
Figure 3.3: Neutral states coming from: a) solitons confinement, b) deformations of SG breathers, c) bound states of the kink (3.3.8)

Obviously, due to the non–integrable nature of this quantum field theory not all these particles belong to the stable part of its spectrum. Apart from a selection rule coming from the conservation of parity, decay processes are expected to be simply controlled by phase–space considerations, i.e. a heavier particle with mass M_h will decay in lighter particles of masses m_i satisfying the condition

$$M_h \geq \sum_i m_i \ .$$

Hence, to determine the stable particles of the theory, one has initially to identify the lightest mesons of odd and even parity with mass $m_-^\star$ and $m_+^\star$ $(m_-^\star < m_+^\star)$, respectively. Then, the stable particles of even parity are those with mass m below the threshold $2m_-^\star$ whereas the stable particles of odd parity are those with mass $m < m_-^\star + m_+^\star$. For instance, in the $\mu \to 0$ limit we know that the only stable mesons are those given by the particles (c), as confirmed by the expansion (3.3.13). Hence, in this limit no one of the other neutral particles is present as asymptotic states. For the mesons of type (a), this can be easily understood since they are all above the threshold dictated by the lightest neutral particle. The situation is more subtle, instead, for the states (b). However, their absence in the theory with $\mu \to 0$ clearly indicates that at some particular value of λ even the lightest of these objects acquires a mass above the

threshold $2m_{(K)}^{(1)}$, with $m_{(K)}^{(1)}$ given by (3.3.12). Analogous analysis can be done for other values of the couplings so that the general conclusion is that most of the above neutral states are nothing else but resonances of the DSG model. As it is well known, unstable particles should have a non–zero imaginary part in their masses, as we have discussed in (1.2.10), but expression (3.3.12) is real. This is due to the fact that, at semiclassical level, the fingerprint of instability is the imaginary nature of some of the frequencies ω_i, eigenvalues of the stability equation (2.1.9), which are not considered in the leading order expression (3.3.12) for the bound states masses. Hence, although at the leading order we are missing the imaginary contributions to the masses, we always have to keep in mind that they come from some of the ω_i.

Another kind of resonances has been numerically observed in the classical scattering of kink and antikinks of the type (3.3.8). The corresponding study, performed in [37], relies on the ideas developed in [35] for the broken ϕ^4 theory, and it is essentially based on the presence of the "shape mode". Along the lines of the discussion presented in Sect. 3.2, this mechanism can be easily interpreted in our formalism. Unfortunately, in the case of DSG we were not able to solve analytically the stability equation around the kink background (3.3.8). However, the conclusion that this kind of resonances is described by the bound states of a normal and an excited kink remains unchanged.

In addition to the above scenario of kink states and bound state thereof, in the region $\lambda < 4\mu$ there is another non-trivial static solution of the theory, defined over the false vacuum placed at $\varphi = \frac{2\pi}{\beta}$. It interpolates between the two values $\frac{2\pi}{\beta}$ and $\frac{4\pi}{\beta} - \frac{2}{\beta}\arccos(1 - \lambda/2\mu)$, and then it comes back (see Fig. 3.4). Its explicit expression is given by

$$\varphi_B(x) = \frac{4\pi}{\beta} - \frac{4}{\beta}\arctan\left[\sqrt{\frac{\lambda}{4\mu - \lambda}}\cosh\left(m_f x\right)\right] , \qquad (3.3.14)$$

where

$$m_f^2 = \mu - \frac{\lambda}{4} \qquad (3.3.15)$$

is the curvature of the relative minimum. Similarly to the kink (3.3.8), it admits an expression in terms of a soliton and an antisoliton of the unperturbed SG model:

$$\varphi_B(x) = \varphi_{SG}(x + R) + \varphi_{SG}(-(x - R)) , \qquad (3.3.16)$$

where now $\varphi_{SG}(x) = \frac{4}{\beta}\arctan\left[e^{m_f x}\right]$ are the Sine-Gordon solitons with the deformed mass parameter (3.3.15) whereas their distance $2R$ is now given by

$$R = \frac{1}{m_f}\operatorname{arcsinh}\sqrt{\frac{4\mu}{\lambda} - 1} . \qquad (3.3.17)$$

In the small λ limit, it is clear that this background describes the confined soliton and antisoliton of the SG model, which become free in the $\lambda = 0$ point, i.e. where $R \to \infty$.

The classical background (3.3.14) is not related to any stable particle in the quantum theory. This can be directly seen from equation (2.1.9); in fact, Lorentz invariance always implies the presence of the eigenvalue $\omega_0^2 = 0$, with corresponding eigenfunction $\eta_0(x) = \frac{d}{dx}\varphi_{cl}(x)$. However, in the case of the solution (3.3.14) the eigenfunction η_0 clearly displays a node, which indicates that the corresponding eigenvalue is not the smallest in the spectrum. Hence, there must be a lower eigenvalue $\omega_{-1}^2 < 0$, with a corresponding imaginary part of the mass relative to this particle state. Furthermore, the instability of (3.3.14) can be related to the theory of false vacuum decay [51, 52]: due to the deep physical interest of this topic, we will discuss it separately in Section 3.3.2.
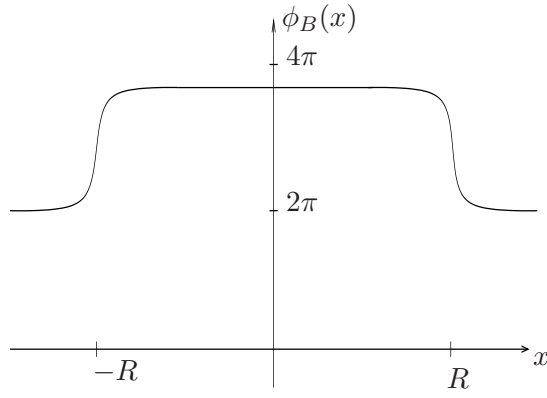
Figure 3.4: Bounce-like solution (3.3.14)
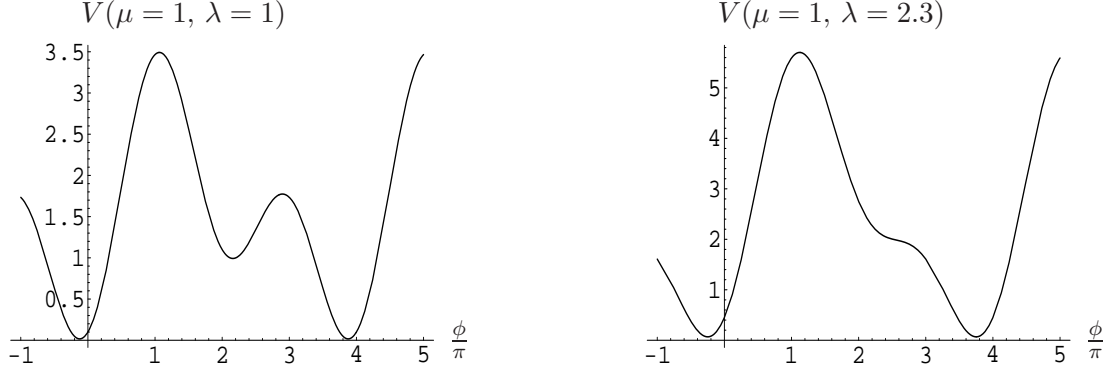
Figure 3.5: DSG potential in the case $\delta = \frac{\pi}{3}$.

Comments on generic δ case

We have already anticipated that the qualitative features of the theory relative to $\delta = 0$ case are common to all other theories associated to the values of δ in the range $0 < \delta < \frac{\pi}{2}$. This can be clearly understood by looking at the shape of the potential, which is shown in Fig. 3.5 for the case $\delta = \frac{\pi}{3}$.

In contrast to the $\delta = 0$ case, parity invariance is now lost in these models, and the minima move to values depending on the couplings. Furthermore, in addition to the change in the nature of the original vacuum at $\frac{2\pi}{\beta}$, which becomes a relative minimum by switching on λ, there is also a lowering of one of the two maxima. These features make much more complicated the explicit derivation of the classical solutions, as we have mentioned at the beginning of the Section.

However, it is clear from Fig. 3.5 that the excitations of these theories share the same nature of the ones in the $\delta = 0$ case. In fact, the original SG solitons undergo a confinement, while a new stable topological kink appears, interpolating between the new degenerate minima. Hence, the analysis performed for $\delta = 0$ still holds in its general aspects, i.e. also in these cases the spectrum consists of a kink, antikink, and three different kinds of neutral particles.

$\delta = \frac{\pi}{2}$ case

The value $\delta = \frac{\pi}{2}$ describes the peculiar case in which no confinement phenomenon takes place, since the two different vacua of the original two–folded SG remain degenerate also in the perturbed theory. As a consequence, the original SG solitons are also asymptotic states in the

perturbed theory. By means of the semiclassical method we can then compute their bound states, which represent the deformations of the two sets of breathers in the original two–folded SG. Hence, in this specific case FFPT and semiclassical method describe the same objects, and their results can be compared in a regime where both β and λ are small.

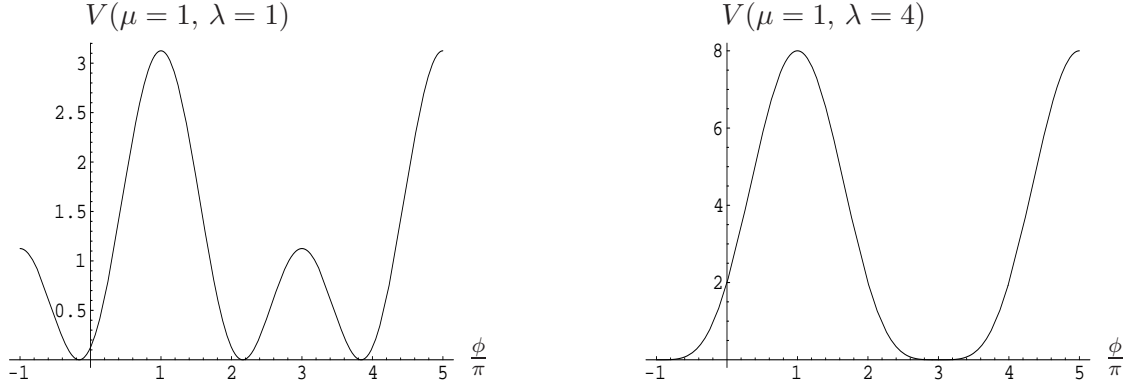$$V(\mu = 1, \lambda = 1) \qquad\qquad V(\mu = 1, \lambda = 4)$$

Figure 3.6: DSG potential in the $\delta = \frac{\pi}{2}$ case.

Fig. 3.6 shows the behavior of this DSG potential. There are two regions, qualitatively different, in the space of parameters, the first given by $0 < \lambda < 4\mu$ and the second given by $\lambda > 4\mu$. They are separated by the value $\lambda = 4\mu$ which has been identified in [36] as a phase transition point. We will explain how this identification is confirmed in our formalism.

Let's start our analysis from the coupling constant region where $\lambda < 4\mu$. Switching on λ, the original inequivalent minima of the two–folded Sine-Gordon, located at $\phi_{\min} = 0, \frac{2\pi}{\beta}$ (mod $\frac{4\pi}{\beta}$), remain degenerate and move to $\phi_{\min} = -\phi_0, \frac{2\pi}{\beta} + \phi_0$ (mod $\frac{4\pi}{\beta}$), with $\phi_0 = \frac{2}{\beta} \arcsin \frac{\lambda}{4\mu}$. The common curvature of these minima is

$$m^2 = \mu - \frac{1}{16} \frac{\lambda^2}{\mu} \,. \tag{3.3.18}$$

Correspondingly there are two different types of kinks, one called "large kink" and interpolating through the higher barrier between $-\phi_0$ and $\frac{2\pi}{\beta} + \phi_0$, the other called "small kink" and interpolating through the lower barrier between $\frac{2\pi}{\beta} + \phi_0$ and $\frac{4\pi}{\beta} - \phi_0$. Their classical expressions are explicitly given by

$$\varphi_L(x) \;=\; \frac{\pi}{\beta} + \frac{4}{\beta} \arctan\left[\sqrt{\frac{4\mu + \lambda}{4\mu - \lambda}} \tanh\left(\frac{m}{2}\,x\right)\right] \qquad (\text{mod } 4\pi)\,, \tag{3.3.19}$$

$$\varphi_S(x) \;=\; \frac{3\pi}{\beta} + \frac{4}{\beta} \arctan\left[\sqrt{\frac{4\mu - \lambda}{4\mu + \lambda}} \tanh\left(\frac{m}{2}\,x\right)\right] \qquad (\text{mod } 4\pi)\,. \tag{3.3.20}$$

With the notation previously introduced, the vacuum structure of the corresponding quantum field theory consists of two sets of inequivalent minima, denoted by $\mid 0 \,\rangle$ and $\mid 1 \,\rangle$, identified modulo 2, i.e. $\mid a + 2n \,\rangle \equiv \mid a \rangle$. The spontaneous breaking of the symmetry $T : \varphi \to 2\pi - \varphi$ selects one of these minima as the vacuum. If we choose to quantize the theory around $\mid 0 \,\rangle$, the admitted quantum kink states are $\mid L \,\rangle = \mid K_{0,1} \,\rangle$ and $\mid \overline{S} \,\rangle = \mid K_{0,-1} \,\rangle$, with the corresponding antikink states $\mid \overline{L} \,\rangle = \mid K_{1,0} \,\rangle$ and $\mid S \,\rangle = \mid K_{-1,0} \,\rangle$, and topological charges

$$Q_L = -Q_{\overline{L}} = 1 + \frac{\beta\phi_0}{\pi} \,,$$
$$Q_S = -Q_{\overline{S}} = 1 - \frac{\beta\phi_0}{\pi} \,.$$

Multi–kink states of this theory satisfy the selection rule coming from the continuity of vacuum indices and are generically given by

$$| \, K_{\alpha_1\alpha_2}(\theta_1) \, K_{\alpha_2\alpha_3}(\theta_2) \cdots K_{\alpha_{n-2}\alpha_{n-1}}(\theta_{n-2}) \, K_{\alpha_{n-1}\alpha_n}(\theta_{n-1}) \, \rangle$$

The leading contributions to the masses of the large and small kink are given by their classical energies, which can be easily computed

$$M_{L,S} = \frac{8\,m}{\beta^2} \left\{ 1 \pm \frac{\lambda}{\sqrt{16\,\mu^2 - \lambda^2}} \left(\frac{\pi}{2} \pm \arcsin \frac{\lambda}{4\mu} \right) \right\} \, . \tag{3.3.21}$$

The expansion of this formula for small λ is given by

$$M_{L,S} \xrightarrow[\lambda \to 0]{} \frac{8\sqrt{\mu}}{\beta^2} \pm \frac{\lambda}{\beta^2} \frac{\pi}{\sqrt{\mu}} + O(\lambda^2) \, , \tag{3.3.22}$$

and the first order correction in λ coincides with the result of FFPT in the semiclassical limit (see Appendix 3.A).

Since two different types of kink $|\,L\,\rangle$ and $|\,S\,\rangle$ are present in this theory, one must be careful in applying eq. (2.2.12) to recover the form factors of each kink separately. In fact, one could expect that both types of kink contribute to the expansion over intermediate states (2.2.4) used in [24] to derive the result. For instance, starting from the vacuum $|\,0\,\rangle$ located at $\phi_{\min} = -\phi_0$ there might be the intermediate matrix elements $_0\langle \bar{S} \,|\, \mathcal{O} \,|\, L \rangle_0$ and $_0\langle L \,|\, \mathcal{O} \,|\, \bar{S} \rangle_0$. However, if $\mathcal{O}$ is a non–charged local operator, it easy to see that these off-diagonal elements have to vanish for the different topological charges of $|\,L\,\rangle$ and $|\,S\,\rangle$. Hence, the expansion over intermediate states diagonalizes and one recovers again eq. (2.2.12).

Therefore, from the dynamical poles of the form factor of φ on the large and small kink-antikink states, reported in Appendix 3.B, we can extract the semiclassical masses of two sets of bound states:

$$m_{(L)}^{(n)} = 2M_L \sin \left(n_L \frac{m}{2M_L} \right) \quad , \quad 0 < n_L < \pi \frac{M_L}{m} \, , \tag{3.3.23}$$

$$m_{(S)}^{(n)} = 2M_S \sin \left(n_S \frac{m}{2M_S} \right) \quad , \quad 0 < n_S < \pi \frac{M_S}{m} \, . \tag{3.3.24}$$

Expanding for small λ, we can see that these states represent the perturbation of the two sets of breathers in the original two–folded Sine-Gordon model:

$$m_{(L,S)}^{(n)} \xrightarrow[\lambda \to 0]{} \frac{16\sqrt{\mu}}{\beta^2} \sin \left(n \frac{\beta^2}{16} \right) \pm 2\pi \frac{\lambda}{\sqrt{\mu}} \left[\frac{1}{\beta^2} \sin \left(n \frac{\beta^2}{16} \right) - \frac{n}{16} \cos \left(n \frac{\beta^2}{16} \right) \right] + O(\lambda^2) \tag{3.3.25}$$

A discussion of these results, in comparison with previous studies of this model [47], is reported in Appendix 3.C.

Concerning the stability of the above spectrum, for $\lambda < 4\mu$ the only stable bound states are the ones with $m_{(L,S)}^{(n)} < 2m_{(S)}^{(1)}$; for λ close enough to 4μ, however, the small kink creates no bound states, hence the stability condition[6] becomes $m_{(L)}^{(n)} < 2m_{(L)}^{(1)}$.

---

[6]Specifically, this stability condition holds for $\lambda > \lambda^*$, where λ^* is defined by

$$\frac{\lambda^*}{\sqrt{16\mu^2 - \lambda^{*2}}} \left(\frac{\pi}{2} - \arcsin \frac{\lambda^*}{4\mu} \right) = 1 - \frac{\beta^2}{8\pi} \, .$$

Resonances in the classical scattering of the small kinks and antikinks (3.3.20) have also been numerically observed in [37]. Our analysis is in agreement with these results, and it adds in this case another possibility. In fact, these resonances can be related both to the bound states of small excited kink–antikink with masses $m_{S*}^{(n)}$ in the range

$$2M_S < m_{S*}^{(n)} < 2M_S + \tilde{\omega}_1 \; ,$$

and to the large kink-antikink bound states with masses in the range

$$2M_S < m_L^{(n)} < 2M_L \; ,$$

where $m_L^{(n)}$ are given by (3.3.23).

In the limit $\lambda \to 4\mu$, ϕ_0 tends to $\frac{\pi}{\beta}$, the two minima at $\frac{2\pi}{\beta} + \phi_0$ and $\frac{4\pi}{\beta} - \phi_0$ coincide and the small kink disappears, becoming a constant solution with zero classical energy. All the large kink bound states masses collapse to zero, and in this limit all dynamical poles of the large kink form factor disappear. This is nothing else but the semiclassical manifestation of the occurrence of the phase transition present in the DSG model (see [36]).

In the second coupling constant region, parameterized by $\lambda > 4\mu$, there is only one minimum at fixed position $-\frac{\pi}{\beta}$ (mod $\frac{4\pi}{\beta}$), with curvature

$$m^2 = \frac{\lambda}{4} - \mu \; . \tag{3.3.26}$$

There is now only one type of kink, given by

$$\varphi_K(x) = \frac{\pi}{\beta} + \frac{4}{\beta} \arctan\left[\sqrt{\frac{\lambda}{\lambda - 4\mu}} \, \sinh(m\,x)\right] \; . \tag{3.3.27}$$

Its classical mass, expanded for small μ, is again in agreement with FFPT (see Appendix 3.A):

$$M_K = \frac{16\,m}{\beta^2} \left\{ 1 + \frac{\lambda}{4\sqrt{\mu(\lambda - 4\mu)}} \left(\frac{\pi}{2} - \arcsin\frac{\lambda - 8\mu}{\lambda} \right) \right\} \to$$

$$\xrightarrow[\lambda \to 0]{} \frac{8\sqrt{\lambda/4}}{(\beta/2)^2} - \frac{\mu}{\beta^2}\frac{32}{3\sqrt{\lambda}} + O(\mu^2) \; . \tag{3.3.28}$$

The bound states of this kink (see Appendix 3.B for the explicit form factors) have masses

$$m_{(K)}^{(n)} = 2M_K \sin\left(n\,\frac{m}{2M_K} \right) \quad , \quad 0 < n < \pi\frac{M_K}{m} \; . \tag{3.3.29}$$

For small μ, these states are nothing else but the perturbed breathers of the Sine-Gordon model with coupling $\beta/2$:

$$m_{(K)}^{(n)} \xrightarrow[\mu \to 0]{} \frac{64}{\beta^2}\sqrt{\frac{\lambda}{4}} \sin\left(n\,\frac{\beta^2}{64} \right) - \frac{2}{3}\frac{\mu}{\sqrt{\lambda}}\left[\frac{32}{\beta^2}\sin\left(n\,\frac{\beta^2}{64} \right) + n\cos\left(n\,\frac{\beta^2}{64} \right) \right] + O(\mu^2)$$

In closing the discussion of the $\delta = \pi/2$ case, it is interesting to mention another model which presents a similar phase transition phenomenon, although in a reverse order. This is the Double Sinh–Gordon Model (DShG), discussed in Appendix 3.D. The similarity is due to the fact that also in this case a topological excitation of the theory becomes massless at the phase transition point, but the phenomenon is reversed, because in DSG the small kink disappears when λ reaches the critical value, while in DShG a topological excitation appears at some value of the perturbing coupling.

3.3.2 False vacuum decay

The semiclassical study of false vacuum decay in quantum field theory has been performed by Callan and Coleman [51], in close analogy with the work of Langer [52]. The phenomenon occurs when the field theoretical potential $U(\varphi)$ displays a relative minimum at φ_+: this classical point corresponds to the false vacuum in the quantum theory, which decays through tunnelling effects into the true vacuum, associated with the absolute minimum φ_- (see Fig. 3.7).
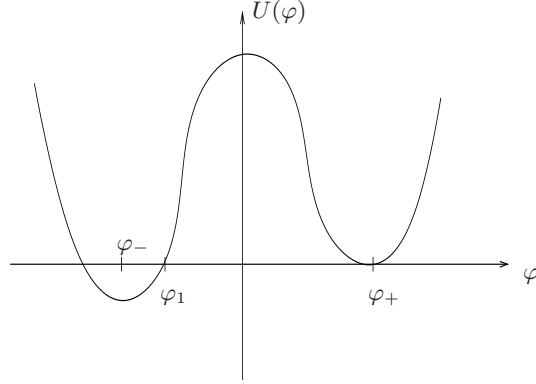

Figure 3.7: Generic potential for a theory with a false vacuum

The main result of [51] is the following expression for the decay width per unit time and unit volume:

$$\frac{\Gamma}{V} \;=\; \left(\frac{B}{2\pi\hbar}\right) e^{-B/\hbar} \left| \frac{\det'[-\partial^2 + U''(\varphi)]}{\det[-\partial^2 + U''(\varphi_+)]} \right|^{-1/2} [1 + O(\hbar)] \;, \qquad (3.3.30)$$

specialized here to the case of two–dimensional space–time. Omitting any discussion of the determinant, about which we refer to the original papers [51], we will present here an explicit analysis of the coefficient B.

It has been shown that B coincides with the Euclidean action of the so–called "bounce" background φ_B:

$$B \;=\; S_E \;=\; 2\pi \int_0^\infty d\rho\, \rho \left[\frac{1}{2}\left(\frac{d\varphi_B}{d\rho}\right)^2 + U(\varphi_B) \right] \;. \qquad (3.3.31)$$

This classical solution is the field–theoretical generalization of the path of least resistance in quantum mechanical tunnelling; it only depends on the Euclidean radius $\rho = \sqrt{\tau^2 + x^2}$ and satisfies the equation

$$\frac{d^2\varphi_B}{d\rho^2} + \frac{1}{\rho}\frac{d\varphi_B}{d\rho} \;=\; U'[\varphi_B] \;, \qquad (3.3.32)$$

with boundary conditions

$$\lim_{\rho\to\infty} \varphi_B(\rho) \;=\; \varphi_+ \;, \qquad \frac{d\varphi_B}{d\rho}(0) = 0 \;.$$

Although in general one does not know explicitly the bounce solution, it is possible to set up some approximation to extract a closed expression for the coefficient B. The so-called "thin wall" approximation consists in viewing the potential $U(\varphi)$ as a perturbation of another potential $U_+(\varphi)$, which displays degenerate vacua at $\varphi_\pm$ and a kink $\varphi_K(x)$ interpolating between them. The small parameter for the approximation is the energy difference $\varepsilon = U(\varphi_+) - U(\varphi_-)$.

In this framework, one can qualitatively guess that the bounce has a value $\varphi(0)$ very close to φ_-, then it remains in this position until some vary large $\rho = R$ and finally it moves quickly towards the final value φ_+. For ρ near R, the first–derivative term in eq. (3.3.32) can be neglected; if in addition one also approximates U with U_+, then one can express the unknown bounce solution as [51]

$$
\varphi_B(\rho) = \begin{cases} \varphi_- & \rho \ll R \\ \varphi_K(\rho - R) & \rho \approx R \\ \varphi_+ & \rho \gg R \,. \end{cases} \tag{3.3.33}
$$

Since the bounce has to represent the path of least resistance, the parameter R, free up to this point, can be fixed by minimizing the action

$$
S_E \;=\; -\pi R^2 \epsilon + 2\pi R \, M_K \,,
$$

which is given by the sum of a volume term and a surface term. Hence, the condition $\frac{dS_E}{dR} = 0$ is realized by the balance of these two different terms in competition, and it finally gives

$$
R \;=\; \frac{M_K}{\varepsilon} \quad \Longrightarrow \quad B \;=\; \pi \, \frac{M_K^2}{\varepsilon} \,. \tag{3.3.34}
$$

In the DSG model, however, we know explicitly the bounce background in the thin wall regime (here we have $\varepsilon = \frac{2\lambda}{\beta^2}$), without any approximation on the potential. This is given by the solution (3.3.14) with x replaced by ρ, that can be directly used to estimate the decay width. Unfortunately the integral in (3.3.31) does not admit a simple expression to be expanded for small λ, but it is clear from eq. (3.3.16) and Fig. 3.4 that the leading contribution is given by

$$
S_E \;\simeq\; 2\pi R \int\limits_{R-\Delta r}^{R+\Delta r} dx \left[\frac{d\varphi_{SG}}{dx}(R - x) \right]^2 \;\simeq\; \frac{8\pi}{\beta^2} \log\left(\frac{16\mu}{\lambda} \right) \,, \tag{3.3.35}
$$

with R given by (3.3.17). This behavior in λ does not agree with the general prediction (3.3.34). The reason can be traced out in the fact that eq. (3.3.16) explicitly realizes the relation between the bounce and the kink of the unperturbed theory, but in a more sophisticated way than (3.3.33). In fact, the mass parameter m_f of the SG kink φ_{SG} is dressed to be the one of the DSG theory, and the parameter R is not free, since (3.3.14) is already the result of a minimization process, being a solution of the Euler–Lagrange equations. The thin wall approximation can be still consistently used because R is very big for small λ, while the crucial difference is that the volume term is now missing from the action, since the value $\varphi_B(0) = \varphi_1$ is the so–called classical turning point (see Fig. 3.7), degenerate with the false vacuum. It is worth noting that the path of least resistance in quantum mechanics precisely interpolates between the false vacuum and the turning point.

Up to the determinant factor, our result for the leading term in the decay width is then

$$
\frac{\Gamma}{V} \;\simeq\; \frac{4}{\beta^2} \left(\frac{\lambda}{16\mu} \right)^{8\pi/\beta^2} \log\left(\frac{16\mu}{\lambda} \right) \,. \tag{3.3.36}
$$

It will be interesting to investigate whether the above mentioned difference with the prediction (3.3.34) is a particular feature of the DSG model or it appears for a generic potential if one improves the approximate description of the bounce along the lines discussed here.

3.4   Summary

In this Chapter we have shown how the semiclassical method is an efficient tool for studying non–integrable QFT. In fact, applied to the broken ϕ^4 theory, it has provided new simple results about mass spectrum, three–particle couplings and resonances.

In cases where also the Form Factor Perturbation Theory can be applied, the semiclassical method may be complementary to this technique or it may provide results comparable with it. We have applied both methods for analysing the mass spectrum of the non–integrable QFT given by the Double Sine–Gordon model, for few qualitatively different regions of its coupling–constants space. This model appears to be an ideal theoretical playground for understanding some of the relevant features of non–integrable models. By moving its coupling constants, in fact, it shows different types of kink excitations and confinement phenomena, a rich spectrum of meson particles, resonance states, false vacuum decay and the occurrence of a phase transition. In light of the many applications it finds in condensed matter systems, it would be interesting to investigate further its properties.

Finally, it is worth mentioning that the semiclassical method can be easily extended to the analysis of several power–like potentials, which have interesting physical interpretations along the lines of the Landau–Ginzburg theory discussed in Sect. 1.3.

Appendix 3.A. Kink mass corrections in the FFPT

In this Appendix we compute by means of the FFPT the corrections to the kink masses in the semiclassical limit, which is relevant for a comparison with our results.

For small λ, we have to consider the DSG model as a perturbation of the two–folded Sine-Gordon [47]. In the $\delta = \pi/2$ case, the perturbing operator is $\Psi = \sin \frac{\beta}{2}\phi$. Its form factors between the vacuum and the two possible kink-antikink asymptotic states are obtained at the semiclassical level by performing the Fourier transform of $\sin \left[\frac{\beta}{2} K^{cl}_{k,k+1}(x) \right]$ [1], with $K^{cl}_{k,k+1}(x)$ given by eq. (3.3.2). Hence we obtain

$$F^{\Psi}_{K_{k,k+1},\bar{K}_{k,k+1}}(\theta) \;=\; \frac{8\pi}{\beta^2} (-1)^k \frac{1}{\cosh \frac{4\pi}{\beta^2}(\theta - i\pi)} \;. \tag{3.A.1}$$

The first order correction in λ to the kink masses is then

$$\delta M_{K_{k,k+1}} \;=\; \frac{\lambda}{\beta^2} \frac{1}{M_K} F^{\Psi}_{K_{k,k+1},\bar{K}_{k,k+1}}(i\pi) \;=\; (-1)^k \frac{\lambda}{\beta^2} \frac{\pi}{\sqrt{\mu}} \;, \tag{3.A.2}$$

in agreement with the correction to the classical masses (3.3.22), since $K_{0,1}$ is associated with the large kink, and $K_{1,2}$ with the small one.

In the $\delta = 0$ case, instead, we can explicitly see how the solitons disappear from the spectrum as soon as λ is switched on. The form factor of the operator $\Psi = \cos \frac{\beta}{2}\phi$ has, in fact, a divergence at $\theta = i\pi$

$$F^{\Psi}_{K_{k,k+1},\bar{K}_{k,k+1}}(\theta) \;=\; -i\frac{8\pi}{\beta^2} (-1)^k \frac{1}{\sinh \frac{4\pi}{\beta^2}(i\pi - \theta)} \;. \tag{3.A.3}$$

The other interesting regime to explore is the small μ limit. In the case $\delta = 0$, this can be seen as the perturbation of the SG model at coupling $\tilde{\beta} = \beta/2$ by means of the operator $\Psi = \cos 2\tilde{\beta}\varphi$. The semiclassical form factor is

$$F^{\Psi}_{K,\bar{K}}(\theta) \;=\; \frac{16}{3} \frac{32}{\beta^2} \frac{i\pi y}{\sin i\pi y}(1 - 2\,y^2) \;, \tag{3.A.4}$$

where we have defined $y = \frac{16}{\beta^2}(i\pi - \theta)$. The corresponding mass correction is given by

$$\delta M_K \;=\; \frac{\mu}{\beta^2} \frac{1}{M_K} F^{\Psi}_{K,\bar{K}}(i\pi) \;=\; \frac{\mu}{\beta^2} \frac{16}{3} \frac{1}{\sqrt{\lambda/4}} \;, \tag{3.A.5}$$

in agreement with (3.3.11).

The case $\delta = \frac{\pi}{2}$ can be described by shifting the original SG field as $\varphi \to \varphi + \frac{\pi}{\beta}$. In this way the perturbing operator becomes $-\Psi$ and we finally obtain the same mass correction but with opposite sign, as in (3.3.28).

Appendix 3.B. Semiclassical form factors

In this Appendix we explicitly present the expressions of the two–particle form factors, on the asymptotic states given by the different kinks appearing in the DSG theory, of the operators $\varphi(x)$ and $\varepsilon(x)$, the last one defined by

$$\varepsilon(x) \equiv \frac{1}{2}\left(\frac{d\varphi}{dx}\right)^2 + V[\varphi(x)] \ .$$

These matrix elements are obtained by performing the Fourier transforms of the corresponding classical backgrounds, as indicated in (2.2.12) and (2.2.14). We use the notation:

$$F_{K\bar{K}}^{\Psi}(\theta) = \langle 0 | \Psi(0) | K(\theta_1) \, \bar{K}(\theta_2) \rangle \ ,$$

with $\theta = \theta_1 - \theta_2$.

For the kink (3.3.8) in the $\delta = 0$ case we have

$$F_{K\bar{K}}^{\varphi}(\theta) = \frac{4\pi^2}{\beta} M_K \, \delta\left[M_K(i\pi - \theta)\right] + i \, \frac{4\pi}{\beta} \frac{1}{i\pi - \theta} \frac{\cos\left[\alpha \frac{M_K}{m}(i\pi - \theta)\right]}{\cosh\left[\frac{\pi}{2}\frac{M_K}{m}(i\pi - \theta)\right]} \ , \tag{3.B.1}$$

where

$$\alpha = \operatorname{arccosh}\sqrt{\frac{\lambda + 4\mu}{\lambda}} \ ,$$

while m and M_K are given by (3.3.9) and (3.3.10), respectively, and

$$F_{K\bar{K}}^{\varepsilon}(\theta) = -\frac{128\pi}{\beta^2} \frac{m^3 M_K}{\lambda} \left\{ \frac{1}{\sinh\left[\pi \frac{M_K}{2m}(i\pi - \theta)\right]} \frac{d}{dc}\left[\frac{\sinh\left[(\operatorname{arccosh} c)\frac{M_K}{2m}(i\pi - \theta)\right]}{\sqrt{c^2 - 1}}\right] + \right.$$

$$\left. - \frac{2\sinh\pi}{\cosh\left[\pi \frac{M_K}{m}(i\pi - \theta)\right] - 1} \frac{d}{dc}\left[\frac{c\sinh\left[(\operatorname{arccosh} c)\frac{M_K}{2m}(i\pi - \theta)\right]}{\sqrt{c^2 - 1}}\right]\right\} \ , \tag{3.B.2}$$

where $c = 1 + \frac{8\mu}{\lambda}$.

For the large kink (3.3.19) in the $\delta = \frac{\pi}{2}$ case (with $\lambda < 4\mu$) we have

$$F_{L\bar{L}}^{\varphi}(\theta) = \frac{2\pi^2}{\beta} M_L \, \delta\left[M_L(i\pi - \theta)\right] + i \, \frac{4\pi}{\beta} \frac{1}{i\pi - \theta} \frac{\sinh\left[\alpha \frac{M_L}{m}(i\pi - \theta)\right]}{\sinh\left[\pi \frac{M_L}{m}(i\pi - \theta)\right]} \ , \tag{3.B.3}$$

where

$$\alpha = 2\arctan\sqrt{\frac{4\mu + \lambda}{4\mu - \lambda}} \ ,$$

while m and M_L are given by (3.3.18) and (3.3.21), respectively, and

$$F_{L\bar{L}}^{\varepsilon}(\theta) = \frac{8\pi}{\beta^2} \frac{m^3 M_L}{\mu} \frac{1}{\sinh\left[\pi \frac{M_L}{m}(i\pi - \theta)\right]} \frac{d}{dc}\left\{\frac{\sinh\left[(\arccos c)\frac{M_L}{m}(i\pi - \theta)\right]}{\sqrt{1 - c^2}}\right\} \ , \tag{3.B.4}$$

where $c = -\frac{\lambda}{4\mu}$.

For the small kink (3.3.20) in the $\delta = \frac{\pi}{2}$ case (with $\lambda < 4\mu$) we have

$$F^\varphi_{S\bar{S}}(\theta) = \frac{6\pi^2}{\beta} M_S \, \delta\left[M_S(i\pi - \theta)\right] + i \frac{4\pi}{\beta} \frac{1}{i\pi - \theta} \frac{\sinh\left[\alpha \frac{M_S}{m}(i\pi - \theta)\right]}{\sinh\left[\pi \frac{M_S}{m}(i\pi - \theta)\right]} \,, \qquad (3.\text{B}.5)$$

where

$$\alpha = 2\arctan\sqrt{\frac{4\mu - \lambda}{4\mu + \lambda}} \,,$$

while m and M_S are given by (3.3.18) and (3.3.21), respectively, and

$$F^\varepsilon_{S\bar{S}}(\theta) = \frac{8\pi}{\beta^2} \frac{m^3 M_S}{\mu} \frac{1}{\sinh\left[\pi \frac{M_S}{m}(i\pi - \theta)\right]} \frac{d}{dc}\left\{ \frac{\sinh\left[(\arccos c)\frac{M_S}{m}(i\pi - \theta)\right]}{\sqrt{1 - c^2}} \right\} \,, \qquad (3.\text{B}.6)$$

where $c = \frac{\lambda}{4\mu}$.

Finally, for the kink (3.3.27) in the $\delta = \frac{\pi}{2}$ case (with $\lambda > 4\mu$) we have

$$F^\varphi_{K\bar{K}}(\theta) = \frac{2\pi^2}{\beta} M_K \, \delta\left[M_K(i\pi - \theta)\right] + i \frac{4\pi}{\beta} \frac{1}{i\pi - \theta} \frac{\cos\left[\alpha \frac{M_K}{m}(i\pi - \theta)\right]}{\cosh\left[\frac{\pi}{2} \frac{M_K}{m}(i\pi - \theta)\right]} \,, \qquad (3.\text{B}.7)$$

where

$$\alpha = \operatorname{arccosh}\sqrt{\frac{\lambda - 4\mu}{\lambda}} \,,$$

while m and M_L are given by (3.3.26) and (3.3.28), respectively, and

$$F^\varepsilon_{K\bar{K}}(\theta) = -\frac{128\pi}{\beta^2} \frac{m^3 M_K}{\lambda} \left\{ \frac{1}{\sinh\left[\pi \frac{M_K}{2m}(i\pi - \theta)\right]} \frac{d}{dc}\left[\frac{\sinh\left[(\arccos c)\frac{M_K}{2m}(i\pi - \theta)\right]}{\sqrt{1 - c^2}} \right] + \right.$$

$$\left. -\frac{2\sinh\pi}{\cosh\left[\pi \frac{M_K}{m}(i\pi - \theta)\right] - 1} \frac{d}{dc}\left[\frac{c\sinh\left[(\arccos c)\frac{M_K}{2m}(i\pi - \theta)\right]}{\sqrt{1 - c^2}} \right] \right\} \,, \qquad (3.\text{B}.8)$$

where $c = 1 - \frac{8\mu}{\lambda}$.

Appendix 3.C. Neutral states in the $\delta = \frac{\pi}{2}$ case

The semiclassical results reported in the text, i.e. eqs. (3.3.23), (3.3.24) and (3.3.25), pose an interesting question about the nature of neutral states in the DSG model at $\delta = \frac{\pi}{2}$. It should be noticed, in fact, that the first order correction in λ obtained by the Semiclassical Method does not match with the results reported in [47] where, by using the FFPT and an extrapolation of numerical data, the authors concluded that this correction was instead identically zero[7]. It is worth discussing this problem in more detail.

In the standard Sine–Gordon model, the breathers $|b_n\rangle$, with n odd (or even), are defined as the bound states of odd (or even) combinations of $|K\bar{K}\rangle$ and $|\bar{K}K\rangle$, where K represents the soliton and $\bar{K}$ the antisoliton. The combinations $|K\bar{K} \pm \bar{K}K\rangle$ are eigenstates of the parity operator $P : \phi \to -\phi$, which commutes with the hamiltonian and acts on the soliton transforming it into the antisoliton. The above mentioned identification of the bound states relies on a very peculiar feature of the Sine–Gordon S–matrix in the soliton sector [16], whose elements are defined as

$$
\begin{aligned}
K(\theta_1)\,\bar{K}(\theta_2) &= S_T(\theta_{12})\,\bar{K}(\theta_2)\,K(\theta_1) + S_R(\theta_{12})\,K(\theta_2)\,\bar{K}(\theta_1)\,, \\
K(\theta_1)\,K(\theta_2) &= S(\theta_{12})\,K(\theta_2)\,K(\theta_1)\,, \\
\bar{K}(\theta_1)\,\bar{K}(\theta_2) &= S(\theta_{12})\,\bar{K}(\theta_2)\,\bar{K}(\theta_1)\,.
\end{aligned}
\tag{3.C.1}
$$

In fact, both the transmission and the reflection amplitudes $S_T(\theta)$ and $S_R(\theta)$ display poles at $\theta_n^* = i(\pi - n\xi)$, with residua which are equal or opposite in sign depending whether n is odd or even. Hence, the diagonal elements

$$
S_-(\theta) = \frac{1}{2}\,[S_T(\theta) - S_R(\theta)]\,, \tag{3.C.2}
$$

$$
S_+(\theta) = \frac{1}{2}\,[S_T(\theta) + S_R(\theta)] \tag{3.C.3}
$$

have only the poles with odd or even n, respectively, and for each n there is only one bound state with definite parity.

However, this is a special feature of the Sine–Gordon model which finds no counterpart, for instance, in other problems with a similar structure. As an explicit example, one can consider the $(\mathrm{RSOS})_3$ scattering theory, which displays a 3-fold degenerate vacuum and two types of kink and antikink with the same mass. The central vacuum is surrounded by two other minima, as in the Sine–Gordon case, and this gives the possibility to define both a kink-antikink state and an antikink-kink state around it. The minimal scattering matrix, given in [53], can be dressed with a CDD factor to generate bound states. It is easy to check that the common poles in the transmission and reflection amplitudes have in this case different residua, giving rise to two distinct bound states, degenerate in mass, over the central vacuum.

Hence, if we call $|b_n^{(0)}\rangle$ the bound states of kink-antikink and $|b_n^{(1)}\rangle$ the bound states of antikink-kink, in general we have to consider them as two distinct excitations, and if they have the same mass we can build two other states from their linear combinations

$$
|b_n^{(\pm)}\rangle = \frac{|b_n^{(0)}\rangle \pm |b_n^{(1)}\rangle}{\sqrt{2}}\,. \tag{3.C.4}
$$

---

[7]It is worth stressing that the linear correction (3.3.25) in λ is very small even for finite values of β (it is easy to check, indeed, that the first term of its expansion is $\frac{\pi}{24}\left(\frac{\beta^2}{16}\right)^2$) and somehow compatible with the numerical data given in [47].

The peculiarity of the Sine–Gordon model is the removal of this double multiplicity due to the fact that the states $|b_{2n+1}^{(+)}\rangle$ and $|b_{2n}^{(-)}\rangle$ decouple from the theory. This feature is shared also by the two-folded version of the model, since the kink scattering amplitudes have the same analytical form as in SG [48].

In the two–folded SG there are two different kink states $|K_{-1,0}\rangle$ and $|K_{0,1}\rangle$ (see Sect. 3.3 and ref. [48] for the notation), and the parity P, which is still an exact symmetry of the theory, acts on them transforming the kink of one type into the antikink of the other type:

$$P:\ |K_{0,1}\rangle \to |K_{0,-1}\rangle, \quad |K_{-1,0}\rangle \to |K_{1,0}\rangle. \qquad (3.C.5)$$

If we quantize the theory around the vacuum $|0\rangle$, we can define $|b_n^{(0)}\rangle$ as the bound states of $|K_{0,1}\,K_{1,0}\rangle$, and $|b_n^{(1)}\rangle$ as the bound states of $|K_{0,-1}\,K_{-1,0}\rangle$. These degenerate states, which transform under P as

$$P:\ |b_n^{(0)}\rangle \to |b_n^{(1)}\rangle, \quad |b_n^{(1)}\rangle \to |b_n^{(0)}\rangle, \qquad (3.C.6)$$

can be still organized in parity eigenstates $|b_n^{(\pm)}\rangle$, and the particular dynamics of the problem causes the decoupling of half of them from the theory. Furthermore, it is easy to see that the form factors of an odd operator between two of these states has to vanish in virtue of the relation

$$\langle 0|\sin\frac{\beta}{2}\phi\,|\,b_n^{(\pm)}b_n^{(\pm)}\rangle\ =\ \langle 0|P^{-1}P\left(\sin\frac{\beta}{2}\phi\right)P^{-1}P|b_n^{(\pm)}b_n^{(\pm)}\rangle\ =$$

$$=\ -\langle 0|\sin\frac{\beta}{2}\phi\,|\,b_n^{(\pm)}b_n^{(\pm)}\rangle\,,$$

leading to the FFPT result that the breathers receive a zero mass correction at first order in λ, as it is claimed in [47].

However, FFPT can be applied by taking into account the nature of neutral states in the DSG model, where the addition to the Lagrangian of the term $-\frac{\lambda}{\beta^2}\sin\frac{\beta}{2}\varphi$ spoils the invariance under P. The kinks $|K_{-1,0}\rangle$ and $|K_{0,1}\rangle$ are deformed into the small and large kinks $|S\rangle$ and $|L\rangle$, respectively, which are not anymore degenerate in mass and cannot be superposed in linear combinations. Hence, the neutral states present in the theory are $|b_n^{(L)}\rangle$ and $|b_n^{(S)}\rangle$, deformations of $|b_n^{(0)}\rangle$ and $|b_n^{(1)}\rangle$ respectively. In virtue of the general considerations presented above, one can see that this interpretation does not lead to any drastic change in the spectrum. In fact, the states $|b_{2n+1}^{(+)}\rangle$ and $|b_{2n}^{(-)}\rangle$ have no reason to decouple in the DSG theory, but they have to carry a coupling which is a function of λ adiabatically going to zero in the two–folded SG limit.

A proper use of the FFPT on $|b_n^{(0)}\rangle$ and $|b_n^{(1)}\rangle$ reproduces indeed the situation described by (3.3.25), in which the two sets of breathers receive mass corrections including also odd terms in λ, but with opposite signs. This is easily seen by considering the P transformations in the two–folded SG model:

$$\langle 0|\sin\frac{\beta}{2}\phi\,|\,b_n^{(0)}b_n^{(0)}\rangle\ =\ \langle 0|P^{-1}P\left(\sin\frac{\beta}{2}\phi\right)P^{-1}P|b_n^{(0)}b_n^{(0)}\rangle\ =$$

$$=\ -\langle 0|\sin\frac{\beta}{2}\phi\,|\,b_n^{(1)}b_n^{(1)}\rangle\,,$$

which gives, at first order in λ,

$$\delta\,m_{(L)} = -\,\delta\,m_{(S)}\,, \qquad (3.C.7)$$

in agreement with our semiclassical result (3.3.25). It is worth noting that also with this interpretation the total spectrum of the DSG model remains unchanged under the action of P,

which corresponds to the transformation $\lambda \to -\lambda$. In fact, the two types of kinks and breathers are mapped one into the other. This is consistent with the observation that P, although it is not anymore a symmetry of the perturbed theory, simply realizes a reflection of the potential, hence the total spectrum should be invariant under it.

Presently the above symmetry considerations seem to us the correct criterion to define the neutral states, and find confirmation in our semiclassical result (3.3.25). However, the available numerical data presented in [47] pose a challenge to this interpretation and further studies are needed to solve this interesting and delicate problem. In fact, although $\delta m_{(L)}$ and $\delta m_{(S)}$ are not forced to vanish by symmetry arguments, there is in principle the possibility that both of them are identically zero in the complete quantum computation. This could follow from the use of the exact kink masses entering eqs. (3.3.23) and (3.3.24), together with a proper shift of the semiclassical pole in the form factors, due to higher order contributions. The exact cancellation of the linear corrections is a very strong requirement, in support of which we have presently no indication in the theory, but a careful analysis of this point is neverthless an interesting open problem.

Appendix 3.D. Double Sinh–Gordon model

Among the different qualitative features taking place in perturbing integrable models, a situation particularly interesting is the one in which the perturbation is adiabatic for small values of the parameters but nevertheless a qualitative change in the spectrum occurs by increasing its intensity.

This is indeed the situation in the $\delta = \frac{\pi}{2}$ case of DSG model, where we have two types of kinks for small λ, but at $\lambda = 4\mu$ one of them disappears from the spectrum. This phenomenon is obviously unaccessible by means of FFPT, hence the semiclassical method is the best tool to describe it.

Here we consider another interesting example of this kind, realized by the Double Sinh-Gordon Model (DShG). In this case the phenomenon is even more evident, because in the unperturbed Sinh-Gordon model there are no kinks at all, but just one scalar particle, while perturbing it, at some critical value of the coupling a kink and antikink appear, i.e. there is a deconfinement phase transition of these particles.

The DShG potential, shown in Fig. 3.8, is expressed as

$$V(\varphi) \;=\; \frac{\mu}{\beta^2}\,\cosh\beta\,\varphi - \frac{\lambda}{\beta^2}\,\cosh\left(\frac{\beta}{2}\,\varphi\right)\,. \tag{3.D.1}$$
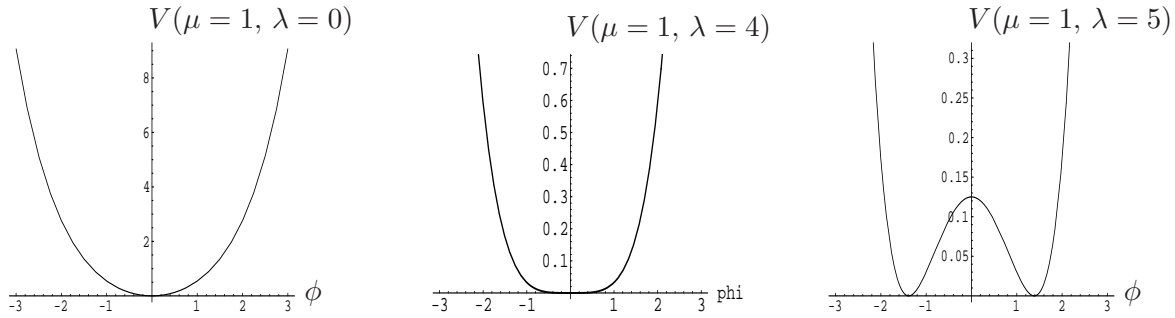

Figure 3.8: DShG potential

In the regime $\lambda < 4\mu$ the qualitative features are the same as in the unperturbed Sinh-Gordon model. At $\lambda = 4\mu$, however, the single minimum splits in two degenerate minima, which for $\lambda > 4\mu$ are located at $\varphi_\pm = \pm\frac{2}{\beta}\mathrm{arccosh}\frac{\lambda}{4\mu}$. A study of the classical thermodynamical properties of the theory in this regime has been performed in [54] with the transfer integral method.

The kink interpolating between the two degenerate vacua is

$$\varphi_K(x) \;=\; \frac{4}{\beta}\,\mathrm{arctanh}\left[\sqrt{\frac{\lambda - 4\mu}{\lambda + 4\mu}}\,\tanh\left(\frac{m}{2}\,x\right)\right]\,, \tag{3.D.2}$$

with

$$m^2 \;=\; \frac{\lambda^2 - 16\mu^2}{16\mu}\,.$$

Its classical mass is given by

$$M_K \;=\; \frac{8m}{\beta^2}\left\{-1 + \frac{2\lambda}{\sqrt{\lambda^2 - 16\mu^2}}\,\mathrm{arctanh}\sqrt{\frac{\lambda - 4\mu}{\lambda + 4\mu}}\right\}\,. \tag{3.D.3}$$

From the form factor of φ on the kink-antikink asymptotic state, expressed as

$$F_2(\theta) = -i\frac{\pi}{\beta}\frac{1}{i\pi - \theta}\frac{\sin\left[\arccosh\frac{\lambda}{4\mu}\frac{M_K}{m}(i\pi - \theta)\right]}{\sinh\left[\pi\frac{M_K}{m}(i\pi - \theta)\right]} \, , \tag{3.D.4}$$

we derive the bound states spectrum

$$m_{(K)}^{(n)} = 2M_K \sin\left(n\frac{m}{2M_K}\right) \quad , \quad 0 < n < \pi\frac{M_K}{m} \tag{3.D.5}$$

All the kink–antikink bound states disappear from the theory at a certain value $\lambda^* > 4\mu$ such that $\pi\frac{M_K}{m}\Big|_{\lambda^*} = 1$, and the kink becomes a constant solution with zero classical energy when $\lambda \to 4\mu$. This is the semiclassical manifestation of a phase transition, analogous to the one observed in DSG with $\delta = \frac{\pi}{2}$. As we have already anticipated, here the phenomenon occurs in a reverse order, since in this case a kink appears in the theory by increasing the coupling λ.

Chapter 4

Finite–size effects

Quantum field theory on a finite volume is a subject of both theoretical and practical interest. It almost invariably enters the extrapolation procedure of numerical simulations, limited in general to rather small samples, but it is also intimately related to quantum field theory at finite temperature. It is therefore important to increase our ability in treating finite size effects by developing efficient analytic means. In the last years, a considerable progress has been registered in particular on the study of finite size behaviour of two dimensional systems. Also for these models, however, an exact treatment of their finite size effects has been obtained only in particular situations, namely when the systems are at criticality or if they correspond to integrable field theories. At criticality, in fact, methods of finite size scaling and Conformal Field Theory permit to determine many universal amplitudes and to extract as well useful information on the entire spectrum of the transfer matrix. Away from criticality, exact results can be obtained only for integrable theories which, on a finite volume, can be further analysed by means of Thermodynamical Bethe Ansatz. This technique provides integral equations for the energy levels, mostly solved numerically. In all other cases, the control of finite size effects in two dimensional QFT has been reached up to now either by perturbative or numerical methods.

The semiclassical method is capable of shedding new light on this topic [1, 3, 4]. In fact, once the proper classical solutions are identified to describe a given geometry, the spectral function in finite volume can be easily estimated by adapting the Goldstone and Jackiw's result. Furthermore, the finite–volume kinks can be quantized semiclassically by adapting the DHN technique, which permits to write in analytic form the discrete energy levels as functions of the size of the system. This procedure can be also extended to geometries with boundaries.

The Chapter is organized as follows. A brief overview of the known non–perturbative techniques to study finite–size effects is presented in Section 4.1. Section 4.2 describes the semiclassical results obtained about form factors and correlation functions in finite volume, for the Sine–Gordon and broken ϕ^4 theories on a cylinder with antiperiodic boundary conditions. Finally, the semiclassical quantization of the Sine–Gordon model on a periodic cylinder and on a strip with Dirichlet boundary conditions are presented in Sections 4.3 and 4.4, respectively. The Chapter also contains few appendices, devoted to some technical discussions. Appendix 4.A presents the quantization of a free bosonic theory in a finite volume and a comparison of finite–volume and finite–temperature computations of the simplest one–point correlation function. Appendix 4.B collects relevant mathematical properties of the elliptic functions used in the text whereas Appendix 4.C displays the main properties of the Lamé equation, which plays a central role in the finite–size quantization.

4.1 Known facts

4.1.1 General results

The understanding of finite–size effects is an important tool in the study of QFT. The finite–volume energy spectrum, in fact, contains a lot of information about the properties of the theory in infinite volume. This was first pointed out by Lüscher [55], who showed how the mass of a particle in a large but finite volume approaches exponentially its asymptotic value in a way controlled by the scattering data of the infinite–volume theory. Lüscher's results were obtained in the context of Monte Carlo simulation of lattice field theories, with the intent of correctly interpreting the numerical data, unavoidably affected by finite–size effects. However, these findings proved to be useful for purposes other than merely controlling a systematic error source. In fact, they can be applied with the opposite spirit, for extracting scattering data from the numerical analyses. It is worth mentioning that this also provides an independent tool for checking the S–matrices of integrable theories, often obtained on the basis of conjectures about the conserved quantities and particle content of the considered theories.

We illustrate here Lüscher's result for the mass corrections in finite–volume, restricting to the case of $(1+1)$–dimensional space–time, with the space variable compactified on a periodic cylinder of circumference R. For the general $d+1$–dimensional result and its proof, see [55, 56]. The deviation of the mass of a particle from its value in infinite volume is shown to originate from polarization effects. In fact, the self–energy of the particle receives contributions from processes in which virtual particles "travel around the finite–size world". The phenomenon can take place at leading order in two different ways, represented in Fig. 4.1. The first, possible only in theories with appropriate cubic couplings and indicated by (1), is a virtual process in which the particle splits in two constituents, which travel around the world before recombining to give back the original particle. The infinite–volume analog of this process is also depicted in Fig. 4.1 (1). The second process, indicated as (2) in Fig. 4.1, is the analog of a tadpole diagram in infinite volume, and involves the scattering amplitudes of the given particle with the others in the theory, which travel around the world before annihilating again.
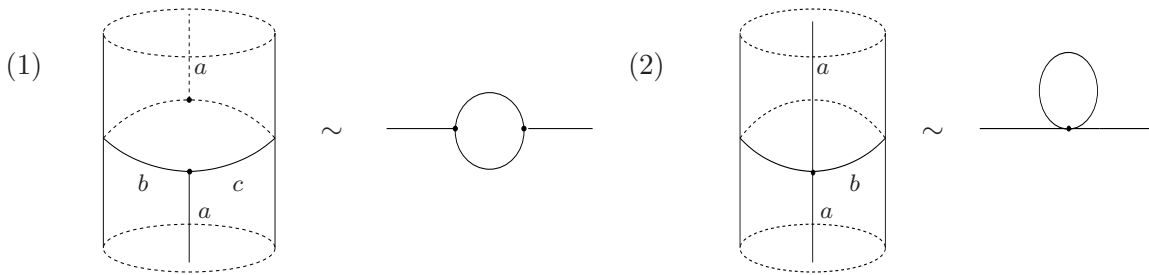

Figure 4.1: The two finite–volume contributions to the self–energy, and their infinite–volume analogs.

Therefore, the finite–size mass of a particle a is given by

$$m_a(R) = m_a(\infty) + \Delta m_a^{(1)}(R) + \Delta m_a^{(2)}(R) + O\left(e^{-\sigma_a R}\right) \;, \qquad (4.1.1)$$

where the constant σ_a indicates the order of the errors, and

$$\Delta m_a^{(1)}(R) \;=\; -\sum_{b,\,c} \theta\left(m_a^2 - |m_b^2 - m_c^2|\right) \mu_{abc}\, R_{abc}\, e^{-\mu_{abc}R}\,, \tag{4.1.2}$$

$$\Delta m_a^{(2)}(R) \;=\; -\sum_{b} \mathcal{P} \int_{-\infty}^{\infty} d\theta\, e^{-m_b R \cosh\theta}\, m_b \cosh\theta\, \left(S_{ab}^{ab}(\theta + i\pi/2) - 1\right) \tag{4.1.3}$$

($\mathcal{P}$ denotes the principal part of the integral). S_{ab}^{ab} is the two–particle scattering amplitude defined in (1.2.2) and θ is the rapidity variable introduced in (1.2.3). In correspondence of a bound state pole at $\theta^* = i u_{ab}^c$, the S–matrix has the residue R_{abc} introduced in (1.2.8). Finally, the quantity μ_{abc} is defined as $\mu_{abc} = m_b \sin u_{ab}^c$, and the step function $\theta\left(m_a^2 - |m_b^2 - m_c^2|\right)$ restricts the sum in (4.1.2) to those processes in which the virtual particles b and c can effectively recombine into a in the forward direction. It is worth noticing that the term $\Delta m_a^{(1)}(R)$ is of order $O\left(e^{-\mu_{abc}R}\right)$, while the term $\Delta m_a^{(2)}(R)$ is of order $O\left(e^{-m_b R}\right)$.

As we have already commented, Lüscher result has been derived in the context of numerical simulations in lattice QFT. Another efficient numerical method for studying two–dimensional QFT in finite–size, which does not require a discretization of space, was suggested in [57], and is called Truncated Conformal Space Approach (TCSA). This method is based on the possibility of viewing a massive QFT as a perturbation of some CFT, and its description gives us the possibility of discussing some general properties of finite–size energy levels.

We have shown in Sect. 1.1 that a conformally invariant theory can be mapped on a cylindrical geometry, and the finite–size Hamiltonian can be expressed in terms of the Virasoro generators and the central charge as

$$H_{CFT} = \frac{2\pi}{R}\left(L_0 + \bar{L}_0 - \frac{c}{12}\right)\,.$$

Perturbing this CFT with a relevant operator Φ with zero spin and scaling dimension $\Delta = h + \bar{h}$, the Hamiltonian becomes (see (1.2.1))

$$H_\lambda \;=\; H_{CFT} + \lambda V\,, \qquad \text{with} \qquad V = \int_0^R \Phi(x,t)\, dx \tag{4.1.4}$$

(we are considering for simplicity a single perturbing operator, but the discussion can be straightforwardly generalized to multiple perturbations). The induced Renormalization Group flow is parameterized by the dimensionless variable $\lambda R^{2-\Delta}$, and the energy eigenvalues E_i can be expressed in terms of *scaling functions* f_i of this variable:

$$E_i(R,\lambda) \;=\; \frac{2\pi}{R}\, f_i\left(\lambda R^{2-\Delta}\right)\,.$$

These functions interpolate between the massless CFT, corresponding to the ultraviolet (UV) limit $\lambda R^{2-\Delta} \to 0$, and the massive infrared (IR) theory, corresponding to $\lambda R^{2-\Delta} \to \infty$. In the two limits the energies are dominated by

$$E_i(R,\lambda) \;\sim\; \frac{2\pi}{R}\left(h_i + \bar{h}_i - \frac{c}{12}\right) \qquad \text{for} \qquad \lambda R^{2-\Delta} \to 0\,, \tag{4.1.5}$$

$$E_i(R,\lambda) \;\sim\; \varepsilon_0\, \lambda^{\frac{2}{2-\Delta}} R + m_i \qquad \text{for} \qquad \lambda R^{2-\Delta} \to \infty\,, \tag{4.1.6}$$

where $h_i, \bar{h}_i$ are the dimensions of the conformal state related to the ith level, ε_0 is the dimensionless bulk vacuum energy and m_i is the (multi)particle mass term of the ith level.

The TCSA technique takes advantage of the fact that the eigenstates of H_{CFT} can be chosen as a basis for the Hilbert space of the perturbed problem. As a consequence, the matrix elements of V in this basis

$$\langle \phi_i \, | \, V \, | \, \phi_j \, \rangle = \frac{R}{2\pi} \langle \phi_i \, | \, \Phi(0,0) \, | \, \phi_j \, \rangle$$

can be computed in terms of the structure constants which enter the OPE in CFT (see (1.1.6)). The obtained Hamiltonian can be finally truncated to the desired level, putting an upper bound on the conformal dimensions of the states in the basis. As a result of its diagonalization, one typically obtains finite–size spectra as shown in Fig. 4.2 (usually, one sets $\lambda = 1$ and plots the spectrum as a function of R).
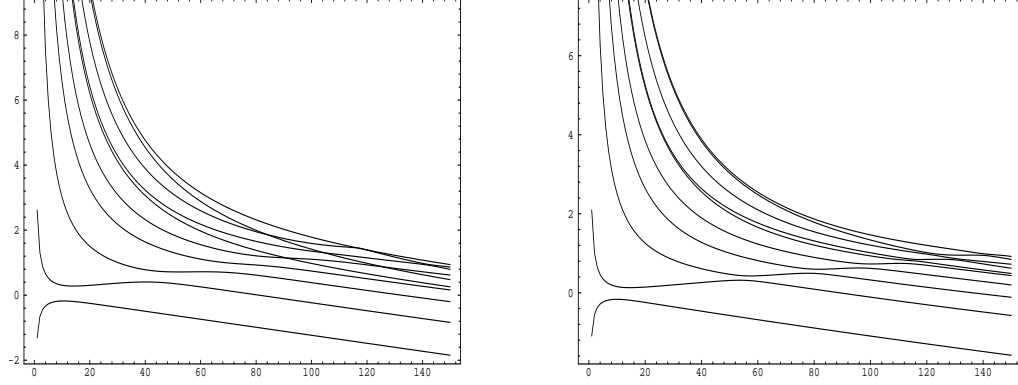

Figure 4.2: TCSA results obtained in [34] for the discrete spectrum $E_i(R)$ in the Ising model with magnetic perturbation (left picture), and in the Ising model with both magnetic and thermal perturbation (right picture).

From the UV and IR asymptotic behaviours of the obtained energy spectra it is therefore possible to extract several conformal and scattering data, according to (4.1.5) and (4.1.6). Furthermore, also the elastic two–particle S–matrix can be measured [58], by considering two–particle states $| A_a \, A_b \, \rangle$ with zero total momentum, relative momentum k and energy

$$E = \sqrt{m_a^2 + k^2} + \sqrt{m_b^2 + k^2} \ .$$

In fact, the momentum k can be extracted from the above equation after the numerical determination of E, m_a and m_b, and the S–matrix can be then deduced by the quantization condition

$$e^{ikR} \, S_{ab}(k) = 1 \ .$$

TCSA can be applied to both integrable and non–integrable theories, and this permits to observe an interesting phenomenon. In fact, in integrable theories it is quite common to observe crossing of different energy levels at finite values of R, while these intersections are immediately removed as one adds a non–integrable perturbation (see for instance Fig. 4.2). In non–relativistic quantum mechanics it is well known that two energy levels can cross only if they belong to different irreducible representations of the symmetry group of the Hamiltonian, otherwise, in absence of any symmetry, they have to repel. This has a clear counterpart in QFT: the presence of conserved charges ensures the stability of particles above threshold, whose lines cross an infinite

number of one–particle lines. As soon as a perturbation is switched on, however, integrability is lost and inelastic processes become allowed, causing the decay of the particle. As a consequence, the particles lines above threshold become broken lines, whose difference in slope with the threshold is proportional to the decay width of the unstable states [59]. Therefore, the study of finite–size effects also gives evidences about the integrability of the theory in exam.

4.1.2 Integrable QFT

We have seen so far how important are finite–size effects for the understanding of QFT. It is therefore useful to have the possibility of controlling them also analytically. Apart from the case of CFT, where conformal invariance permits a complete treatment of the problem, interesting results can be obtained for integrable QFT, passing through a thermodynamic interpretation of the finite size of the system.

The cylindrical geometry can be physically interpreted in two different ways, illustrated in Fig. 4.3. One is the finite–volume picture described above, in which the space variable is compactified on a circle of circumference R while the time evolution takes place along an unbounded direction. The other picture is the finite–temperature one, in which the space variable is unbounded but the (euclidean) time lives on a circle of circumference R. In the Matsubara formalism, this corresponds to introducing a finite temperature in the system, related to the compactification size by the inverse proportionality $R \propto 1/T$.
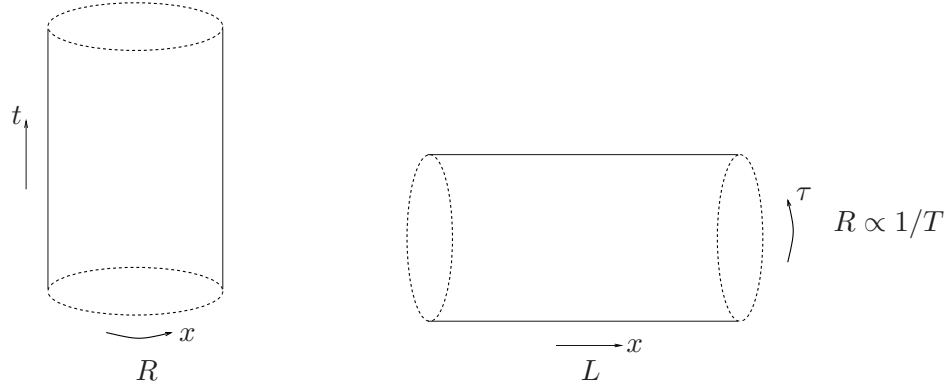

Figure 4.3: Finite volume and finite temperature interpretations of the cylindrical geometry.

In the case of integrable QFT, a lot of information about the thermodynamics can be obtained from the knowledge of the S–matrix. In fact, the partition function

$$Z = \text{Tr}\left(e^{-RH}\right)$$

can be determined by means of the so–called Thermodynamic Bethe Ansatz (TBA) technique, proposed in [60]. Here we limit ourselves to illustrate the basic ideas underlying this method, referring to the original literature for a consistent description. If we put the theory on a large box $0 < x < L$, assuming for simplicity that the spectrum contains only one type of particle with mass m and scattering matrix S, the quantization conditions of the momenta are given by the Bethe Ansatz equations

$$e^{imL\sinh\theta_i} \prod_{j \neq i} S(\theta_i - \theta_j) = 1 \, ,$$

with the rapidity variable θ defined in (1.2.3). The thermodynamic limit of the equivalent condition

$$mL \sinh \theta_i + \sum_{j \neq i} \delta(\theta_i - \theta_j) = 2\pi n_i , \qquad n_i \in \mathbb{Z} , \tag{4.1.7}$$

with $\delta(\theta) = -i \log S(\theta)$, is given by

$$m \cosh \theta + 2\pi \, \varphi(\theta) * \rho_1(\theta) = 2\pi \rho(\theta) ,$$

where $\rho(\theta)$ and $\rho_1(\theta)$ represent, respectively, the density of levels and of occupied states per unit volume, $*$ indicates the convolution operator and $\varphi(\theta) = \frac{d}{d\theta}\delta(\theta)$. The minimization of the free energy with respect to the density of states leads to the integral equation

$$\varepsilon(\theta) = mR \cosh \theta - \varphi(\theta) * \log(1 + e^{-\varepsilon(\theta)}) \tag{4.1.8}$$

for the so–called pseudo–energy $\varepsilon(\theta)$, defined as

$$\frac{\rho_1}{\rho} = \frac{1}{1 + e^{\varepsilon}} .$$

The partition function can be then expressed in terms of the pseudo–energy, which is numerically determined from (4.1.8), as

$$Z(R, L) = \exp\left[mL \int \frac{d\theta}{2\pi} \cosh \theta \, \log\left(1 + e^{-\varepsilon(\theta)}\right)\right] .$$

If we now come back to the finite–volume picture, performing the $L \to \infty$ limit we realize that the partition function has to be dominated by

$$Z(R, L) = \text{Tr}\left(e^{-LH_R}\right) \simeq e^{-LE_0(R)} ,$$

where $E_0(R)$ is the ground state eigenvalue of the finite–volume Hamiltonian H_R. Parameterizing it conveniently as $E_0(R) = \frac{2\pi}{R} f_0(mR)$, we therefore obtain the scaling function [60, 61]

$$f_0(mR) = -\frac{mR}{2\pi} \int \frac{d\theta}{2\pi} \cosh \theta \, \log\left(1 + e^{-\varepsilon(\theta)}\right) , \tag{4.1.9}$$

which in the UV limit has to reduce to $f(mR) \to h_0 + \bar{h}_0 - c/12$, where h_0 and c are the lowest conformal dimension and the central charge of the corresponding CFT (see (1.1.13)).

In this framework, the determination of excited energy levels is not possible or extremely involved. To this respect, however, other techniques exploiting integrability have been developed and applied for instance in [62, 63, 64].

Besides energy levels, the understanding of QFT obviously requires also the knowledge of correlation functions. In the finite–temperature picture, the matrix elements are computed by performing a thermodynamic averaging over the usual infinite–volume particle states:

$$\langle \mathcal{O}_1 \, \ldots \, \mathcal{O}_n \rangle_R \equiv \frac{1}{Z} \, \text{Tr}\left(e^{-RH} \mathcal{O}_1 \, \ldots \, \mathcal{O}_n\right) ,$$

where H is the infinite–volume Hamiltonian and Z is the partition function. Therefore, in the case of integrable QFT, a method has been proposed in [65] for expressing the finite–temperature

correlators in terms of the infinite volume form factors and some thermodynamical quantities available from TBA. For instance, the one–point functions are given as

$$\langle\,\mathcal{O}(x,t)\,\rangle_R \;=\; \frac{1}{Z}\sum_{n=0}^{\infty}\frac{1}{n!}\int\frac{d\theta_1}{2\pi}\,\cdots\,\frac{d\theta_n}{2\pi}\left(\prod_{i=1}^{n}f(\theta_i)\,e^{-\varepsilon(\theta_i)}\right)\langle\,\theta_n,\,\ldots\,,\theta_1\,|\,\mathcal{O}(0,0)\,|\,\theta_1,\,\ldots\,,\theta_n\,\rangle\,,$$

where the "filling fractions" are defined as $f(\theta)=\left(1+e^{-\varepsilon(\theta)}\right)^{-1}$, with the pseudo–energy $\epsilon(\theta)$ given by the solutions of (4.1.8). Higher point correlation functions can be in principle expressed in a conceptually similar way, although there is some controversy about their correct determination [66].

Further insight on this topic could come from a comparison with the finite–volume picture, as it was done for the ground state energy. In this case, the computation of matrix elements involves the notion of finite–size ground state $|\,0\,\rangle_R$:

$$\langle\,\mathcal{O}_1\,\ldots\,\mathcal{O}_n\,\rangle_R \;\equiv\; {}_R\langle\,0\,|\,\mathcal{O}_1\,\ldots\,\mathcal{O}_n\,|\,0\,\rangle_R\,.$$

Unfortunately, at present the precise structure of this ground state is not clear, and moreover, the finite–size matrix elements of operators are still poorly understood. It is precisely from this problem that we will start, in the next Section, our discussion of the semiclassical results obtained in finite volume.

4.2   Semiclassical form factors in finite volume

A particularly interesting problem in the study of QFT in finite volume regards the possibility of defining a "form factor representation" for the correlation functions, in analogy to the infinite volume expression (1.2.11). There are reasons to expect, in fact, a fast convergent behaviour of these series also for finite volume correlators, as it happens in infinite volume (see, for instance [21]). If this would be indeed the case, accurate estimates of finite volume correlators and other related physical quantities, could be obtained by just using few exact terms of their spectral representations, having consequently a great simplification of the problem. This observation makes clear that it is worth pursuing the research on finite–volume form factors, looking in particular for an efficient scheme of approximation.

In the non–perturbative study of form factors at a finite volume, there are so far only semiclassical results relative to a conformal theory [67] as well as exact calculations relative to the Ising model [68] (for a Bethe Ansatz approach see, however, [69]). Although these findings are very interesting, the techniques employed in the above papers are however strictly related either to the specific integrable structure of the considered models or to the free nature of the Majorana fermion field of the Ising model.

In [1], we have proposed to face this problem with a semiclassical approach based on Goldstone and Jackiw's result. This method, contrary to the ones previously mentioned, does not require integrability and it is then of more general applicability, of course within its range of approximation. It is worth to recall an important feature that has come out from the study of the semiclassical form factors in infinite volume. As we have seen in Sect. 2.3, their accuracy seems to extend, somehow, beyond the regime in which they were supposed to be valid. Together with the known fast convergency properties of the spectral series, the above result suggests that the semiclassical method may provide a rather precise estimate of finite volume correlation functions, an outcome which may be useful for many applications.

The application of the procedure described in Sect. 2.2 to the finite volume case is straightforward, thanks to the possibility of choosing $\hat{f}(a)$ as a solution of eq. (2.1.4) with any constant A. As explicitly shown by the examples discussed below, this is equivalent to define a kink solution configuration on a finite volume, with the constant A directly related to the size of the system. We have now to consider the matrix elements of $\phi(0)$ between two eigenstates $|p_{n_1}\rangle$ and $|p_{n_2}\rangle$ of the finite volume hamiltonian H_R. These states can be naturally labelled with the so-called "quasi-momentum" variable p_n, which corresponds to the eigenvalues of the translation operator on the cylinder (multiples of π/L), and appears in the space dependent part of eq. (2.2.3) in the case of finite volume. The Bethe ansatz equations (4.1.7), valid for large R, are exactly a relation between this variable and the free momentum p^∞ of the infinite volume asymptotic states, through a phase shift $\delta(p^\infty)$ which encodes the information about the interaction:

$$p_n^\infty + \frac{\delta(p_n^\infty)}{R} = \frac{2n\pi}{R} \equiv p_n \;.$$

Defining θ_n as the "quasi-rapidity" of the kink states by

$$p_n = M(R)\sinh\theta_n \simeq M(R)\theta_n \;,$$

we can now write the form factor at a finite volume by replacing the Fourier integral transform with a Fourier series expansion:

$$f(\theta_n) = \langle p_{n_2}|\,\phi(0)\,|p_{n_1}\rangle = M(R)\int\limits_{-R/2}^{R/2} da\, e^{i\,M(R)\theta_n a}\phi_{cl}(a)\;, \tag{4.2.1}$$

$$\phi_{cl}(a) = \frac{1}{R\,M(R)}\sum_{n=-\infty}^{\infty} e^{-i\,M(R)\theta_n a}f(\theta_n)\;, \tag{4.2.2}$$

where

$$M(R)\,\theta_n \simeq p_{n_1}-p_{n_2} = \frac{(2n_1-1)\pi}{R} - \frac{(2n_2-1)\pi}{R} \equiv \frac{2n\pi}{R}\;.$$

Since the energy eigenvalues of the finite volume hamiltonian cannot be related to the quasi-rapidity as in eq. (1.2.3), in principle we are not allowed to express the crossed channel form factor $F_2(\theta)$ via the change of variable $\theta \to i\pi - \theta$. However, it is easy to show that in our regime of approximations the deviations of the kink energy from (1.2.3) are of higher order in the coupling and can be neglected at this stage.

On the cylinder, the spectral function can be expressed as a series expansion on the form factors:

$$\rho^{(\phi)}(E_k,p_k) = 2\pi\sum_n \frac{1}{n!}\frac{1}{(2R)^n}\sum_{k_1,\ldots,k_n}\frac{1}{E_{k_1}E_{k_2}\ldots E_{k_n}}\,\delta(E_k - E_{k_1}\ldots - E_{k_n})\,\delta(p_k - p_{k_1}\ldots - p_{k_n})\times$$

$$\times|\,\langle 0|\,\phi(0)|\,n\,\rangle\,|^2\;, \tag{4.2.3}$$

where p_{k_i} are the quasi-momenta of the intermediate states, and E_{k_i} are the finite volume energy eigenvalues, that will be discussed in the following Sections. For the moment their knowledge is not necessary, because at leading semiclassical order the spectral function $\hat{\rho}^{(\phi)}(E_k,p_k)$ is given by the trivial vacuum term plus the kink–antikink contribution, and the kink energies can be

consistently approximated with their classical masses M, which can be exactly computed as functions of the volume. We then have

$$\hat{\rho}^{(\phi)}(E_k, p_k) = 2\pi\delta(E_k)\delta(p_k)|\langle 0| \phi(0)|0\rangle|^2 + \frac{\pi}{4} \frac{\delta\left(\frac{E_k}{M} - 2\right)}{M^2} \sum_{\theta_{k_1}} \left| F_2\left(2\theta_{k_1} + i\pi - \frac{p_k}{M}\right)\right|^2 .$$

(4.2.4)

As in the infinite volume case, the consistency of the semi–classical approximation selects as the relevant values of the above series those with $\theta_k \simeq 0$ and therefore it can can be roughly estimated by simply evaluating $|F_2|^2$ at $\theta_{k_1} = 0$.

We will now explicitly construct the form factors on the kink states in the sine–Gordon model (2.3.1) and in the broken ϕ^4 theory (2.1.5), both defined on a cylindrical geometry with antiperiodic boundary conditions, respectively given by

$$\begin{cases} \phi(x + R) = \frac{2\pi}{\beta} - \phi(x) & \text{for sine–Gordon} , \\ \phi(x + R) = -\phi(x) & \text{for broken } \phi^4 . \end{cases}$$

(4.2.5)

Sine–Gordon model

In order to identify a kink on the twisted cylinder, we have to look for a static finite energy solution of the SG model satisfying the anti–periodic boundary condition (4.2.5). For the first order equation

$$\frac{1}{2}\left(\frac{\partial\phi_{cl}}{\partial x}\right)^2 = \frac{m^2}{\beta^2}\left(1 - \cos\beta\phi_{cl} + A\right)$$

(4.2.6)

a solution with this property can be found for $-2 < A < 0$, and it is expressed as

$$\phi_{cl}(x) = \frac{2}{\beta}\arccos\left[k\,\text{sn}\left(m(x - x_0),\, k^2\right)\right] ,$$

(4.2.7)

where $\text{sn}(u, k^2)$ is the Jacobi elliptic function with modulus $k^2 = \frac{A+2}{2}$, and the presence of a free parameter x_0, which represents the kink's center of mass position, is due to the translational invariance of the theory around the cylinder axis. The plot of (4.2.7) as a function of the real variable x is drawn in Fig.4.4. For a given value of A, this solution oscillates with a period $4\mathbf{K}(k^2)$ between ϕ_0 and $\frac{2\pi}{\beta} - \phi_0$, where ϕ_0 is defined by the condition $V(\phi_0) = -\frac{m^2}{\beta^2}A$, and $\mathbf{K}(k^2)$ is the complete elliptic integral of the first kind. For the definitions and properties of elliptic integrals and Jacobi elliptic functions, see Appendix 4.B.

The solution (4.2.7) has been proposed in [70] as a model of a crystal of solitons and antisolitons in the sine-Gordon theory in infinite volume. In our finite volume case, the solution (4.2.7) has to be interpreted, instead, as a single (anti)soliton defined on a cylinder of circumference

$$R = \frac{1}{m}\,2\mathbf{K}\left(k^2\right) .$$

(4.2.8)

Within this interpretation, the periodic oscillations of the solution represent the soliton circling around the cylinder. Eq. (4.2.8) is the explicit relation between the size of the system and the integration constant A; one can consistently recover the infinite volume limit for $A \to 0$: in this limit R goes to infinity and the function (4.2.7) goes to the standard (anti)soliton solution (2.3.3).
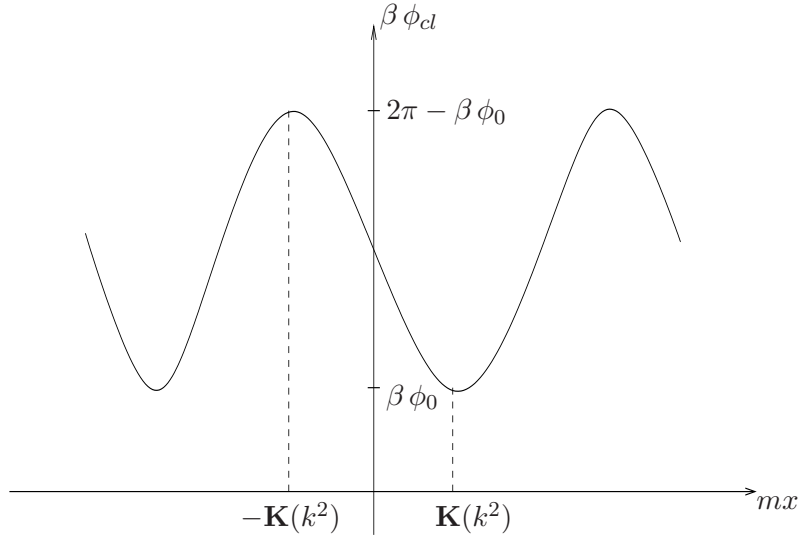
Figure 4.4: Solution of eq. (4.2.6) with $-2 < A < 0$ and $x_0 = 0$.

We can now write the finite volume form factor (4.2.1) in terms of the antikink background (4.2.7):

$$f(-\theta_n) = \frac{2M}{\beta} \int\limits_{-R/2}^{R/2} da \, e^{i\,M\theta_n a} \arccos\left[\,k\,\mathrm{sn}(ma)\right] = \qquad (4.2.9)$$

$$= -\frac{2}{\beta\theta_n} \left[e^{iM\theta_n \frac{R}{2}} \log\left(k + ik'\right) - e^{-iM\theta_n \frac{R}{2}} \log\left(-k + ik'\right) \right] - \frac{2\pi i}{\beta} \frac{1}{\theta_n \cosh\left[\frac{\mathbf{K}'}{m} M\theta_n\right]} \quad,$$

where $k' = \sqrt{1 - k^2}$ and $\mathbf{K}'(k^2) = \mathbf{K}(k'^2)$. The kink mass M is represented at this order by the classical energy, given by

$$\mathcal{E}_{cl}(R) = \int\limits_{-R/2}^{R/2} dx \left[\frac{1}{2}\left(\frac{\partial\phi_{cl}}{\partial x}\right)^2 + \frac{m^2}{\beta^2}(1 - \cos\beta\phi_{cl}) \right] = 8\frac{m}{\beta^2}\left[\mathbf{E}(k^2) - \frac{1}{2}(1 - k^2)\mathbf{K}(k^2)\right] \quad,$$

$$(4.2.10)$$

where $\mathbf{E}(k^2)$ is the complete elliptic integral of the second kind. In order to obtain the result (4.2.9) one has to use the relation

$$\arccos\left[k\,\mathrm{sn}(ma)\right] = \frac{1}{i}\log\left[k\,\mathrm{sn}(ma) + i\,\mathrm{dn}(ma)\right] \quad,$$

and, after an integration by parts, finally compare the inverse Fourier transform (4.2.2) with the expansion [90]

$$\mathrm{cn}(ma) = \frac{2\pi}{k}\frac{1}{mR}\sum_{n=1}^{\infty}\frac{\cos\left[\frac{(2n-1)\pi}{R}a\right]}{\cosh\left[\frac{(2n-1)\pi}{R}\frac{\mathbf{K}'}{m}\right]} \quad.$$

The form factor (4.2.9) has the correct IR limit[1], and leads to the following expressions for

_____

[1]The function $\frac{e^{-ixR/2}}{x}$ can be shown to tend to $-i\pi\delta(x)$ in the distributional sense for $R \to \infty$, and in the same way one can show that $\frac{\cos(xR/2)}{x}$ tends to zero.

$F_2(\theta)$ and for the spectral function:

$$F_2(\theta_n) = \frac{4\pi i}{\beta(i\pi - \theta_n)} \left\{ \frac{1}{\cosh\left[\frac{M}{m}\mathbf{K}'(i\pi - \theta_n)\right]} + \left(-1 + \frac{2}{\pi}\arctan\frac{k'}{k}\right) \cos\left[M(i\pi - \theta_n)\frac{R}{2}\right] \right\},$$

(4.2.11)

$$\hat{\rho}(E_n, p_n) = 4\pi^3\,\delta\left(\frac{E_n}{M} - 2\right) \frac{1}{\beta^2(p_n)^2} \left\{ \frac{1}{\cosh\left[\frac{\mathbf{K}'}{m}p_n\right]} + \left(-1 + \frac{2}{\pi}\arctan\frac{k'}{k}\right) \cos\left[p_n\frac{R}{2}\right] \right\}^2.$$

(4.2.12)

Note that the finite volume dependence of both the form factor (4.2.11) and the spectral function (4.2.12) is not restricted to the second term only. The $M(R)\,\mathbf{K}'(k^2)$ factor in the first term carries the main R-dependence, although it is not manifest but implicitly defined by eq. (4.2.8).

Broken ϕ^4 theory

The differential equation

$$\frac{1}{2}\left(\frac{\partial\phi_{cl}}{\partial x}\right)^2 = \frac{\lambda}{4}\left(\phi^2 - \frac{m^2}{\lambda}\right)^2 + A$$

has a solution given by

$$\bar{\phi}_{cl}(\bar{x}) = (\pm)\sqrt{2 - \bar{\phi}_0^2}\ \text{sn}\left(\frac{\bar{\phi}_0}{\sqrt{2}}(\bar{x} - \bar{x}_0),\ k^2\right),$$

(4.2.13)

with $k^2 = \frac{2}{\bar{\phi}_0^2} - 1$, $V(\phi_0) = -A$ and $1 < \bar{\phi}_0 < \sqrt{2}$, where we have rescaled the variables as

$$\bar{\phi} = \frac{\sqrt{\lambda}}{m}\phi, \qquad \bar{x} = mx.$$

This function oscillates with period

$$2R = \frac{4}{m}\frac{\sqrt{2}}{\bar{\phi}_0}\mathbf{K}(k^2)$$

(4.2.14)

between the two values $-\sqrt{2 - \bar{\phi}_0^2}$ and $\sqrt{2 - \bar{\phi}_0^2}$, and it satisfies the anti–periodic boundary condition (4.2.5). Moreover, it goes to the standard (anti)kink solution (2.1.6) for $\bar{\phi}_0 \to 1$, i.e. when $R \to \infty$.

From the analytic knowledge of the background (4.2.13), we can immediately extract an important scattering data of the non–integrable ϕ^4 theory. In fact, the leading term in the kink mass is given by the classical energy, expressed for generic R as

$$\mathcal{E}_{cl}(R) = \frac{m^3}{\lambda}\frac{\sqrt{2}}{\bar{\phi}_0}\left(-\frac{1}{6}\bar{\phi}_0^4\,\mathbf{K}(k^2) + \frac{1}{3}\bar{\phi}_0^2\left[2\mathbf{E}(k^2) - \mathbf{K}(k^2)\right] + \frac{\mathbf{K}(k^2)}{2}\right).$$

(4.2.15)

It is easy to see that for $R \to \infty$ this quantity indeed reproduces the infinite–volume energy (2.1.7). From its asymptotic expansion for large R, we can obtain the leading order of the kink mass correction in finite volume, and compare it with Lüscher's result (4.1.2, 4.1.3). Taking into

account the $k \to 1$ ($k' \to 0$) expansions of $\mathbf{E}$ and $\mathbf{K}$ (see Appendix 4.B) and noting from (4.2.14) that

$$e^{-\sqrt{2}mR} = \frac{1}{256}(k')^4 + \cdots ,$$

we derive the following asymptotic expansion of $\mathcal{E}_{cl}$ for large R:

$$\mathcal{E}_{cl}(R) = M_\infty - 8\sqrt{2}\,\frac{m^3}{\lambda}e^{-\sqrt{2}mR} + O\left(e^{-2\sqrt{2}mR}\right) . \tag{4.2.16}$$

The counterpart of this behaviour in Lüscher's theory is given by the process (1) in Fig. 4.1, where particle a is the kink, particle b is the elementary meson, and particle c is another kink. In fact, in the broken ϕ^4 theory the elementary boson has semiclassical leading mass $m_b = \sqrt{2}\,m$, which is much lower than the kink one (2.1.7), therefore the dynamical pole relative to this process is located at $u^k_{kb} \simeq \frac{\pi}{2}$. From the comparison with (4.1.2) we finally extract the leading semiclassical expression for the residue of this 3–particle process:

$$R_{k\,k\,b} = 8\,\frac{m^2}{\lambda} .$$

It is easy to see that this result correctly reproduces, as required by (1.2.8), the square of the value (3.2.4) previously obtained for the 3-particle coupling $\Gamma_{k\bar{k}b}$ by looking at the residue of the kink–antikink form factor in infinite volume[2].

Moving then to the finite–volume form factors, these can be computed by comparing the inverse Fourier transform (4.2.2) with the expansion [90]

$$\mathrm{sn}(u) = \frac{\pi}{k\mathbf{K}} \sum_{n=1}^{\infty} \frac{\sin\left[\frac{(2n-1)\pi}{2\mathbf{K}}u\right]}{\sinh\left[\frac{(2n-1)\pi}{2\mathbf{K}}\mathbf{K}'\right]} ,$$

obtaining the expression

$$
\begin{aligned}
F_2(\theta_n) &= M\frac{m}{\sqrt{\lambda}}\sqrt{2 - \bar{\phi}_0^2}\int_{-R/2}^{R/2} da\, e^{i\,M(i\pi - \theta_n)a}\mathrm{sn}\left(\frac{\bar{\phi}_0}{\sqrt{2}}ma\right) = \\
&= i\pi\sqrt{\frac{2}{\lambda}}M\frac{1}{\sinh\left[\frac{\sqrt{2}}{m\phi_0}\mathbf{K}'M(i\pi - \theta_n)\right]} .
\end{aligned} \tag{4.2.17}
$$

Therefore, the $1/\lambda$ leading contribution to the spectral function is given by

$$\hat{\rho}(E_n, p_n) = \frac{2\pi}{\lambda}\,\delta\left(E_n/m\right)\delta\left(p_n/m\right) + \frac{\pi^3}{2\lambda}\,\delta\left(\frac{E_n}{M} - 2\right)\frac{1}{\sinh^2\left[\frac{\sqrt{2}}{m\phi_0}\mathbf{K}'p_n\right]} . \tag{4.2.18}$$

Again, as in the Sine-Gordon case, the finite volume dependence of these quantities comes from the factor $M(R)\mathbf{K}'(k^2)$, where $M(R)$ is the kink mass given by (4.2.15).

4.3   Sine–Gordon model on the cylinder

As we have discussed, the knowledge of form factors permits to estimate the the spectral density representation of correlation functions at a finite volume in both integrable and non–integrable

---

[2]Crossing symmetry implies the equality $R_{k\bar{k}b} = R_{kkb}$.

theories. However, correlation functions need another set of data for their complete determination, precisely the energies of the intermediate states at a finite volume.

The paper [3] has been mainly devoted to fill this gap, that is, to face the problem of a semiclassical computation of the energies $E_i(R)$ of vacua and excited states as functions of the circumference R of a cylindrical geometry. The analytic form of the semiclassical scaling functions for two–dimensional QFT admitting static kink solutions can be achieved by suitably adapting the DHN method to the finite geometry. The example discussed in [3] is the sine–Gordon model, which is particularly appealing for its simplified semiclassical results whereby the significant physical effects are not masked by other additional complications. Moreover, due to the integrable nature of this theory, its finite size effects have been previously studied by means of Thermodynamical Bethe Ansatz [62, 64], and it would be interesting to perform a quantitative comparison between these results and the semiclassical ones, in order to directly control their range of validity. However, as already pointed out, semiclassical methods apply not only to integrable theories and this opens the way to describe analytically the finite size effects also in non–integrable models.

The Sine–Gordon model (2.3.1) on a cylindrical geometry admits quasi–periodic boundary conditions (b.c.)

$$\phi(x+R,t) \;=\; \phi(x,t) + \frac{2n\pi}{\beta}$$

(the arbitrary winding number $n \in \mathbb{Z}$ originates from the invariance of the potential (2.3.1) under $\phi \rightarrow \phi + \frac{2n\pi}{\beta}$). In particular, since we are interested in the one–kink sector, which is defined by $n = 1$, we will impose the b.c.

$$\phi(x+R,t) \;=\; \phi(x,t) + \frac{2\pi}{\beta} \quad . \tag{4.3.1}$$

The first step for applying the semiclassical method to this problem is to find the finite size analog of the kink solution, satisfying now the b.c.'s (4.3.1). However, the success in constructing the scaling functions depends on whether one is able to solve the corresponding Schrödinger equation (2.1.9) and to derive an analytical expression for its frequencies ω_k. It turns out that the semiclassical finite size effects in SG model are intrinsically related to the simplest ($N = 1$) Lamè equation, which admits a complete analytical study.

The subject is organized as follows: after the introductory Section 4.3.1, where we discuss the simplest scaling function in a finite volume in order to clarify the nature of divergencies encountered in such computations, in Section 4.3.2 we present the complete semiclassical analysis of the energy levels in the one–kink sector. Finally, Section 4.3.3 is devoted to the finite–size form factors for the SG model on a periodic cylinder.

4.3.1 Ground state energy regularization

As shown by eq. (2.1.11), quantum corrections to energy levels are given by the series on the frequencies ω_n. However, this series is generally divergent (this is the usual UV divergence in field theory) and a criterion is needed to regularize it. It is quite instructive to consider the simplest example where such divergence occur, i.e. in the calculation of the ground state energy $\mathcal{E}_0^{\text{vac}}(R)$ of the vacuum sector of the SG theory on a cylindrical geometry of circumference R. This can be constructed by implementing the DHN procedure for one of the constant solutions, for instance $\phi_{\text{cl}}^{\text{vac}} = 0$, imposing periodic boundary conditions for the corresponding fluctuations

$\eta^{\mathrm{vac}}(x)$. Obviously, what comes out is nothing else but the Casimir energy of a free bosonic field $\phi(x,t)$ with mass m. In this case the frequency eigenvalues are fixed to be

$$\omega_n = \sqrt{p_n^2 + m^2} \ ,$$

with $p_n = 2\pi n/R$ and $n = 0, \pm1, \pm2, \ldots$.

The ground state energy has to be regularized by subtracting its infinite–volume continuous limit: this ensures in fact the proper normalization of this quantity, expressed by

$$\lim_{R \to \infty} \mathcal{E}_0^{\mathrm{vac}}(R) = 0 \ .$$

The ground state energy at a finite volume is therefore defined by

$$\mathcal{E}_0^{\mathrm{vac}}(R) = \frac{1}{2} \sum_{n=-\infty}^{\infty} \sqrt{\left(\frac{2\pi n}{R}\right)^2 + m^2} - \frac{1}{2} \int_{-\infty}^{\infty} dn \sqrt{\left(\frac{2\pi n}{R}\right)^2 + m^2} \ . \tag{4.3.2}$$

Isolating the zero mode, it can be conveniently rewritten as

$$\mathcal{E}_0^{\mathrm{vac}}(R) = \frac{m}{2} + \frac{2\pi}{R} \sum_{n=1}^{\infty} \sqrt{n^2 + \left(\frac{r}{2\pi}\right)^2} - \frac{2\pi}{R} \int_0^{\infty} dn \sqrt{n^2 + \left(\frac{r}{2\pi}\right)^2} \ ,$$

where $r \equiv mR$. Since the divergence of the series is due to the large n behaviour of the first two terms in the expansion

$$\sqrt{n^2 + \left(\frac{r}{2\pi}\right)^2} \simeq n + \frac{1}{2}\left(\frac{r}{2\pi}\right)^2 \frac{1}{n} + \mathcal{O}\left(\frac{1}{n^2}\right) \ ,$$

we begin our calculation by subtracting and adding these divergent terms to it:

$$S(r) \equiv \sum_{n=1}^{\infty} \sqrt{n^2 + \left(\frac{r}{2\pi}\right)^2} = \sum_{n=1}^{\infty} \left\{ \sqrt{n^2 + \left(\frac{r}{2\pi}\right)^2} - n - \frac{1}{2}\left(\frac{r}{2\pi}\right)^2 \frac{1}{n} \right\} +$$

$$+ \sum_{n=1}^{\infty} n + \frac{1}{2}\left(\frac{r}{2\pi}\right)^2 \sum_{n=1}^{\infty} \frac{1}{n} \ . \tag{4.3.3}$$

The first series in the right hand side of the above expression is now convergent, whereas the last two terms should be coupled to the analogous ones coming from the integral, whose divergencies have to be handled in strict correspondence with those coming from the series. Hence, by subtracting and adding the leading divergence to the integral

$$I(r) \equiv \int_0^{\infty} dn \sqrt{n^2 + \left(\frac{r}{2\pi}\right)^2} =$$

$$= \int_0^{\infty} dn \left\{ \sqrt{n^2 + \left(\frac{r}{2\pi}\right)^2} - n \right\} + \int_0^{\infty} dn\, n \ , \tag{4.3.4}$$

we can combine the last term in this expression with the one in (4.3.3) and implement the well known regularization

$$\sum_{n=0}^{\infty} n - \int_0^{\infty} n\, dn = \lim_{\alpha \to 0} \left[\sum_{n=0}^{\infty} n\, e^{-\alpha n} - \int_0^{\infty} n\, e^{-\alpha n}\, dn \right] = -\frac{1}{12} \ . \tag{4.3.5}$$

However, the first term in (4.3.4) still contains a subleading logarithmic divergence, as it can be seen by explicitly computing the integral by using a cut-off Λ, in the limit $\Lambda \to \infty$

$$\int_0^\Lambda dn \left\{ \sqrt{n^2 + \left(\frac{r}{2\pi}\right)^2} - n \right\} = \frac{1}{2}\left(\frac{r}{2\pi}\right)^2 \ln 2\Lambda + \frac{1}{4}\left(\frac{r}{2\pi}\right)^2 - \frac{1}{2}\left(\frac{r}{2\pi}\right)^2 \ln\frac{r}{2\pi} \ . \tag{4.3.6}$$

This divergence can be cured by subtracting and adding the term $\frac{1}{2}\left(\frac{r}{2\pi}\right)^2 \ln \Lambda$. By combining this last term with its analogous in the series we have

$$\lim_{\Lambda\to\infty}\left(\sum_{n=1}^\Lambda \frac{1}{n} - \ln\Lambda\right) = \gamma_E \ , \tag{4.3.7}$$

where γ_E is the Euler-Mascheroni constant, while the remaining part of (4.3.6) with the above subtraction is now finite.

Collecting the above results, the finite expression of the ground state energy on a cylinder is then given by

$$\mathcal{E}_0^{\text{vac}}(R) = \frac{1}{R}\left[-\frac{\pi}{6} + \frac{r}{2} + \frac{r^2}{4\pi}\left(\ln\frac{r}{4\pi} + \gamma_E - \frac{1}{2}\right) + \sum_{n=1}^\infty \left(\sqrt{(2\pi n)^2 + r^2} - 2\pi n - \frac{r^2}{4\pi n}\right) \right] \ . \tag{4.3.8}$$

It is now easy to see that (4.3.8) nicely coincide with the analogous expression obtained in the finite–temperature picture, given by the TBA result (4.1.9) for the free case, in which the pseudo–energy is simply given by $\varepsilon(\theta) = mR\cosh\theta$:

$$\mathcal{E}_0^{\text{vac}}(R) = -m\int_0^\infty \frac{d\theta}{2\pi} \cosh\theta \ln\left(1 - e^{-r\cosh\theta}\right) \ .$$

In fact, this integral formula can be expressed in terms of Bessel functions, which admit a series representation that directly leads to (4.3.8) (see Ref. [61]). Moreover, one can also check that the above regularization scheme ensures the agreement between the finite–volume and finite–temperature calculations of the one–point functions $\langle\phi^{2k}\rangle$. The interested reader can find the simplest example of these calculations in Appendix 4.A.

Finally, it is worth noting that the result (4.3.8) can also be obtained by using a simpler prescription which automatically includes the subtraction of the various divergencies, fastening the calculation. This consists in ignoring the divergent part of the integral, keeping only its finite part, and in regularizing the divergent series as

$$\sum_{n=1}^\infty n \bigg|_{\text{reg}} = -\frac{1}{12} \ , \tag{4.3.9}$$

$$\sum_{n=1}^\infty \frac{1}{n} \bigg|_{\text{reg}} = \gamma_E + \ln\frac{r}{2\pi} \ . \tag{4.3.10}$$

Formula (4.3.9) is the standard regularization of the Riemann zeta function $\zeta(-1)$, where $\zeta(s) = \sum_{n=1}^\infty \frac{1}{n^s}$, and usually corresponds to normal ordering with respect to the infinite volume vacuum (see, for instance, [71], chapter 4). On the contrary, the regularization of the second series is a–priori ambiguous due to its logarithmic divergence, and its finite value (4.3.10) was chosen according to the above discussion.

4.3.2 Scaling functions

We will now develop a complete semiclassical scheme to analyse the energy of the quantum states in the one–kink sector of SG model on the cylinder. This can be achieved by applying the DHN method to an appropriate kink background.

Properties of the periodic kink solution

In order to identify a kink on the cylinder, we have to look for a static finite energy solution of the SG model satisfying the quasi–periodic boundary condition (4.3.1). For the first order equation (4.2.6) a solution which has this property can be found for $A > 0$. It can be expressed as

$$\phi_{cl}(x) = \frac{\pi}{\beta} + \frac{2}{\beta} \, \text{am} \left(\frac{m(x - x_0)}{k}, k^2 \right) , \qquad k^2 = \frac{2}{2 + A} , \qquad (4.3.11)$$

provided the circumference R of the cylinder is identified with

$$R = \frac{2}{m} k \, \mathbf{K} \left(k^2 \right) , \qquad (4.3.12)$$

where $\mathbf{K}(k^2)$ denotes the complete elliptic integral of the first kind[3]. The parameter x_0 in (4.3.11) represents the kink's center of mass position, and its arbitrariness is due to the translational invariance of the theory around the cylinder axis. The behaviour of (4.3.11) as a function of the real variable x is shown in Figure 4.5.
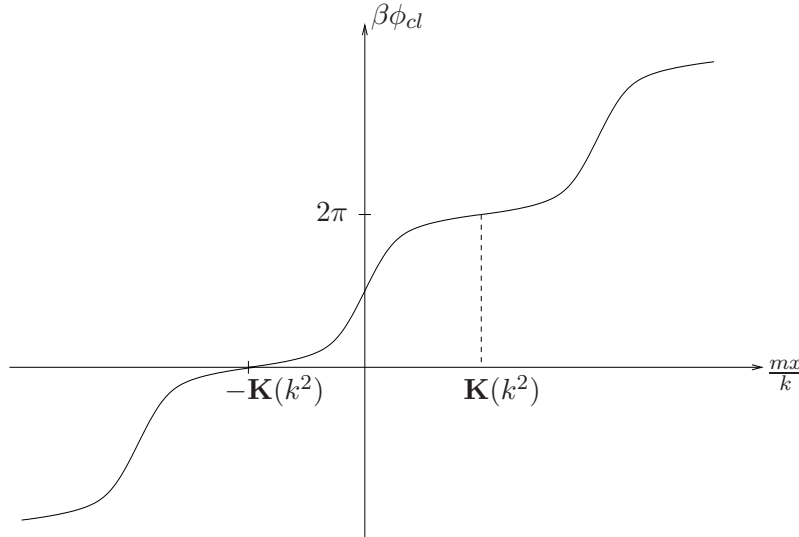

Figure 4.5: Solution of eq. (4.2.6) with $A > 0$ and $x_0 = 0$.

The function (4.3.11) has been first proposed in [70] and interpreted as a crystal of solitons in the sine-Gordon theory in infinite volume. In our finite volume case, instead, (4.3.11) has to be seen as a single soliton defined on a cylinder of circumference R (given by eq. (4.3.12)), while its quasi-periodic oscillations represent winding around the cylinder. As shown in eq. (4.3.12), there is an explicit relation between the size of the system and the integration constant A. It

---

[3]The definition and basic properties of $\mathbf{K}(k^2)$ and the Jacobi elliptic amplitude $\text{am}(u, k^2)$ can be found in Appendix 4.B.

is easy to see that the infinite volume solution (2.3.3) is consistently recovered from (4.3.11) in the limit $A \to 0$, i.e. when R goes to infinity.

The classical energy of the kink on the cylinder is given by

$$\mathcal{E}_{cl}(R) = \int_{-R/2}^{R/2} dx \left[\frac{1}{2} \left(\frac{\partial \phi_{cl}}{\partial x} \right)^2 + \frac{m^2}{\beta^2} (1 - \cos \beta \phi_{cl}) \right] = \frac{8m}{\beta^2} \left[\frac{\mathbf{E}(k^2)}{k} + \frac{k}{2} \left(1 - \frac{1}{k^2} \right) \mathbf{K}(k^2) \right] ,$$

(4.3.13)

where $\mathbf{E}(k^2)$ is the complete elliptic integral of the second kind. In the $R \to \infty$ limit (which corresponds to $k' \to 0$, with $(k')^2 \equiv 1 - k^2$), $\mathcal{E}_{cl}(R)$ approaches exponentially the correct value $M_\infty = \frac{8m}{\beta^2}$. This can be seen expanding $\mathbf{E}$ and $\mathbf{K}$ for small k' (see Appendix 4.B), and expressing the result in terms of mR, which can be itself expanded in k' in virtue of the relation (4.3.12):

$$e^{-mR} = \frac{1}{16} (k')^2 + \cdots .$$

Hence the large R expansion of the classical energy is

$$\mathcal{E}_{cl}(R) = M_\infty + \frac{32}{\beta^2} m \, e^{-mR} + O\left(e^{-2mR} \right) .$$

(4.3.14)

We will comment more on the interpretation of this result in the following.

Similarly, one can derive the behaviour of $\mathcal{E}_{cl}(R)$ for small $r = mR$, which corresponds to the limit $A \to \infty$ (or $k^2 \to 0$):

$$\mathcal{E}_{cl}(R) = \frac{2\pi}{R} \frac{\pi}{\beta^2} + m \frac{r}{\beta^2} - m \left(\frac{r}{2\pi} \right)^3 \frac{\pi}{2\beta^2} + \cdots$$

(4.3.15)

This formula will be relevant in the later discussion of the UV properties of the scaling functions.

Before moving to the quantization of the kink–background (4.3.11), it is worth recalling that another simple kind of elliptic function, given in (4.2.7), was also proposed in [70] and interpreted as a crystal of solitons and antisolitons in the infinite volume SG. This background corresponds as well to a kink on the cylinder geometry but satisfying the *antiperiodic* boundary conditions

$$\phi(x + R, t) = \frac{2\pi}{\beta} - \phi(x, t) .$$

The associated form factors were obtained in [1] and have been described in Sect. 4.2. Although the quantization of this second kink solution is technically similar to the one of (4.3.11) presented here, it displays however some different interpretative features that justify its discussion in a separate future publication [72].

Semiclassical quantization in finite volume

The application of the DHN method to the periodic kink (4.3.11) requires the solution of eq. (2.1.9) for the quantum fluctuations η_ω, which in this case takes the form

$$\left\{ \frac{d^2}{d\bar{x}^2} + k^2 \left(\bar{\omega}^2 + 1 \right) - 2k^2 \operatorname{sn}^2(\bar{x}, k^2) \right\} \eta_{\bar{\omega}}(\bar{x}) = 0 ,$$

(4.3.16)

where $\operatorname{sn}(\bar{x}, k^2)$ is the Jacobi elliptic function defined in Appendix 4.B, and we have introduced the rescaled variables

$$\bar{x} = \frac{mx}{k} , \qquad \bar{\omega} = \frac{\omega}{m} .$$

Due to the periodic properties of $\phi_{cl}(x)$ expressed by eq. (4.3.11), the boundary condition (4.3.1) translates in the requirement for $\eta_{\bar{\omega}}(\bar{x})$

$$\eta_{\bar{\omega}}\left(\bar{x} + \frac{mR}{k}\right) = \eta_{\bar{\omega}}(\bar{x}) \ . \tag{4.3.17}$$

Eq. (4.3.16) can be cast in the so–called Lamé form, which admits the two linearly independent solutions

$$\eta_{\pm a}(\bar{x}) = \frac{\sigma(\bar{x} + i\mathbf{K}' \pm a)}{\sigma(\bar{x} + i\mathbf{K}')} \, e^{\mp \bar{x} \zeta(a)} \ ,$$

where the auxiliary parameter a is defined as a root of the equation

$$\mathcal{P}(a) = \frac{2 - k^2}{3} - k^2 \bar{\omega}^2 \ .$$

The Weierstrass functions $\mathcal{P}(u)$, $\zeta(u)$ and $\sigma(u)$ are defined in Appendix 4.C, where the Lamé equation and its relation with (4.3.16) are discussed in detail.

As it is usually the case for a Schrödinger–like equation with periodic potential, the spectrum of eq. (4.3.16) has a band structure, determined by the properties of the Floquet exponent

$$F(a) = 2i \left[\mathbf{K}\, \zeta(a) - a\, \zeta(\mathbf{K})\right] \ , \tag{4.3.18}$$

which is defined as the phase acquired by $\eta_{\pm a}$ in circling once the cylinder

$$\eta_{\pm a}(\bar{x} + 2\mathbf{K}) = e^{\pm iF(a)}\, \eta_{\pm a}(\bar{x}) \ .$$

We have two allowed bands for real $F(a)$, i.e.

$$0 < \bar{\omega}^2 < \frac{1}{k^2} - 1 \quad \text{and} \quad \bar{\omega}^2 > \frac{1}{k^2} \ ,$$

and two forbidden bands for $F(a)$ complex, i.e.

$$\bar{\omega}^2 < 0 \quad \text{and} \quad \frac{1}{k^2} - 1 < \bar{\omega}^2 < \frac{1}{k^2} \ .$$

The band $0 < \bar{\omega}^2 < \frac{1-k^2}{k^2}$ is described by $a = \mathbf{K} + iy$, where y varies between 0 and $\mathbf{K}'$ and, correspondingly, $F(a)$ goes from 0 to π. The other allowed band $\bar{\omega}^2 > \frac{1}{k^2}$ corresponds instead to $a = iy$ and, by varying y, $F(a)$ goes from π to infinity, as it is shown in Fig. 4.6.

By imposing the periodic boundary conditions (4.3.17) on the fluctuation $\eta(\bar{x})$, one selects the values of $\bar{\omega}^2$ for which the Floquet exponent is an even multiple of π, thus making the spectrum of eq. (4.3.16) discrete. These eigenvalues are $\bar{\omega}_0^2 = 0$, which is the zero mode associated with translational invariance and has multiplicity one, and the infinite series of points

$$\bar{\omega}_n^2 \equiv \frac{1}{k^2}\left[\frac{2 - k^2}{3} - \mathcal{P}(iy_n)\right] \tag{4.3.19}$$

with multiplicity two, placed in the highest band $\bar{\omega}^2 > \frac{1}{k^2}$, with y_n determined by the equation

$$F(iy_n) = 2\mathbf{K}\, i\, \zeta(iy_n) + 2y_n\, \zeta(\mathbf{K}) = 2n\pi \ , \qquad n = 1, 2, \ldots \tag{4.3.20}$$

In the IR limit ($A \to 0$) the spectrum goes to the one related to the standard background (2.3.3): the allowed band $0 < \bar{\omega}^2 < \frac{1}{k^2} - 1$, in fact, shrinks to the eigenvalue $\bar{\omega}_0^2 = 0$, while the other
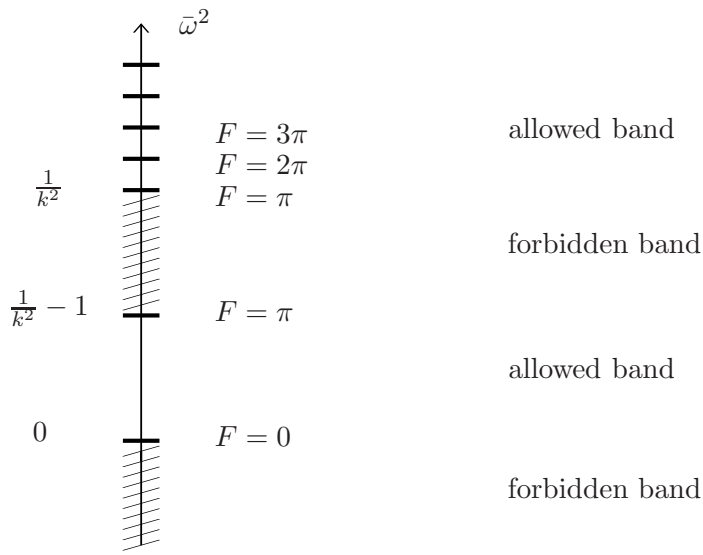
Figure 4.6: Spectrum of eq. (4.3.16)

allowed band $\bar{\omega}^2 > \frac{1}{k^2}$ merges in the continuous part of the spectrum $\bar{\omega}_q^2 = 1 + q^2$. Therefore, by recalling the interpretation of the continuous spectrum in infinite volume as representing the scattering states of the kink with breathers, we can now give to the requirement (4.3.20) the physical meaning of a quantization condition for the momenta of the states constituted by a kink and a breather on the finite volume, analogous to the Bethe ansatz equation (4.1.7) but valid for any value of the size of the system. In particular, using the small–k' expansions of the elliptic integrals and Weierstrass functions presented in Appendices 4.B and 4.C, it easy to check that for large R the condition (4.3.20) indeed reduces to the form

$$m R\, q\, +\, \delta(q)\, =\, 2n\pi\ ,$$

where mq represents the momentum of the lightest breather, and $\delta(q)$ is the semiclassical phase shift (2.3.4).

It is useful to note that, although the R dependence of the frequencies (4.3.19) is quite implicit, since it passes through the inversion of eq. (4.3.12), nevertheless these are analytic functions of R and it is extremely simple to plot them. The corresponding curves, shown in Figure 4.7, provide an important piece of information, since they are nothing else but the energies of the excited states with respect to their ground state $\mathcal{E}_0(R)$.

To complete the analysis, it remains then to determine the finite volume ground state energy $\mathcal{E}_0(R)$ of the kink sector. In analogy with the infinite volume case (see eq. (2.3.5)), this is defined by

$$\mathcal{E}_0(R)\, =\, \mathcal{E}_{cl}(R) + \sum_{n=1}^{\infty} \omega_n(R) - \frac{\delta\mu^2}{\beta^2} \int\limits_{-R/2}^{R/2} dx\, [1 - \cos\beta\phi_{cl}] - \mathcal{E}_0^{\text{vac}}(R)\ . \tag{4.3.21}$$

Before commenting in detail each of these terms, let's focus first on the main problem in deriving a closed expression for $\mathcal{E}_0(R)$, which consists in the evaluation of the infinite sum on the frequencies $\omega_n(R)$ or, better, in isolating its finite part. We need therefore a method for solving the transcendental equation (4.3.20) for $y_n(k^2)$ in order to make the expression (4.3.19) for the frequencies $\omega_n(k^2)$ explicit. As we have already seen for the classical energy, two kinds of expansion are possible, one in the elliptic modulus k and the other in the complementary modulus k',
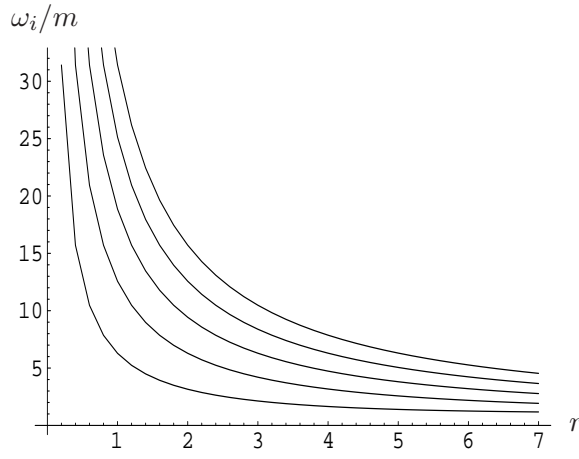
Figure 4.7: The first few levels defined in (4.3.19)

which are efficient approximation schemes in the small and large r regimes, respectively. Here for simplicity we only present the small r expansion. By taking into account the series expansion in k for $\mathbf{K}$, $\zeta(u)$ and $\mathcal{P}(u)$ (see Appendices 4.B and 4.C), we are led to look for a solution of eq. (4.3.20) in the form

$$y_n(k^2) = \sum_{s=0}^{\infty} (k^2)^s \, y_n^{(s)} \; .$$

Here we give the result for the first few coefficients $y_n^{(s)}$, $s = 0, 1, 2$:

$$
\begin{aligned}
y_n^{(0)} &= \operatorname{arctanh}\frac{1}{2n} \; , \\
y_n^{(1)} &= \frac{1}{4} \, y_n^{(0)} \; , \\
y_n^{(2)} &= \frac{9}{64} \, y_n^{(0)} - \frac{n}{16(4n^2 - 1)^2} \; ,
\end{aligned}
$$

which are those relevant in the later analysis of the UV properties of the scaling function. As a consequence, we obtain the following simple expression for the frequencies:

$$\frac{\omega_n}{m} = \frac{2n}{k}\left[1 - \frac{k^2}{4} - \frac{k^4}{64}\frac{20n^2 - 9}{4n^2 - 1} + O(k^6)\right] \; .$$

Comparing it order by order with the small–k expansion of eq. (4.3.12)

$$r = mR = \pi k \left[1 + \frac{k^2}{4} + \frac{9}{64} k^4 + O(k^6)\right] \; ,$$

we finally obtain the explicit R–dependence

$$\frac{\omega_n(R)}{m} = \frac{2\pi}{r} n + \left(\frac{r}{2\pi}\right)^3 \frac{n}{4n^2 - 1} + \dots \qquad (4.3.22)$$

It is worth noting that this series expansion in r, which can be easily extended up to desired accuracy, efficiently approximates the exact energy levels also for rather large values of the scaling variable. Fig. 4.8 shows a numerical comparison between the first energy level given by
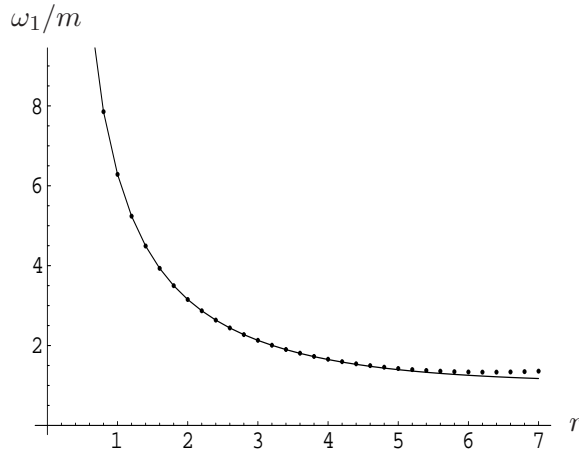
Figure 4.8: Comparison between the exact energy level ω_1/m given by (4.3.19) (continuous line) and the approximate expression (4.3.22) (dotted line).

(4.3.19) and its approximate expression (4.3.22), and for the higher levels it is possible to see that the agreement is even better.

With the above analysis, the sum over frequencies in the ground state energy (4.3.21) takes the form

$$\sum_{n=1}^{\infty} \frac{\omega_n(R)}{m} = \frac{2\pi}{r} \sum_{n=1}^{\infty} n + \left(\frac{r}{2\pi}\right)^3 \sum_{n=1}^{\infty} \frac{n}{4n^2 - 1} + \dots \tag{4.3.23}$$

As we will see below, the subtraction of counterterm and vacuum energy in (4.3.21) leads to the cancellation of all the divergencies, producing a finite expression for the ground state energy in the kink sector.

Moving now to the analysis of the remaining terms in (4.3.21), a similar series expansion can be easily performed on each of them. The classical energy $\mathcal{E}_{cl}(R)$, given in eq. (4.3.13), has already be treated in this way in eq. (4.3.15). The finite volume counterterm (C.T.), where the one–loop mass renormalisation is given by

$$\delta\mu^2 = -\frac{m^2\beta^2}{8\pi} \frac{2\pi}{R} \sum_{n=-\infty}^{\infty} \frac{1}{\sqrt{m^2 + \frac{(2n\pi)^2}{R^2}}}$$

and ϕ_{cl} is given by (4.3.11), takes the explicit form

$$\text{C.T.} = m \left[k\mathbf{K}\left(k^2\right) - \frac{\mathbf{K}\left(k^2\right) - \mathbf{E}\left(k^2\right)}{k} \right] \sum_{n=-\infty}^{\infty} \frac{1}{\sqrt{(2n\pi)^2 + r^2}} \ .$$

The first terms of its expansion in R are then

$$\frac{\text{C.T.}}{m} = \frac{1}{4} + \frac{r}{4\pi} \sum_{n=1}^{\infty} \frac{1}{n} - \frac{r^2}{32\pi^2} - \frac{1}{4}\left(\frac{r}{2\pi}\right)^3 \sum_{n=1}^{\infty} \left(\frac{1}{n} + \frac{1}{n^3}\right) + \dots \ , \tag{4.3.24}$$

Finally, the vacuum energy $\mathcal{E}_0^{\text{vac}}(R)$ is the one precisely computed in Sec. 4.3.1. Since its role is to cancel certain divergencies present in the other terms of $\mathcal{E}_0(R)$, in complete analogy with the

infinite volume case (see eq. (2.3.5)), we will now consider its "naive" formulation, given by

$$\frac{\mathcal{E}_0^{\text{vac}}(R)}{m} = \frac{1}{2m}\sum_{n=-\infty}^{\infty}\sqrt{\left(\frac{2n\pi}{R}\right)^2 + m^2} = \frac{1}{2} + \frac{2\pi}{r}\sum_{n=1}^{\infty}n + \frac{r}{4\pi}\sum_{n=1}^{\infty}\frac{1}{n} - \frac{1}{8}\left(\frac{r}{2\pi}\right)^3\sum_{n=1}^{\infty}\frac{1}{n^3} + \dots$$

(4.3.25)

Hence, in the final expression for the ground state energy all the divergent series present in the sum over frequencies, in the counterterm and in the vacuum energy cancel out, and one obtains

$$\frac{\mathcal{E}_0(R)}{m} = \frac{2\pi}{r}\frac{\pi}{\beta^2} - \frac{1}{4} + \frac{1}{\beta^2}r - \frac{1}{8}\left(\frac{r}{2\pi}\right)^2 - \left(\frac{r}{2\pi}\right)^3\left[\frac{1}{8}\zeta(3) - \frac{1}{4}(2\log 2 - 1) - \frac{\pi}{2\beta^2}\right] + \dots ,$$

(4.3.26)

where we have used [90]

$$\sum_{n=1}^{\infty}\frac{2n^2-1}{8n^3(4n^2-1)} = \frac{1}{8}\zeta(3) - \frac{1}{4}(2\log 2 - 1)$$

in order to evaluate explicitly the coefficient of the r^3 term.

Repeating the above calculations, one can also easily write the finite expressions of the excited energy levels (2.1.10), whose series expansion in r is given by

$$\begin{aligned}\frac{\mathcal{E}_{\{k_n\}}(R)}{m} &= \frac{2\pi}{r}\left(\frac{\pi}{\beta^2} + \sum_n k_n\,n\right) - \frac{1}{4} + \frac{1}{\beta^2}r - \frac{1}{8}\left(\frac{r}{2\pi}\right)^2 + \\ &\quad - \left(\frac{r}{2\pi}\right)^3\left[\frac{1}{8}\zeta(3) - \frac{1}{4}(2\log 2 - 1) - \frac{\pi}{2\beta^2} + \sum_n k_n\frac{n}{4n^2-1}\right] + \dots\end{aligned}$$

(4.3.27)

where $\{k_n\}$ is a set of integers defining a particular excited state of the kink.

UV–IR correspondence

The semiclassical quantization of the periodic kink (4.3.11) provides us with analytic expressions, albeit implicit, for the scaling functions in the kink sector for arbitrary values of the scale $r = mR$. These quantities control analytically the interpolation between the Hilbert spaces of the ultraviolet (UV) and infrared (IR) limiting theories. It is worth noting that, although we obtain them in the framework of a particle–like description proper of the IR limit, the kink background (4.3.11) is intrinsically formulated on a finite size, leading to the possibility of extracting UV data. Hence, it is important to check whether our scaling functions reproduce both the expected results for the IR ($r \to \infty$) and UV ($r \to 0$) limits.

Concerning the IR behaviour, we have already seen that in the $R \to \infty$ limit all the quantities in exam, i.e. the classical solution, its classical energy and the stability frequencies, correctly reach their asymptotic values. In addition, we can now analyse the asymptotic approach of the kink mass to the infinite–volume limit, in order to compare it with the known scattering data of the SG theory, according to Lüscher's theory described in Sect. 4.1. Restricting for simplicity our analysis to the leading term in β in the kink mass (which, in our approach, is simply given by the classical energy), we have then to compare the expansion presented in (4.3.14) with the term that dominates Lüscher's result for small β. This is given by formula (4.1.2) evaluated for the process in which a kink splits into the lightest breather and another kink, i.e.

$$\Delta M(R) = -m_b\sin u_{kb}^k\,R_{kbk}\,e^{-m_b\sin u_{kb}^k R} + \dots ,$$

(4.3.28)

Recalling the kink–breather S–matrix [16]

$$S_{kb}(\theta) = \frac{\sinh\theta + i\cos\frac{\gamma}{16}}{\sinh\theta - i\cos\frac{\gamma}{16}} \quad , \quad \gamma = \frac{\beta^2}{1 - \beta^2/8\pi}$$

and selecting its s-channel pole $\theta^* = iu_{kb}^k = i\left(\frac{\pi}{2} + \frac{\gamma}{16}\right)$, we find[4]

$$R_{kbk} = -2\cotg\frac{\gamma}{16} \ .$$

Substituting in (4.3.28), for small β^2 we have

$$\Delta M(R) = m\frac{32}{\beta^2}e^{-mR} + \dots \ ,$$

which therefore reproduces eq. (4.3.14). It is a remarkable fact that the classical energy alone, being the leading term in the mass for $\beta^2 \to 0$, contains the IR scattering information which controls the large–distance behaviour of $\mathcal{E}_0(R)$.

As we have seen in Sect. 4.1, the UV behaviour for $r \to 0$ of the ground state energy $E_0(R)$ of a given off–critical theory is related instead to the Conformal Field Theory (CFT) data $(\Delta, \bar{\Delta}, c)$ of the corresponding critical theory and to the bulk energy term as

$$E_0(R) \simeq \frac{2\pi}{R}\left(h + \bar{h} - \frac{c}{12}\right) + BR + \cdots \tag{4.3.29}$$

where c is the central charge, $h + \bar{h}$ is the lowest anomalous dimension in a given sector of the theory and B the bulk coefficient. For the Sine–Gordon model the bulk energy term is given by [62, 73]

$$B = 16\frac{m^2}{\gamma^2}\tan\frac{\gamma}{16} \ , \tag{4.3.30}$$

while its UV limit is described by the CFT given by the gaussian action (1.1.14) with the normalization constant fixed to the value[5] $g = 1$

$$\mathcal{A}_G = \frac{1}{2}\int d^2x \, \partial_\mu\phi \, \partial^\mu\phi \ ,$$

and the free bosonic field compactified on a circle of radius $\mathcal{R} = \frac{1}{\beta}$ (see eq.(1.1.15)). We have described the main properties of this CFT in Sect. 1.1. In particular, the central charge takes the value $c = 1$, and the theory is divided into sectors labelled by two integers s and n. In each sector, the state with lowest anomalous dimension (1.1.17) is created by the vertex primary operator $V_{s,n}$, introduced in (1.1.16). It is worth noticing that the SG action can be seen as the perturbed gaussian CFT of the form (4.1.4) with $\lambda = \frac{m^2}{\beta^2}$ and $\Phi = V_{1,0} + V_{-1,0}$. These perturbing operators carry anomalous dimension $\Delta_{\pm 1,0} = h_{\pm 1,0} + \bar{h}_{\pm 1,0} = \frac{\beta^2}{4\pi}$, which is zero in the semiclassical limit, determining the form of the scaling variable as $r = mR$.

The vacuum sector is described by $s = n = 0$, with $h_{vac} + \bar{h}_{vac} = 0$, while the kink sector, defined by the boundary condition (4.3.1), naturally corresponds to $s = 0, n = 1$, in which the lowest anomalous dimension is

$$\Delta_{0,1} = h_{0,1} + \bar{h}_{0,1} = \frac{\pi}{\beta^2} \ . \tag{4.3.31}$$

---

[4]The negative sign of the residue is due to the odd parity of the lightest breather, which implies $\Gamma_k^{kb} = -\Gamma_{kb}^k$ in (1.2.8)

[5]Note that the usual normalization adopted in the CFT literature is instead $g = \frac{1}{4\pi}$.

The conformal vertex operator $V_{0,1}$ has been put in exact correspondence with the soliton–creating operator of SG in Ref. [74].

The question to be addressed now is whether the small r expansion of $\mathcal{E}_0^{vac}(R)$ and $\mathcal{E}_0(R)$ given by eqs. (4.3.8) and (4.3.26) reproduces, in semiclassical approximation, the above data controlling the UV limit of SG model. For the vacuum sector, comparing (4.3.8) with (4.3.29), we correctly obtain $c = 1$ and $h_{vac} = \bar{h}_{vac} = 0$. We do not expect, however, to obtain the bulk term B relative to SG model by looking at (4.3.8), simply because the semiclassical expression of the ground state energy in the vacuum sector applies equally well to any theory which has a quadratic expansion near the vacuum state. Namely, apart from the value of the mass m, eq. (4.3.8) is a universal expression that does not refer then to SG model. The kink scaling function (4.3.26) has instead a richer structure. The obtained scaling dimension

$$h + \bar{h} = \frac{\pi}{\beta^2}$$

is the expected one, given by (4.3.31), for the soliton-creating operator in Sine-Gordon, while the central charge contribution $c = 1$ is absent, simply because in (4.3.26) we have subtracted the vacuum ground state energy from the kink one[6]. Moreover, the bulk coefficient $B = \frac{m^2}{\beta^2}$ present in (4.3.26) correctly reproduces the semiclassical limit of the exact one, given in eq. (4.3.30). In principle, this bulk term should be present in all the energy levels, included the ground state energy in the vacuum sector, but its non–perturbative nature makes impossible to see it in the semiclassical expansion around the vacuum solution, which is in fact purely perturbative. Hence it is not surprising that to extract the bulk energy term we have to look at the kink ground state energy, in virtue of the non–perturbative nature of the corresponding classical solution. Finally, the expression (4.3.27) for the excited energy levels explicitly show their correspondence with the conformal descendants of the kink ground state. In fact, their anomalous dimension is given by

$$h_{\{k_n\}} + \bar{h}_{\{k_n\}} = \frac{\pi}{\beta^2} + \sum_n k_n \, n \ . \tag{4.3.32}$$

The successful check with known UV and IR asymptotic behaviours confirms the ability of the semiclassical results to describe analytically the scaling functions of SG model in the one–kink sector. It would be interesting to further test them at arbitrary values of r through a numerical comparison with the results of [62, 64] in an appropriate range of parameters. This was not pursued here because the results presently available in the literature were obtained for values of β which are beyond the semiclassical regime and moreover the energy levels were plotted as functions of a different scaling variable, i.e. the one defined in terms of the kink mass. We hope however to come back to this problem in the future.

4.3.3 Form factors and correlation functions

The semiclassical scaling functions, derived in Sect. 4.3.2, provide an important information about the finite size effects in SG model. As in the infinite volume case, however, the complete description of the finite volume QFT requires to find, in addition to the energy eigenvalues (4.3.27), the kink form factors and the correlation functions of local operators. This section

---

[6]The value $c = 1$, coming out from the regularization of the leading term of the series on the frequencies (4.3.22), is in fact exactly cancelled by the same term in the vacuum energy.

is devoted to the analysis of this problem, i.e. to the determination of the finite volume form factors and the corresponding spectral functions.

The form factors can be determined with the same procedure described in Sect. 4.2 and applied to the SG model and the broken ϕ^4 field theory, both defined on a cylindrical geometry with *antiperiodic* boundary conditions. In what follows we will apply it instead to the case of SG model with *periodic* boundary conditions. The corresponding finite volume form factor (4.2.1) can be written in terms of the soliton background (4.3.11):

$$f(\theta_n) = M \int_{-R/2}^{R/2} da\, e^{i\, M\theta_n a} \left[\frac{\pi}{\beta} + \frac{2}{\beta} \operatorname{am}\left(\frac{mx}{k}, k^2 \right) \right] = \tag{4.3.33}$$

$$= \frac{2\pi}{\beta} \left\{ \frac{M}{2} R\, \delta_{M\theta_n,0} - i\, \frac{1 - \delta_{M\theta_n,0}}{\theta_n} \left[\cos\left(M\theta_n\, R/2 \right) - \frac{\sin\left(M\theta_n\, R/2 \right)}{M\theta_n R/2} \right] + i\, \frac{1}{\theta_n \cosh\left(k\, \mathbf{K}' \frac{M}{m} \theta_n \right)} \right\} .$$

In order to obtain this result one has to compare the inverse Fourier transform (4.2.2) with the expansion [90]

$$\operatorname{am}(u) = \frac{\pi\, u}{2\mathbf{K}} + \sum_{n=1}^{\infty} \frac{1}{n\, \cosh\left[n\pi \frac{\mathbf{K}'}{\mathbf{K}} \right]} \sin\left[n\pi \frac{u}{\mathbf{K}} \right] .$$

The form factor (4.3.33) has the correct IR limit[7], and leads to the following expressions for $F_2(\theta)$ and for the spectral function[8]:

$$F_2(\theta_n) = \frac{4\pi i}{\beta\, \hat{\theta}_n} \left\{ \frac{1}{\cosh\left[k\, \mathbf{K}' \frac{M}{m} \hat{\theta}_n \right]} + \right.$$
$$\left. - \left(1 - \delta_{\hat{\theta}_n,0} \right) \left[\cos\left(M\, \hat{\theta}_n\, R/2 \right) - \frac{\sin\left(M\hat{\theta}_n\, R/2 \right)}{M\, \hat{\theta}_n\, R/2} \right] \right\} \tag{4.3.34}$$

$$\hat{\rho}(E_n, p_n) = 4\pi^3 \delta\left(\frac{E_n}{M} - 2 \right) \frac{1}{\beta^2 (p_n)^2} \left\{ \frac{1}{\cosh\left[\frac{k\, \mathbf{K}'}{m} p_n \right]} + \right.$$
$$\left. - (1 - \delta_{p_n,0}) \left[\cos\left(p_n\, R/2 \right) - \frac{\sin\left(p_n\, R/2 \right)}{p_n R/2} \right] \right\}^2 , \tag{4.3.35}$$

where $\hat{\theta} = i\pi - \theta$. Note that the finite volume dependence of both the form factor (4.3.34) and the spectral function (4.3.35) is not restricted to the second term only. The $k\, \mathbf{K}'(k^2)\, M(R)$ factor in the first term carries the main R-dependence, although it is not manifest but implicitly defined by eq. (4.3.12).

Another quantity of interest is the two–point function $\langle 0 | \varepsilon(x)\varepsilon(0) | 0 \rangle$ of the energy density operator. One can calculate it by evaluating its spectral function

$$\rho^{(\varepsilon)}(p^2) = \int_{-R/2}^{R/2} dx\, \langle 0 | \varepsilon(x)\varepsilon(0) | 0 \rangle\, e^{-ip\cdot x}$$

---

[7]The functions $\frac{\cos(xR/2)}{x}$ and $\frac{\sin(xR/2)}{x^2 R/2}$ can be shown to tend to zero in the distributional sense for $R \to \infty$.

[8]Here we are considering the matrix elements on the antisymmetric combinations of kink and antikink.

in terms of the form factors of $\varepsilon(x)$, similarly to what we have done for the field ϕ above. In order to find the semiclassical form factor

$$f_\varepsilon(\theta_n) = \langle p_{n_2} | \varepsilon(0) | p_{n_1} \rangle \,,$$

we need to compute the Fourier transform of

$$\varepsilon(\phi_{\rm cl}) = \frac{2m^2}{\beta^2 k^2}(1 + k^2) - \frac{4m^2}{\beta^2} \, {\rm sn}^2 \left(\frac{mx}{k} \right) \,.$$

This can be easily obtained from the following expansion

$${\rm sn}^2 u = \frac{1}{k^2 \mathbf{K}} \left\{ \mathbf{K} - \mathbf{E} - \frac{\pi^2}{\mathbf{K}} \sum_{n=1}^\infty \frac{n \, \cos \frac{n\pi u}{\mathbf{K}}}{\sinh \frac{n\pi \mathbf{K}'}{\mathbf{K}}} \right\} \,, \tag{4.3.36}$$

and we finally have

$$f_\varepsilon(\theta_n) = M^2 \left\{ \delta_{M\theta_n,0} + \frac{4\pi}{\beta^2} \frac{\theta_n}{\sinh \left(k \, \mathbf{K}' \frac{M}{m} \, \theta_n \right)} \right\} \,. \tag{4.3.37}$$

The corresponding semiclassical spectral function is thus given by

$$\hat{\rho}^{(\varepsilon)}(E_n, p_n) = \frac{4\pi^3}{\beta^4} \, \delta \left(\frac{E_n}{M} - 2 \right) \frac{p_n^2}{\sinh^2 \left(\frac{k \, \mathbf{K}'}{m} \, p_n \right)} \,. \tag{4.3.38}$$

It is worth mentioning that it is also possible to obtain the two–point functions of certain vertex operators $V_b^\pm(x,t) = e^{\pm i\beta b\phi(x,t)}$ (for $b = \frac{1}{2}, 1, \frac{3}{2}, 2, ...$), since the required Fourier expansion formulas of the type (4.3.36) are known in these cases [91].

4.4   Strip geometry

In our study of finite–size effects, we have focused so far only on the cylindrical geometry, since the relevant features we were interested to underline can be already observed in this simple case. However, an even richer phenomenology is produced by including non–trivial boundaries, and the semiclassical techniques are also suited to describe such geometries. In this Section, after a brief overview of boundary effects in CFT, we will describe how the semiclassical method has been applied in [4] to study a quantum field theory defined on a strip of width R, with certain boundary conditions at its edges. In particular, the example discussed is the sine–Gordon model subjected to Dirichlet boundary conditions at both edges of the strip.

4.4.1   Boundary effects in CFT

With the purpose of giving an intuitive idea of boundary effects in QFT, we focus here on the case of conformally invariant theories, due to the powerful analytical techniques available in this situation. We limit ourselves to a brief description of the main results, referring to the original literature for a complete discussion [10, 11]. Furthermore, it should be mentioned that several exact results have been obtained also for integrable QFT with boundary, in virtue of the factorization property of the scattering in the bulk and off the boundary [75].

In a critical system with a boundary, conformal transformations must map the boundary onto itself and preserve the boundary conditions. As a consequence, holomorphic and antiholomorphic

fields no longer decouple, and only half of the conformal generators remain. This can be easily seen in the prototype geometry for a two-dimensional system with boundary, i.e. the upper half plane. In fact, infinitesimal local conformal transformations of the form $z \to z + \epsilon(z)$ map the real axis onto itself if and only if $\epsilon(\bar{z}) = \bar{\epsilon}(z)$, i.e. ϵ is real on the real axis, and this constraint eliminates half of the conformal generators.

A powerful tool for describing the half–plane geometry is the so–called method of images. It consists in regarding the dependence of the correlators on antiholomorphic coordinates $\bar{z}_i$ on the upper half-plane as a dependence on holomorphic coordinates $z_i^* = \bar{z}_i$ on the lower (unphysical) half-plane. Having introduced in this way a mirror image of the system, the definition of the stress–energy tensor $T(z)$ can be extended into the lower half-plane as $T(z^*) = \overline{T}(z)$. Such an extension is compatible with the boundary conditions, because

$$T|_B = \overline{T}|_B \tag{4.4.1}$$

at the boundary, which in cartesian coordinates means $T_{xy}|_B = 0$, i.e. there is no energy or momentum flux across the surface. In this framework, it is possible to show that a n–point correlation function $\langle\, \phi_1(z_1) \dots \phi_n(z_n)\, \rangle_{hp}$ on the half–plane can be identified with the $2n$–point function on the entire plane $\langle\, \phi_1(z_1)\, \phi_1(z_1^*) \dots \phi_n(z_n)\, \phi_n(z_n^*)\, \rangle_p$, in which a mirror image is associated to each field. The role of the boundary is therefore simulated by the interaction between mirror images of the same holomorphic field.

The most intriguing feature of boundary CFT is the existence of a relation between boundary conditions and the bulk operator content of the theory. In fact, condition (4.4.1) is expressed in terms of the Virasoro generators acting on a boundary state $|\alpha\rangle$ as

$$\left(L_n - \bar{L}_{-n}\right)|\,\alpha\,\rangle = 0\,,$$

and the solutions are the so-called Ishibashi states

$$|\,j\,\rangle\rangle \equiv \sum_N |j;\, N\rangle \otimes U\overline{|j;\, N\rangle}\,,$$

where $|\,j;\, N\,\rangle$ and $\overline{|j;\, N\rangle}$ are the holomorphic and antiholomorphic states belonging to the conformal family of the bulk primary operator labelled by j, and U is an antiunitary operator introduced for technical reasons. The boundary states $|\,\alpha\,\rangle$ are therefore linear combinations of Ishibashi states associated with different primary operators

$$|\,\alpha\,\rangle = \sum_j C_{\alpha j}\,|\,j\,\rangle\rangle\,,$$

and the coefficients $C_{\alpha j}$ can be determined by exploiting the modular invariance of the theory. This procedure consists in first mapping the half plane on a strip through the conformal transformation

$$z \to w(z) = \frac{R}{\pi}\ln z\,, \tag{4.4.2}$$

and then in interpreting the strip geometry in two different physical ways, similarly to what we have discussed in Sect. 4.1 for the cylinder (see Fig. 4.9).

In the first physical picture the boundaries are placed at $x = 0, R$, and the partition function is obtained by evolving the Hamiltonian $H_{\alpha\beta}$ along the time direction, while in the second
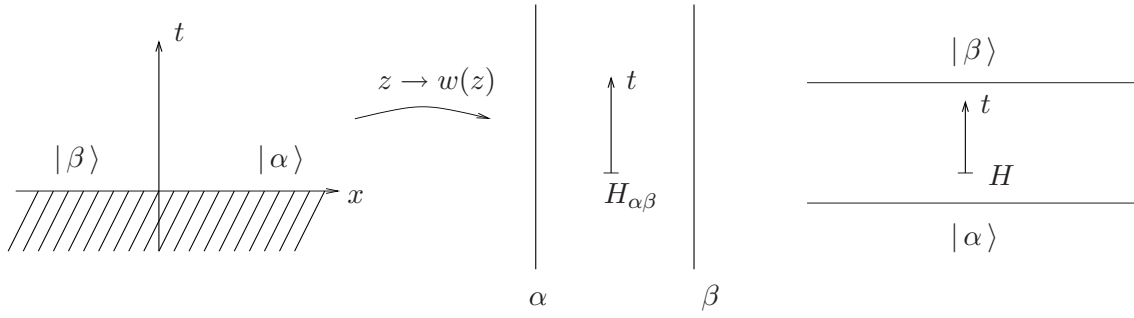
Figure 4.9: Conformal map (4.4.2) from the half plane to the strip.

scheme space is unbounded, and the infinite–volume Hamiltonian H evolves from a state $|\alpha\rangle$ to another state $|\beta\rangle$. The equality of the result in the two different pictures permits to express the coefficients $C_{\alpha j}$ in terms of the so–called modular matrix of the system, establishing a $1:1$ correspondence between boundary states and primary operators of the bulk theory. For instance, in the Ising model (introduced in Sect. 1.1) there are three possible boundary states, symbolically indicated as $|\tilde{j}\rangle$ and given by

$$
\begin{aligned}
|\tilde{\mathbb{I}}\rangle &= \frac{1}{\sqrt{2}}|\mathbb{I}\rangle\rangle + \frac{1}{\sqrt{2}}|\varepsilon\rangle\rangle + \frac{1}{\sqrt[4]{2}}|\sigma\rangle\rangle \\
|\tilde{\varepsilon}\rangle &= \frac{1}{\sqrt{2}}|\mathbb{I}\rangle\rangle + \frac{1}{\sqrt{2}}|\varepsilon\rangle\rangle - \frac{1}{\sqrt[4]{2}}|\sigma\rangle\rangle \\
|\tilde{\sigma}\rangle &= |\mathbb{I}\rangle\rangle - |\varepsilon\rangle\rangle
\end{aligned}
$$

Finally, it is useful for the future discussions to illustrate the features of the Gaussian CFT, described in Sect. 1.1, defined here on a strip with Neumann or Dirichlet boundary conditions. The transformation (4.4.2) leads to the following expression for the Hamiltonian on the strip [11, 89]:

$$
H = \frac{\pi}{R}\left(L_0 - \frac{c}{24}\right) . \tag{4.4.3}
$$

In the case of Neumann boundary conditions

$$
\partial_x \phi(0,t) = \partial_x \phi(R,t) = 0 ,
$$

there is no winding, and the sectors of the theory are only labelled by the momentum index s. The lowest eigenvalue of L_0 in each sector is given by

$$
h_s = \frac{1}{2\pi g}\frac{s^2}{\mathcal{R}^2} . \tag{4.4.4}
$$

On the contrary, Dirichlet boundary conditions

$$
\phi(0,t) = \phi_0 , \qquad \phi(R,t) = \phi_R
$$

constrain the momentum index to zero, but leave the winding free. In this case, the lowest conformal dimension in each sector is expressed as

$$
h_n = \frac{g}{2\pi}\left[(\phi_R - \phi_0) + 2\pi n\mathcal{R}\right]^2 . \tag{4.4.5}
$$

4.4.2 Sine–Gordon model on the strip

The Sine–Gordon model (2.3.1) can be defined on a strip $x \in [0, R]$. Among the several possible boundary conditions which preserve the integrability of the model, a particularly interesting example is given by the Dirichlet boundary conditions (D.b.c.)

$$\phi(0, t) = \phi_0 + \frac{2\pi}{\beta} n_0 , \qquad \phi(R, t) = \phi_R + \frac{2\pi}{\beta} n_R , \qquad \forall t \qquad (4.4.6)$$

with $0 \leq \phi_{0,R} < \frac{2\pi}{\beta}$ and $n_{0,R} \in \mathbb{Z}$. The topological charge of this model is conserved also in the presence of boundaries and it can be conveniently defined as

$$Q \equiv \frac{\beta}{2\pi} \left\{ \int_0^R \partial_x \phi \, dx - (\phi_R - \phi_0) \right\} = n_R - n_0 .$$

Hence the space of states is split in topological sectors with $Q = 0, \pm 1, \pm 2...$, and within a given Q-sector the states are characterized by their energies only.

It is worth mentioning that, in recent years, this problem (and variations thereof) has attracted the attention of several groups: the case of half–plane geometry, for instance, has been discussed by bootstrap methods in [75, 76, 77] and by semiclassical ones in [78, 79, 80] whereas the thermodynamics of different cases in a strip geometry has been studied in a series of publications (see [81, 82, 83, 84, 85, 86, 87]). In completing the work [4], a paper on a (semi)classical analysis of Sine–Gordon model on a strip [88] also appeared, which partially overlaps with it.

The semiclassical quantization presented in [4] adds new pieces of information on this subject and it may be seen as complementary to the aforementioned studies. For the Sine–Gordon model with periodic boundary conditions, alias in a cylindrical geometry, this program has been completed in [3] and presented in Sect. 4.3. Given the similarity of the outcoming formulas with the ones appearing in [3], in the sequel we will often refer to Sect. 4.3 for the main mathematical definitions as well as for the discussion of some technical details. There is though a conceptual difference between the periodic example and the one studied here: in the periodic case, in fact, the vacuum sector is trivial at the semiclassical level (it simply corresponds to the constant classical solution) and therefore the semiclassical quantization provides non-perturbative results just starting from the one-kink sector. Contrarily, on the strip with Dirichlet b.c., the vacuum sector itself is represented by a non-trivial classical solution and its quantization is even slightly more elaborated than the one of the kink sectors.

In order to describe the classical solutions of this problem, it is worth to preliminarily recall some results already obtained. As we have seen in the previous sections, the SG equation of motions admit three kinds of static solution, depending on the sign of the constant A in (4.2.6). The simplest corresponds to $A = 0$ and it describes the standard kink in infinite volume (2.3.3). In the following, we will be concerned with the solutions relative to the case $A \neq 0$, which can be expressed in terms of Jacobi elliptic functions. In particular, for $A > 0$ we have

$$\phi_{cl}^+(x) = \frac{\pi}{\beta} + \frac{2}{\beta} \, \text{am} \left(\frac{m(x - x_0)}{k}, k \right) , \qquad k^2 = \frac{2}{2 + A} ,$$

which has the monotonic and unbounded behaviour in terms of the real variable $u^+ = \frac{m(x - x_0)}{k}$ shown in Fig. 4.10. For $-2 < A < 0$, the solution is given instead by

$$\phi_{cl}^-(x) = \frac{2}{\beta} \, \text{arccos} \left[k \, \text{sn} \left(m(x - x_0), k \right) \right] , \qquad k^2 = 1 + \frac{A}{2} ,$$

and it oscillates in the real variable $u^- = m(x - x_0)$ between the k-dependent values $\tilde{\phi}$ and $\frac{2\pi}{\beta} - \tilde{\phi}$ (see Fig. 4.10).
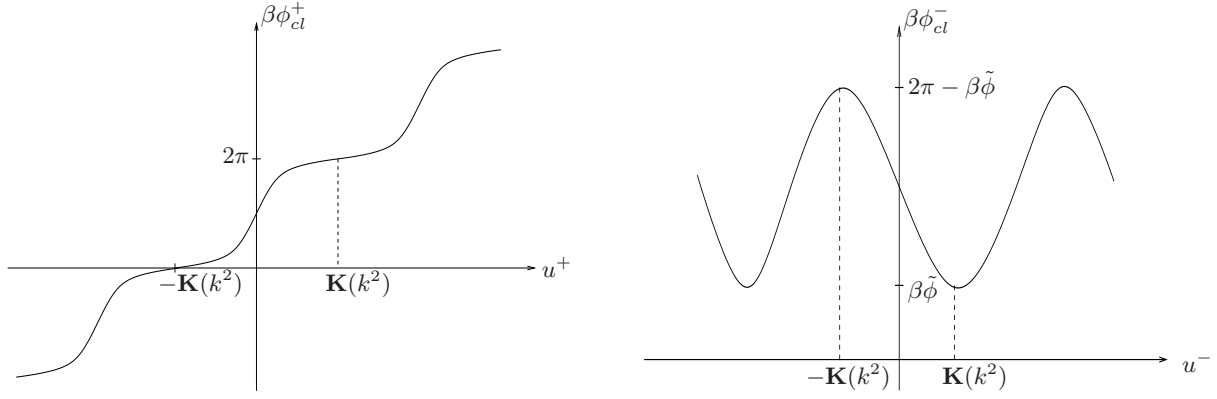

Figure 4.10: Solutions of eq. (4.2.6), $A > 0$ (left hand side), $-2 < A < 0$ (right hand side).

The SG model with the Dirichlet b.c. (4.4.6) can be classically described by using the two building functions $\phi_{cl}^+(x)$ and $\phi_{cl}^-(x)$, thanks to their free parameters x_0 and k, which can be fixed in terms of ϕ_0, ϕ_R and R. However, in order to simplify the notation, in writing down our solutions we will rather use R and x_0, both considered as functions of ϕ_0, ϕ_R and k (as a matter of fact, k can be recovered by inverting the elliptic integrals which enter the corresponding expression of R).

As shown below, both types of solutions $\phi_{cl}^+(x)$ and $\phi_{cl}^-(x)$ are needed, in general, to define the classical background in the vacuum sector whereas only one of them, $\phi_{cl}^+(x)$, is employed for implementing the Dirichlet b.c. in the kink sector.

The vacuum sector: $Q = 0$

To discuss the vacuum sector, it is sufficient to restrict the attention to the case[9] $n_0 = n_R = 0$, $\phi_0 < \phi_R$ and $\left|\cos\frac{\beta}{2}\phi_0\right| > \left|\cos\frac{\beta}{2}\phi_R\right|$. It is also convenient to introduce the compact notation

$$c_{0,R} \equiv \cos\frac{\beta}{2}\phi_{0,R} \ .$$

In order to write down explicitly the classical background corresponding to the vacuum state with Dirichlet b.c., it is necessary to introduce preliminarily two particular values R_1 and R_2 of the width R of the strip, which mark a change in the nature of the solution. They are given by

$$\begin{cases} mR_1 = \operatorname{arctanh}(c_0) - \operatorname{arctanh}(c_R) \ , \\ mR_2 = \mathbf{K}(\tilde{k}) - F\left(\arcsin\frac{c_R}{\tilde{k}}, \tilde{k}\right) \ , \end{cases} \qquad \tilde{k} = |c_0| \ .$$

With these definitions, the classical vacuum solution, as a function of $x \in [0, R]$, has the following behaviour in the three regimes of R:

$$\phi_{cl}^{\text{vac}}(x) = \begin{cases} \phi_{cl}^{(1)}(x) & \text{for} & 0 < R < R_1 \\ \phi_{cl}^{(2)}(x) & \text{for} & R_1 < R < R_2 \\ \phi_{cl}^{(3)}(x) & \text{for} & R_2 < R < \infty \end{cases} \tag{4.4.7}$$

[9]All other cases can be described in a similar way, defining properly x_0 and R, and by using antikinks when necessary.

where

$$\phi_{cl}^{(1)}(x) = \phi_{cl}^{(+)}(x) \qquad \text{with} \qquad \begin{cases} mx_0 = -k\, F\left(\frac{\beta}{2}\phi_0 - \frac{\pi}{2}\,,\, k\right) \\ mR = k\left[F\left(\frac{\beta}{2}\phi_R - \frac{\pi}{2}\,,\, k\right) - F\left(\frac{\beta}{2}\phi_0 - \frac{\pi}{2}\,,\, k\right)\right] \\ 0 < k < 1 \end{cases}$$

$$\phi_{cl}^{(2)}(x) = \phi_{cl}^{(-)}(x) \qquad \text{with} \qquad \begin{cases} mx_0 = -2\mathbf{K}(k) + F\left(\arcsin\frac{c_0}{k}\,,\, k\right) \\ mR = F\left(\arcsin\frac{c_0}{k}\,,\, k\right) - F\left(\arcsin\frac{c_R}{k}\,,\, k\right) \\ \tilde{k} < k < 1 \end{cases}$$

$$\phi_{cl}^{(3)}(x) = \phi_{cl}^{(-)}(x) \qquad \text{with} \qquad \begin{cases} mx_0 = -F\left(\arcsin\frac{c_0}{k}\,,\, k\right) \\ mR = 2\mathbf{K}(k) - F\left(\arcsin\frac{c_0}{k}\,,\, k\right) - F\left(\arcsin\frac{c_R}{k}\,,\, k\right) \\ \tilde{k} < k < 1 \end{cases}$$

In addition to the quantities already defined, we have introduced here the incomplete elliptic integrals

$$F(\varphi, k) = \int_0^\varphi \frac{d\alpha}{\sqrt{1 - k^2 \sin^2 \alpha}}\,, \qquad E(\varphi, k) = \int_0^\varphi d\alpha \sqrt{1 - k^2 \sin^2 \alpha}\,,$$

which reduce to the complete ones at $\varphi = \pi/2$. It is easy to check that at the particular values R_1 and R_2, the different definitions of the background nicely coincide. Fig. 4.11 shows the classical solution at some values of R, one for each of the three regimes[10].
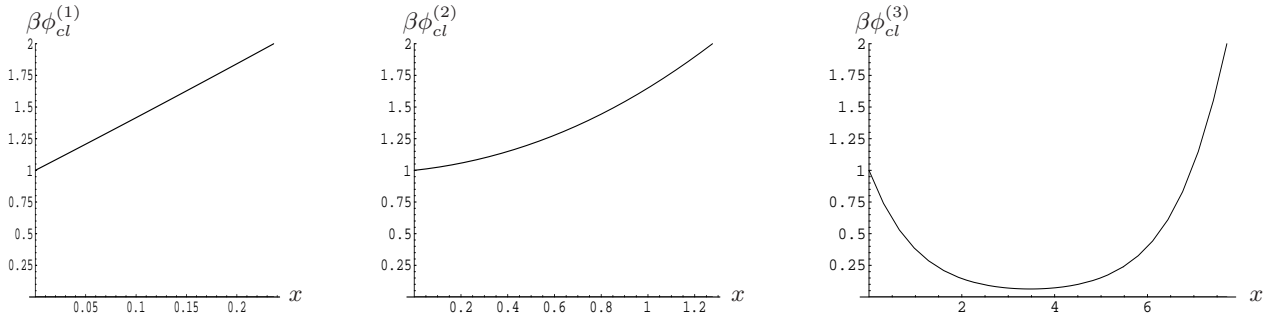

Figure 4.11: Classical solution (4.4.7) at some value of R, in the case $\beta\phi_0 = 1$ and $\beta\phi_R = 2$.

The classical energy of the background (4.4.7) is expressed as

$$\mathcal{E}_{cl}^{\text{vac}}(R) = \begin{cases} \mathcal{E}_{cl}^{(1)}(R) & \text{for} \quad 0 < R < R_1 \\ \mathcal{E}_{cl}^{(2)}(R) & \text{for} \quad R_1 < R < R_2 \\ \mathcal{E}_{cl}^{(3)}(R) & \text{for} \quad R_2 < R < \infty \end{cases} \tag{4.4.8}$$

---

[10]We have chosen for the plot the specific values $\beta\phi_0 = 1$ and $\beta\phi_R = 2$, for which $mR_1 = 0.76$ and $mR_2 = 1.49$. The same values will be considered in all other pictures since their qualitative features do not sensibly depend on these parameters, except for few particular values of $\phi_{0,R}$ discussed separately

where

$$
\mathcal{E}_{cl}^{(1)}(R) \;=\; \frac{2m}{\beta^2} \left\{ \left(1 - \frac{1}{k^2}\right) mR + \frac{2}{k} \left[E\left(\frac{\beta}{2}\phi_R - \frac{\pi}{2}, k\right) - E\left(\frac{\beta}{2}\phi_0 - \frac{\pi}{2}, k\right) \right] \right\} ,
$$

$$
\mathcal{E}_{cl}^{(2)}(R) \;=\; \frac{2m}{\beta^2} \left\{ (k^2 - 1) mR + 2 \left[E\left(\arcsin\frac{c_0}{k}, \, k\right) - E\left(\arcsin\frac{c_R}{k}, \, k\right) \right] \right\} ,
$$

$$
\mathcal{E}_{cl}^{(3)}(R) \;=\; \frac{2m}{\beta^2} \left\{ (k^2 - 1) mR + 2 \left[2\mathbf{E}(k) - E\left(\arcsin\frac{c_0}{k}, \, k\right) - E\left(\arcsin\frac{c_R}{k}, \, k\right) \right] \right\} ,
$$

and it is plotted in Fig. 4.12. As expected, the quantity (4.4.8) has a smooth behaviour at R_1 and R_2, which correspond to the minimum and the point of zero curvature of this function, respectively. The non monotonic behaviour of the classical energy gives an intuitive motivation for the classical background being differently defined in the three regimes of R.
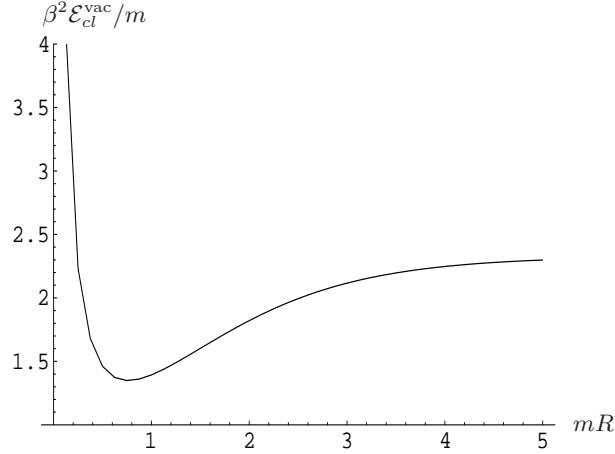
Figure 4.12: Classical energy (4.4.8) for $\beta\phi_0 = 1$ and $\beta\phi_R = 2$.

Furthermore, the classical energy can be easily expanded in the ultraviolet (UV) or infrared (IR) limit, i.e. for small or large values of mR, which correspond to $k \to 0$ in the regime $0 < R < R_1$ or to $k \to 1$ in the regime $R_2 < R < \infty$, respectively.

In fact, expanding the elliptic integrals in (4.4.8) (see [90] and Appendix 4.B for the relative formulas), and comparing the result order by order with the small-k expansion of mR defined in the first regime of (4.4.7)

$$
mR = k\frac{\beta}{2}(\phi_R - \phi_0) \left[1 + \frac{k^2}{4}\left(1 + \frac{\sin\beta\phi_R - \sin\beta\phi_0}{\beta(\phi_R - \phi_0)}\right) + \cdots \right] , \tag{4.4.9}
$$

one obtains the small-mR behaviour

$$
\mathcal{E}_{cl}^{(1)}(R) = \frac{1}{2R}(\phi_R - \phi_0)^2 + R\frac{m^2}{\beta^2}\left[1 - \frac{\sin\beta\phi_R - \sin\beta\phi_0}{\beta(\phi_R - \phi_0)} \right] + \cdots . \tag{4.4.10}
$$

Later we will comment on the meaning of this result in the UV analysis of the ground state energy. On the other hand, comparing the expansion for $k \to 1$ of $\mathcal{E}_{cl}^{(3)}(R)$ in the third regime with

$$
mR = -\log\left\{ \frac{1 - k^2}{16} \frac{1}{\tan\frac{\beta}{4}\phi_0 \, \tan\frac{\beta}{4}\phi_R} \right\} + \cdots , \tag{4.4.11}
$$

one obtains the large-mR behaviour

$$\mathcal{E}_{cl}^{(3)}(R) = \frac{4m}{\beta^2}\left(2 - \cos\frac{\beta}{2}\phi_R - \cos\frac{\beta}{2}\phi_0\right) - \frac{32m}{\beta^2}\tan\frac{\beta}{4}\phi_0\tan\frac{\beta}{4}\phi_R\, e^{-mR} + \cdots. \qquad (4.4.12)$$

The first term of this expression is the classical limit of the boundary energy of the vacuum sector [81], since it is the term that needs to be subtracted by choosing to normalise the energy to zero at $R \to \infty$.

The classical description of the vacuum sector can be completed by mentioning the existence of two particular cases in which the three different regimes of R are not needed. The first is given by $\phi_0 = \phi_R$, for which the whole range of R is described by $\phi_{cl}^{(3)}(x)$ in (4.4.7), since $mR_2 = 0$ in this situation. The second case, defined by ϕ_0 arbitrary and $\phi_R = 0$, can be instead described by the antikink $\bar{\phi}_{cl}^{(1)}(x) = \phi_{cl}^{(1)}(-x)$ alone, since $mR_1 = \infty$ for these values of the boundary parameters (note that x_0 and R have to be defined as opposite to the ones in (4.4.7)). As a consequence, these two cases display a monotonic behaviour of the classical energy, whose UV and IR asymptotics, respectively, require a separate derivation, which can be performed by simply adapting the above procedure.

Finally, it is also worth discussing an interesting feature which emerges in the IR limit of the classical solution (4.4.7). As it can be seen from Fig. 4.11, by increasing R the static background is more and more localised closely to the constant value $\phi(x) \equiv 0$ and this guarantees the finiteness of the classical energy in the $R \to \infty$ limit, given by the first term in $(4.4.12)$[11]. However, if the IR limit is performed directly on the classical solution, we obtain one of the static backgrounds[12] studied in [80]

$$\phi_{cl}^{(3)}(x) \xrightarrow[R\to\infty]{} \frac{2}{\beta}\arccos\left[\tanh m(x - x_0^\infty)\right], \qquad \text{with} \qquad x_0^\infty = -\text{arctanh}(c_0).$$

The last expression tends to zero as $x \to \infty$ and consequently has classical energy $\mathcal{E}_{cl} = \frac{4m}{\beta^2}\left(1 - \cos\frac{\beta}{2}\phi_0\right)$. This phenomenon can be easily understood by noting that the minimum of $\phi_{cl}^{(3)}(x)$ (which goes to zero in the IR limit), is placed at $m\bar{x} = mx_0 + \mathbf{K}(k)$ (see Fig. 4.10) and this point tends itself to infinity as $k \to 1$. Hence, the information about the specific value of ϕ_R is lost when $R \to \infty$, i.e. only the states with $\phi_R = 0$ survive in the IR limit.

We will now perform the semiclassical quantization in the vacuum sector, around the background (4.4.7). Depending on the value of mR, the stability equation (2.1.9) takes the form

$$\left\{\frac{d^2}{d\bar{x}^2} + k^2\left(\bar{\omega}^2 + 1\right) - 2k^2\,\text{sn}^2(\bar{x} - \bar{x}_0, k)\right\}\eta_{\bar{\omega}}^{(1)}(\bar{x}) = 0, \qquad \text{with} \quad \bar{x} = \frac{mx}{k}, \quad \bar{\omega} = \frac{\omega}{m},$$
$$(4.4.13)$$

when $0 < R < R_1$, and

$$\left\{\frac{d^2}{d\bar{x}^2} + \bar{\omega}^2 + 1 - 2k^2\,\text{sn}^2(\bar{x} - \bar{x}_0, k)\right\}\eta_{\bar{\omega}}^{(2,3)}(\bar{x}) = 0, \qquad \text{with} \quad \bar{x} = mx, \quad \bar{\omega} = \frac{\omega}{m}, \quad (4.4.14)$$

when $R_1 < R < R_2$ and $R_2 < R < \infty$.

Equations (4.4.13) and (4.4.14) can be cast in the Lamé form with $N = 1$, which is described in Appendix 4.C and has been studied in detail for the periodic case in Sect. 4.3. The only

---

[11]When $|c_0| < |c_R|$, the same qualitative phenomenon occurs, but the constant value is $\phi(x) \equiv \frac{2\pi}{\beta}$ in this case.

[12]Obviously, the same function is obtained as $\lim_{R\to\infty}\bar{\phi}_{cl}^{(1)}(x)$, in the case $\phi_R = 0$ mentioned above.

differences with the periodic case are the presence of a non-trivial center of mass x_0 and the larger number of parameters entering the expression of the size R of the system: these make more complicated the so–called "quantization condition" that determines the discrete eigenvalues, although they do not alter the general procedure to derive it.

The boundary conditions (4.4.6), which translate in the requirement

$$\eta_{\bar{\omega}}(0) = \eta_{\bar{\omega}}(R) = 0 \ ,$$

select in this case the following eigenvalues, all with multiplicity one,

$$\omega_n^{\text{vac}}(R) = \begin{cases} \omega_n^{(1)}(R) & \text{for} & 0 < R < R_1 \\ \omega_n^{(2)}(R) & \text{for} & R_1 < R < R_2 \\ \omega_n^{(3)}(R) & \text{for} & R_2 < R < \infty \end{cases} \ , \tag{4.4.15}$$

where

$$\omega_n^{(1)}(R) = \frac{m}{k}\sqrt{\frac{2-k^2}{3} - \mathcal{P}(iy_n)} \ ,$$

$$\omega_n^{(2,3)}(R) = m\sqrt{\frac{2k^2-1}{3} - \mathcal{P}(iy_n)} \ ,$$

and the y_n's are defined through the "quantization condition"

$$2\bar{R}\,i\,\zeta(iy_n) + i\,\log\left[\frac{\sigma(-\bar{x}_0 + i\mathbf{K}' + iy_n)\,\sigma(\bar{R} - \bar{x}_0 + i\mathbf{K}' - iy_n)}{\sigma(-\bar{x}_0 + i\mathbf{K}' - iy_n)\,\sigma(\bar{R} - \bar{x}_0 + i\mathbf{K}' + iy_n)}\right] = 2n\pi \ , \qquad n = 1, 2, \dots \tag{4.4.16}$$

This equation comes from the consistency condition associated to the boundary values

$$\begin{cases} D_+\,\eta_a(0) + D_-\,\eta_{-a}(0) = 0 \ , \\ D_+\,\eta_a(R) + D_-\,\eta_{-a}(R) = 0 \ , \end{cases}$$

where $\eta_{\pm a}$ are the two linearly independent solutions of the Lamé equation which are used to build the general solution $\eta(x) = D_+\,\eta_a(x) + D_-\,\eta_{-a}(x)$ (see Appendix 4.C for details). Along the same lines discussed for (4.3.20) in the periodic case, the requirement (4.4.16) can be physically interpreted as a quantization condition for the momentum of a state containing a neutral particle between the two Dirichlet boundary states. The agreement between the large-R limit of this expression and the Bethe ansatz equations involving the appropriate reflection matrices has been verified in [88].

As it can be seen directly from (2.1.10), the frequencies (4.4.15) are nothing else but the energies of the excited states with respect to the ground state $E_0^{\text{vac}}(R)$. They can be easily determined from the above equations and their behaviour, as functions of R, is shown in Fig. 4.13.

As in the periodic case, a more explicit expression for the energy levels (4.4.15) can be obtained by expanding them for small or large values of mR. The UV expansion, for instance, can be performed extracting from (4.4.16) a small-k expansion for y_n, inserting it in (4.4.15), and finally comparing the result order by order with (4.4.9). Exploiting the several properties of Weierstrass functions which follow from their relation with θ–functions (see for instance [91]), one gets

$$y_n = \operatorname{arctanh}\frac{f}{2n\pi} + \frac{k^2}{4}\left\{\operatorname{arctanh}\frac{f}{2n\pi} + s\,\frac{2n\pi(4n^2\pi^2 - 3f^2)}{(4n^2\pi^2 - f^2)^2}\right\} + \cdots \ ,$$
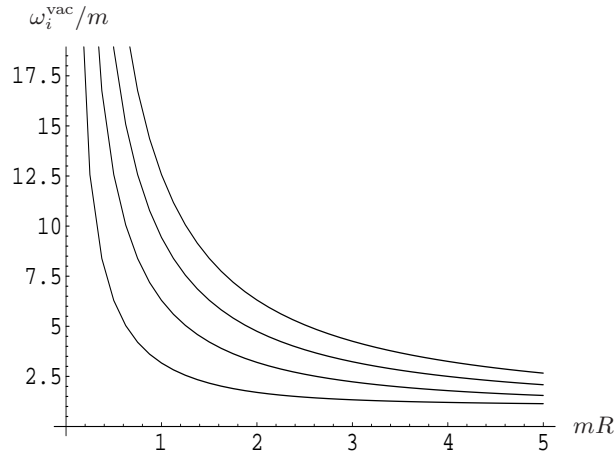
Figure 4.13: The first few energy levels (4.4.15) for $\beta\phi_0 = 1$ and $\beta\phi_R = 2$.

and

$$\omega_n^{(1)} = \frac{m}{k}\frac{2n\pi}{f}\left\{1 - \frac{k^2}{4}\left[1 + \frac{s}{f} - \frac{2fs}{4n^2\pi^2 - f^2}\right] + \cdots\right\} ,$$

where we have introduced the compact notation $f \equiv \beta(\phi_R - \phi_0)$, $s \equiv (\sin\beta\phi_R - \sin\beta\phi_0)$. This leads to the UV expansion

$$\omega_n^{(1)}(R) = \frac{n\pi}{R} + m^2 R\,\frac{s}{f}\frac{2n\pi}{4n^2\pi^2 - f^2} + \cdots \tag{4.4.17}$$

In order to complete the above analysis and obtain the reference value of the energy levels, i.e. the ground state energy $E_0^{\mathrm{vac}}(R)$ of the vacuum sector, we need the classical energy (4.4.8) and the sum on the stability frequencies given in (4.4.15), i.e.

$$E_0^{\mathrm{vac}}(R) = \mathcal{E}_{cl}^{\mathrm{vac}}(R) + \frac{1}{2}\sum_{n=1}^{\infty}\omega_n^{\mathrm{vac}}(R) . \tag{4.4.18}$$

The above series is divergent and its regularization has to be performed by subtracting to it a mass counterterm and the divergent term coming from the infinite volume limit – a procedure that is conceptually analogous to the one discussed in Sect. 4.3 for the periodic case and therefore it is not repeated here. Furthermore, as already mentioned, equation (4.4.18) can be made more explicit by expanding it for small or large values of mR. Here, for simplicity, we limit ourselves to the discussion of the leading $1/R$ term in the UV expansion since it does not receive contributions from the counterterm and therefore it can be simply regularised by using the Riemann ζ–function prescription (see Sect. 4.3.1 for a detailed discussion). The higher terms, instead, require a technically more complicated regularization, although equivalent to the one presented in [3].

The UV behaviour of the ground state energy is dominated by

$$E_0^{\mathrm{vac}}(R) = \frac{\pi}{R}\left[\frac{1}{2\pi}\left(\phi_R - \phi_0\right)^2 - \frac{1}{24}\right] + \cdots \tag{4.4.19}$$

where the coefficient $-1/24$ comes from the regularization of the leading term in the series of frequencies (4.4.17), while the first term simply comes from the expansion of the classical energy

(4.4.10). It is easy to see that the above expression correctly reproduces the expected ground state energy (4.4.3, 4.4.5) for the gaussian Conformal Field Theory (CFT) on a strip of width R with Dirichlet boundary conditions.

Finally, it is simple to check that also the excited energy levels display the correct UV behaviour, being expressed as

$$E_{\{k_n\}}^{\text{vac}}(R) = \frac{\pi}{R}\left[\frac{1}{2\pi}(\phi_R - \phi_0)^2 + \sum_n k_n\, n - \frac{1}{24}\right] + \cdots \tag{4.4.20}$$

The kink sector: $Q = 1$

In discussing the kink sector we can restrict to $n_0 = 0$, $n_R = 1$, since all other cases, as well as the antikink sector with $Q = -1$, are described by straightforward generalizations of the following formulas.

The classical solution can be now expressed only in terms of the function $\phi_{cl}^{(+)}(x)$ as

$$\phi_{cl}^{\text{kink}}(x) = \phi_{cl}^{(+)}(x) \qquad \text{with} \qquad \begin{cases} mx_0 = -k\, F\left(\frac{\beta}{2}\phi_0 - \frac{\pi}{2}, k\right) \\ mR = k\left[2\mathbf{K}(k) + F\left(\frac{\beta}{2}\phi_R - \frac{\pi}{2}, k\right) - F\left(\frac{\beta}{2}\phi_0 - \frac{\pi}{2}, k\right)\right] \\ 0 < k < 1 \end{cases} ,$$
$$\tag{4.4.21}$$

since in this case the whole range $0 < mR < \infty$ is spanned by varying k in $[0, 1]$. This can be intuitively understood by looking at the behaviour of (4.4.21) in Fig. 4.14.
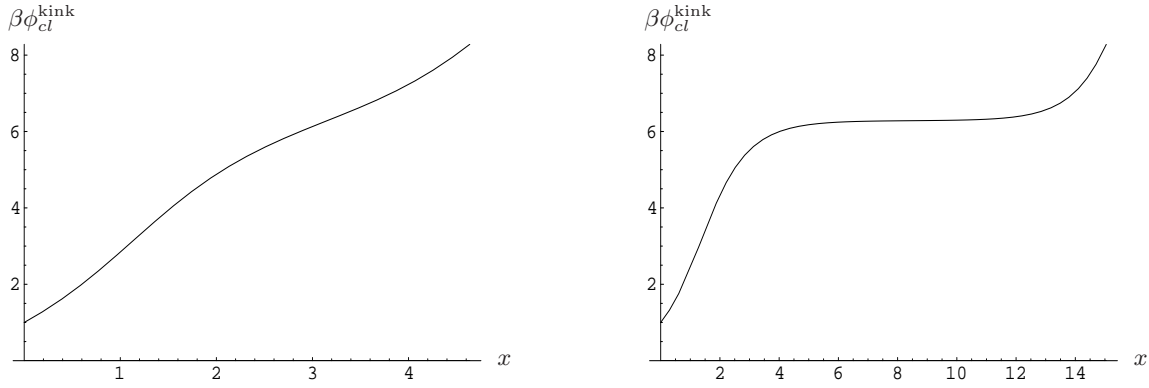

Figure 4.14: Classical solution (4.4.21) at some values of R, in the case $\beta\phi_0 = 1$ and $\beta\phi_R = 2$.

As a consequence, the classical energy and the stability frequencies of this sector can be obtained from $\mathcal{E}_{cl}^{(1)}$ and $\omega_n^{(1)}$ of the vacuum (given respectively in eq. (4.4.8) and (4.4.15)), by simply replacing $\phi_R \to \phi_R + \frac{2\pi}{\beta}$. The leading UV behaviour of the energy levels in this sector, given by

$$E_{\{k_n\}}^{\text{kink}}(R) = \frac{\pi}{R}\left[\frac{1}{2\pi}\left((\phi_R - \phi_0) + \frac{2\pi}{\beta}Q\right)^2 + \sum_n k_n\, n - \frac{1}{24}\right] + \cdots \tag{4.4.22}$$

with $Q = 1$, correctly matches the CFT prediction.

The only result which cannot be directly extracted from the vacuum sector analysis is the IR asymptotic behaviour of the classical energy, since now the $k \to 1$ limit has to be performed

on $\mathcal{E}_{cl}^{(1)}$. We have in this case

$$mR = -\log \left\{ \frac{1-k^2}{16} \frac{\tan \frac{\beta}{4}\phi_0}{\tan \frac{\beta}{4}\phi_R} \right\} + \cdots , \qquad (4.4.23)$$

which leads to

$$\mathcal{E}_{cl}^{(1)}(R) = \frac{4m}{\beta^2} \left(2 - \cos \frac{\beta}{2}\phi_R + \cos \frac{\beta}{2}\phi_0 \right) + \frac{32m}{\beta^2} \frac{\tan \frac{\beta}{4}\phi_R}{\tan \frac{\beta}{4}\phi_0} e^{-mR} + \cdots . \qquad (4.4.24)$$

Analogously to the vacuum sector, the first term of this expression is related to the classical limit of the boundary energy in the one–kink sector. Notice that, differently from the vacuum case, where the asymptotic IR value of the classical energy was approached from below (see (4.4.12)), the coefficient of the exponential correction has now positive sign, in agreement with the monotonic behaviour of the classical energy shown in Fig. 4.15.
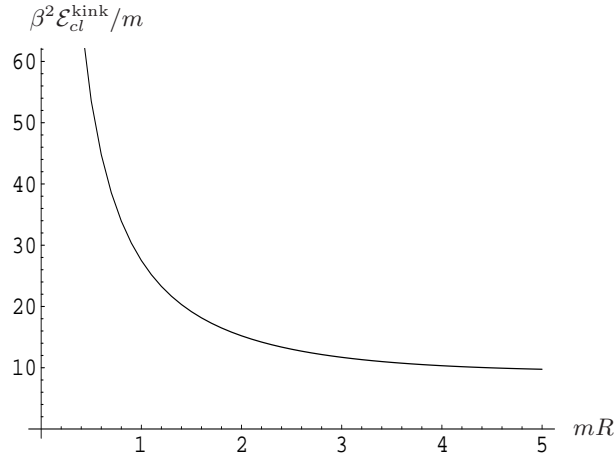
Figure 4.15: Classical energy in the $Q = 1$ kink sector for $\beta\phi_0 = 1$ and $\beta\phi_R = 2$.

When $R \to \infty$, a mechanism analogous to the one discussed for the vacuum also takes place here: the classical energy is finite for any value of ϕ_R, but since $\phi_{cl}^{\text{kink}}(x)$ assumes the value $\frac{2\pi}{\beta}$ at $m\bar{x} = mx_0 + k\mathbf{K}(k)$ (see Fig. 4.10), a point which tends to infinity as $k \to 1$, only the states with $\phi_R = 0$ survive in this limit.

It is worth noticing that $\phi_{cl}^{(+)}(x)$ can be also used to satisfy, at finite values of R, Dirichlet b.c. in sectors with arbitrary topological charge (see Fig. 4.16), giving rise to the correct UV behaviour (4.4.22) with $Q = n_R - n_0$. However, since $\phi_{cl}^{(+)}(x)$ always assumes the value $\frac{2\pi}{\beta}(n_0 + 1)$ at $m\bar{x} = mx_0 + k\mathbf{K}(k)$, which is once again the point going to infinity when $k \to 1$, in the IR limit it can only correspond to $Q = 1$. This result seems natural though, since in infinite volume, static classical solutions can only describe those sectors of the theory with $Q = 0, \pm 1$, while time–dependent ones are needed for higher values of Q. Hence, in the topological sectors with $|Q| > 1$ the space of states will contain, at classical level, the time–dependent backgrounds, defined for any value of R (which are not discussed here), plus the static ones of the form $\phi_{cl}^{(+)}(x)$, which however disappear from the spectrum as $R \to \infty$.
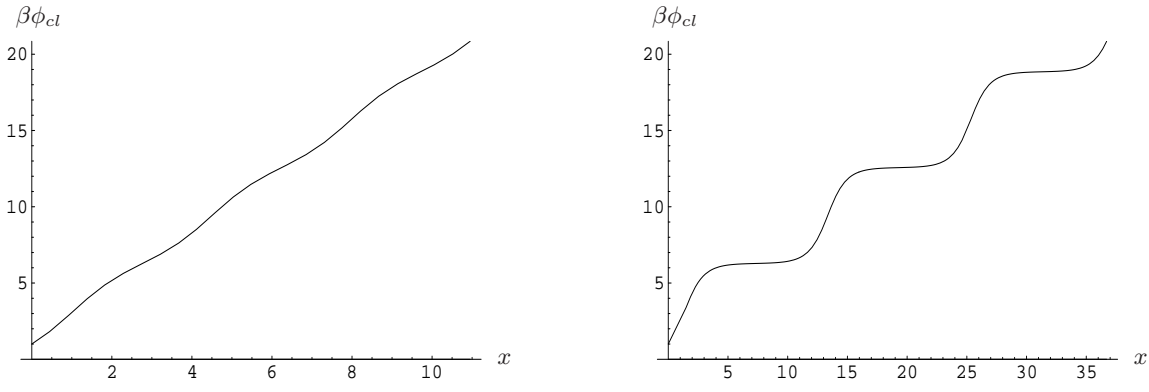
Figure 4.16: Classical solution in the $Q = 3$ sector ($n_0 = 0$, $n_R = 3$) at some values of R, in the case $\beta\phi_0 = 1$ and $\beta\phi_R = 2$.

4.5 Summary

In this Chapter we have shown how the semiclassical methods can provide an analytic description of finite size effects in two–dimensional quantum field theories displaying degenerate vacua. In particular, we have applied the form factors technique to study the correlation functions in SG and broken ϕ^4 theories on a cylindrical geometry. Furthermore, implementing on the cylinder the DHN quantization method, we have derived the scaling functions of the ground (and excited) states in the one–kink (with $Q = 1$) sector of the SG model. The semiclassical approach provides analytic and non–perturbative expressions for the energy levels, valid for arbitrary values of the size R of the system, which permit to link the IR data of the massive theory with the UV conformal data of CFT. It is particularly interesting the application to non–integrable models, where the large R behaviour of the obtained scaling functions can be compared with Lüscher's theory to extract information about the unknown scattering properties of the model, as we have shown in the broken ϕ^4 case at the level of classical energy.

For the integrable case of sine–Gordon model, the next step in the semiclassical program is the extension of the DHN method to describe the multi–kink states ($Q = \pm 2, \pm 3, ...$) as well as the non–vacua ("breather"–like) part of the $Q = 0$ sector. These states are related to certain time–dependent solutions on the cylinder, i.e. to the finite volume analog of soliton–soliton, soliton–antisoliton and breather solutions. Although more complicated from the technical point of view, the determination of these classical solutions and the study of their scaling functions and form factors is a well stated open problem in the semiclassical framework, which deserves further attention. Another interesting problem to be studied is related to the the exactness (or very high accuracy) of the semiclassical results, which is a peculiar feature of SG model in infinite volume, as we have observed in Sect. 2.3. It would be very useful to understand whether similar phenomena take place for the semiclassical scaling functions and form factors in finite volume as well. An indication on this issue could be found by extending to finite volume the analysis of higher loop quantum corrections in the semiclassical expansion.

The semiclassical method is suited also for the description of finite geometries with boundaries, and the example of the SG model on a strip with Dirichlet b.c. has been considered. The resulting analytic expressions for the energy levels permit to link the IR data on the half-line with the UV conformal data of boundary CFT at $c = 1$. In comparison with a cylindrical geometry, an interesting new feature of the quantum field theory defined on a strip consists in

a non–trivial (and non–perturbative) semiclassical description of its vacuum sector. Therefore, we have discussed in detail the classical solutions and energy levels in the $Q = 0$ case, together with the $Q = 1$ that can also be described by static backgrounds. As we have already mentioned, however, the semiclassical methods are not restricted to static backgrounds only, and a complete description of the theory in all sectors requires also the study of time–dependent solutions. Finally, it is worth noticing that the analysis performed here has natural and direct extension to other quantum field theories with various kinds of boundary conditions.

One of the advantages of the semiclassical method is that it works equally well for both integrable and non–integrable models, if they admit kink–type solutions. In fact, we have chosen to test the efficiency of the semiclassical quantization on the example of SG model, mainly because it leads to the simplest $N = 1$ Lamé equation. Static elliptic solutions for other models can be easily obtained by integrating equation (2.1.4) with $A \neq 0$ and appropriate boundary conditions. This was done, for instance in [1], where we have derived the form factors between kink states in the broken ϕ^4 model on the cylinder with twisted boundary conditions. In this case, the quantization of the finite volume kink involves a Lamé equation with $N = 2$ and will be presented in [72]. Lamé equations with $N > 2$ are also expected to enter the quantization of other theories.

Appendix 4.A. Free theory quantization on a finite geometry

Let us consider a free bosonic field $\phi(x, t)$ of mass m defined on a cylinder of circumference R, i.e. satisfying the periodic boundary condition

$$\phi(x + R, t) = \phi(x, t) . \tag{4.A.1}$$

Imposing the equation of motion and the commutation relation

$$[\phi(x, t), \Pi(y, t)] = i\delta_P(x - y) ,$$

where $\Pi(x, t) = \frac{\partial \phi}{\partial t}(x, t)$ is the conjugate momentum of the field whereas

$$\delta_P(x) = \frac{1}{R} \sum_{n=-\infty}^{\infty} e^{\frac{2\pi i n}{R} x} \quad , \quad \delta_P(x + R) = \delta_P(x)$$

is the periodic version of the Dirac delta function, we obtain the mode expansion of the field $\phi(x, t)$. This is given by

$$\phi(x, t) = \sum_{n=-\infty}^{\infty} \frac{1}{2\omega_n R} \left[A_n e^{i(p_n x - \omega_n t)} + A^\dagger e^{-i(p_n x - \omega_n t)} \right] , \tag{4.A.2}$$

where

$$[A_n, A_m^\dagger] = \delta_{n,m} ,$$

and

$$\omega_n = \sqrt{p_n^2 + m^2} \quad , \quad p_n = \frac{2\pi n}{R} \quad n = 0, \pm 1, \ldots \tag{4.A.3}$$

Using the above expansion together with the commutation relation of A and $A^\dagger$, it is easy to compute the propagator of the field, given by

$$\Delta_F(x - x', t - t') = \langle \phi(x, t)\phi(x', t') \rangle = \sum_{n=-\infty}^{\infty} \frac{1}{2\omega_n R} e^{-i[\omega_n(t-t') - p_n(x-x')]} . \tag{4.A.4}$$

The vacuum expectation value of the operator $\phi^2(x, t)$ is then formally given by

$$\langle \phi^2(x, t) \rangle = \Delta_F(0) \tag{4.A.5}$$

and, by translation invariance, is independent from x and t. However this expression is divergent and needs therefore to be regularized. Analogously to what has been done in the text for the ground state energy $\mathcal{E}_0^{\text{vac}}(R)$, we need to subtract the corresponding expression in the infinite volume, so that the finite quantity, simply denoted by $\phi_0^2(R)$, satisfies the usual normalization condition

$$\lim_{R \to \infty} \phi_0^2(R) = 0 .$$

Hence we define

$$\phi_0^2(R) = \frac{1}{2R} \sum_{n=-\infty}^{\infty} \frac{1}{\sqrt{\left(\frac{2\pi n}{R}\right)^2 + m^2}} - \frac{1}{2R} \int_{-\infty}^{\infty} dn \frac{1}{\sqrt{\left(\frac{2\pi n}{R}\right)^2 + m^2}} . \tag{4.A.6}$$

Isolating its zero mode, the series needs just one subtraction, i.e.

$$
\mathcal{S}(r) \equiv \sum_{n=1}^{\infty} \frac{1}{\sqrt{n^2 + \left(\frac{r}{2\pi}\right)^2}} = \sum_{n=1}^{\infty} \left\{ \frac{1}{\sqrt{n^2 + \left(\frac{r}{2\pi}\right)^2}} - \frac{1}{n} \right\} + \sum_{n=1}^{\infty} \frac{1}{n} \ .
$$

$(r = mR)$. In the above expression, the first series is now convergent whereas the second series, which is divergent, has to be combined with a divergence coming from the integral. Indeed we have

$$
\mathcal{I}(r) \equiv \int_0^{\infty} dn \frac{1}{\sqrt{n^2 + \left(\frac{r}{2\pi}\right)^2}} = \lim_{\Lambda \to \infty} \left\{ \ln 2\Lambda - \ln \frac{r}{2\pi} \right\} - \lim_{\Lambda \to \infty} \ln \Lambda + \lim_{\Lambda \to \infty} \ln \Lambda \ ,
$$

and the last term can be used to compose (4.3.7). Collecting the above expressions, it is now easy to see that $\phi_0^2(R)$ coincides with the one obtained doing the calculation in the other quantization scheme, i.e. at a finite temperature. In fact, using the results of Ref. [65], this quantity can be expressed as

$$
\phi_0^2(R) = \int_{-\infty}^{\infty} \frac{d\theta}{2\pi} \frac{1}{e^{r \cosh \theta} - 1} \ , \tag{4.A.7}
$$

whose expansion in r is given by

$$
\phi_0^2(R) = \frac{1}{2r} + \frac{1}{2\pi} \left(\log \frac{r}{2\pi} + \gamma_E - \log 2 \right) + \sum_{n=1}^{\infty} \left(\frac{1}{\sqrt{(2n\pi)^2 + r^2}} - \frac{1}{2n\pi} \right) \ . \tag{4.A.8}
$$

Also this result could have been directly obtained computing only the finite part of the integral and using the prescription (4.3.10).

Appendix 4.B. Elliptic integrals and Jacobi's elliptic functions

In this appendix we collect the definitions and basic properties of the elliptic integrals and functions used in the text. Exhaustive details can be found in [90].

The complete elliptic integrals of the first and second kind, respectively, are defined as

$$\mathbf{K}(k^2) = \int_0^{\pi/2} \frac{d\alpha}{\sqrt{1 - k^2 \sin^2 \alpha}} \ , \qquad \mathbf{E}(k^2) = \int_0^{\pi/2} d\alpha \sqrt{1 - k^2 \sin^2 \alpha} \ . \qquad (4.B.1)$$

The parameter k, called elliptic modulus, has to be bounded by $k^2 < 1$. It turns out that the elliptic integrals are nothing but specific hypergeometric functions, which can be easily expanded for small k:

$$\mathbf{K}(k^2) = \frac{\pi}{2} F\left(\frac{1}{2}, \frac{1}{2}, 1; k^2\right) = \frac{\pi}{2} \left\{1 + \frac{1}{4}k^2 + \frac{9}{64}k^4 + \ldots + \left[\frac{(2n-1)!!}{2^n n!}\right]^2 k^{2n} + \ldots\right\} ,$$

$$\mathbf{E}(k^2) = \frac{\pi}{2} F\left(-\frac{1}{2}, \frac{1}{2}, 1; k^2\right) = \frac{\pi}{2} \left\{1 - \frac{1}{4}k^2 - \frac{3}{64}k^4 + \ldots - \left[\frac{(2n-1)!!}{2^n n!}\right]^2 \frac{k^{2n}}{2n-1} + \ldots\right\} .$$

Furthermore, for $k^2 \to 1$, they admit the following expansion in the so–called complementary modulus $k' = \sqrt{1 - k^2}$:

$$\mathbf{K}(k^2) = \log \frac{4}{k'} + \left(\log \frac{4}{k'} - 1\right) \frac{k'^2}{4} + \ldots ,$$

$$\mathbf{E}(k^2) = 1 + \left(\log \frac{4}{k'} - \frac{1}{2}\right) \frac{k'^2}{2} + \ldots .$$

Note that the complementary elliptic integral of the first kind is defined as

$$\mathbf{K}'(k^2) = \mathbf{K}(k'^2) .$$

The function $\mathrm{am}(u, k^2)$, depending on the parameter k, and called Jacobi's elliptic amplitude, is defined through the first order differential equation

$$\left(\frac{d\,\mathrm{am}(u)}{du}\right)^2 = 1 - k^2 \sin^2\left[\mathrm{am}(u)\right] , \qquad (4.B.2)$$

and it is doubly quasi–periodic in the variable u:

$$\mathrm{am}\left(u + 2n\mathbf{K} + 2im\mathbf{K}'\right) = n\pi + \mathrm{am}(u) .$$

The Jacobi's elliptic function $\mathrm{sn}(u, k^2)$, defined through the equation

$$\left(\frac{d\,\mathrm{sn}u}{du}\right)^2 = \left(1 - \mathrm{sn}^2 u\right)\left(1 - k^2 \mathrm{sn}^2 u\right) , \qquad (4.B.3)$$

is related to the amplitude by $\mathrm{sn}\,u = \sin\left(\mathrm{am}\,u\right)$, and it is doubly periodic:

$$\mathrm{sn}\left(u + 4n\mathbf{K} + 2im\mathbf{K}'\right) = \mathrm{sn}(u) .$$

Appendix 4.C. Lamé equation

The second order differential equation

$$\left\{ \frac{d^2}{du^2} - E - N(N+1)\mathcal{P}(u) \right\} f(u) = 0 \,, \tag{4.C.1}$$

where E is a real quantity, N is a positive integer and $\mathcal{P}(u)$ denotes the Weierstrass function, is known under the name of N-th Lamé equation. The function $\mathcal{P}(u)$ is a doubly periodic solution of the first order equation (see [90])

$$\left(\frac{d\mathcal{P}}{du} \right)^2 = 4 \left(\mathcal{P} - e_1 \right) \left(\mathcal{P} - e_2 \right) \left(\mathcal{P} - e_3 \right) \,, \tag{4.C.2}$$

whose characteristic roots e_1, e_2, e_3 uniquely determine the half–periods ω and ω', defined by

$$\mathcal{P}\left(u + 2n\omega + 2m\omega' \right) = \mathcal{P}(u) \,.$$

The stability equation (4.3.16) can be identified with eq. (4.C.1) for $N = 1$, $u = \bar{x} + i\mathbf{K}'$ and $E = \frac{2-k^2}{3} - k^2\bar{\omega}^2$ in virtue of the relation between $\mathcal{P}(u)$ and the Jacobi elliptic function $\mathrm{sn}(u, k)$ (see formulas 8.151 and 8.169 of [90]):

$$k^2\mathrm{sn}^2(\bar{x}, k) = \mathcal{P}(\bar{x} + i\mathbf{K}') + \frac{k^2 + 1}{3} \,. \tag{4.C.3}$$

Relation (4.C.3) holds if the characteristic roots of $\mathcal{P}(u)$ are expressed in terms of k^2 as

$$e_1 = \frac{2 - k^2}{3} \,, \qquad e_2 = \frac{2k^2 - 1}{3} \,, \qquad e_3 = -\frac{1 + k^2}{3} \,,$$

and, as a consequence, the real and imaginary half periods of $\mathcal{P}(u)$ are given by the elliptic integrals of the first kind

$$\omega = \mathbf{K}(k) \,, \qquad \omega' = i\mathbf{K}'(k) \,.$$

All the properties of Weierstrass functions that we will use in the following are specified to the case when this identification holds.

In the case $N = 1$ the two linearly independent solutions of (4.C.1) are given by (see [91])

$$f_{\pm a}(u) = \frac{\sigma(u \pm a)}{\sigma(u)} \, e^{\mp u \zeta(a)} \,, \tag{4.C.4}$$

where a is an auxiliary parameter defined through $\mathcal{P}(a) = E$, and $\sigma(u)$ and $\zeta(u)$ are other kinds of Weierstrass functions:

$$\frac{d\,\zeta(u)}{du} = -\mathcal{P}(u) \,, \qquad \frac{d\,\log\sigma(u)}{du} = \zeta(u) \,, \tag{4.C.5}$$

with the properties

$$\begin{aligned}
\zeta(u + 2\mathbf{K}) &= \zeta(u) + 2\zeta(\mathbf{K}) \,, \\
\sigma(u + 2\mathbf{K}) &= -\,e^{2(u+\mathbf{K})\zeta(\mathbf{K})}\sigma(u) \,.
\end{aligned} \tag{4.C.6}$$

As a consequence of eq. (4.C.6) one obtains the Floquet exponent of $f_{\pm a}(u)$, defined as

$$f(u + 2\mathbf{K}) = f(u)e^{iF(a)} \,, \tag{4.C.7}$$

in the form

$$F(\pm a) = \pm 2i \left[\mathbf{K}\,\zeta(a) - a\,\zeta(\mathbf{K}) \right] \ . \tag{4.C.8}$$

The spectrum in the variable E of eq. (4.C.1) with $N = 1$ is divided in allowed/forbidden bands depending on whether $F(a)$ is real or complex for the corresponding values of a. We have that $E < e_3$ and $e_2 < E < e_1$ correspond to allowed bands, while $e_3 < E < e_2$ and $E > e_1$ are forbidden bands. Note that if we exploit the periodicity of $\mathcal{P}(a)$ and redefine $a \to a' = a + 2n\omega + 2m\omega'$, this only shifts F to $F' = F + 2m\pi$.

The function $\zeta(u)$ admits a series representation [92] that will be very useful for our purposes in Sect. 4.3.2:

$$\zeta(u) = \frac{\pi}{2\mathbf{K}} \cot\left(\frac{\pi u}{2\mathbf{K}}\right) + \left(\frac{\mathbf{E}}{\mathbf{K}} + \frac{k^2 - 2}{3}\right) u + \frac{2\pi}{\mathbf{K}} \sum_{n=1}^{\infty} \frac{h^{2n}}{1 - h^{2n}} \sin\left(\frac{n\pi u}{\mathbf{K}}\right) , \tag{4.C.9}$$

where $h = e^{-\pi \mathbf{K}'/\mathbf{K}}$. The small-$k$ expansion of this expression gives

$$\zeta(u) = \left(\cot u + \frac{u}{3}\right) + \frac{k^2}{12}\left(u - 3\cot u + 3u\cot^2 u\right) + \tag{4.C.10}$$

$$+ \frac{k^4}{64}\left(-3u + (4u^2 - 5)\cot u + u\cot^2 u + 4u^2\cot^3 u + \sin 2u\right) + \ldots$$

(note that $h \approx \left(\frac{k}{4}\right)^2 + O\left(k^4\right)$). A similar expression takes place for $\mathcal{P}(u)$, by noting that $\mathcal{P}(u) = -\frac{d\zeta(u)}{du}$.

Finally, in the complementary limit $k' = \sqrt{1 - k^2} \to 0$, the Weierstrass functions can be expanded as

$$\zeta(u) = \coth u - \frac{u}{3} + \frac{(k')^2}{6}\left(u - \frac{3}{2}\coth u + \frac{3}{2}u\,\mathrm{csch}^2 u\right) + \ldots$$

$$\mathcal{P}(u) = \coth^2 u - \frac{2}{3} + \frac{(k')^2}{6}\left(2 - 3\coth^2 u + 3u\,\coth u\,\mathrm{csch}^2 u\right) + \ldots$$

Conclusions and Outlook

In this thesis, we have described some fruitful applications of the semiclassical methods in the study of non–integrable QFT and finite–size effects in two dimensions.

The mass spectrum of a generic QFT can be explored non–perturbatively by exploiting the analytic properties of semiclassical form factors of the local fields between kink states, which are available as the Fourier transforms of the classical kinks. With this technique, we have specifically studied two non–integrable theories, given by the ϕ^4 interaction in the $\mathbb{Z}_2$ broken symmetry phase and by the double sine–Gordon model, which describe relevant physical phenomena and find many applications in statistical mechanics and condensed matter physics. Along similar lines, it would be worthwhile to extend the semiclassical analysis to other non–integrable theories which describe the scaling region of interesting statistical systems, like for instance the ϕ^6 potential with three degenerate vacua, associated to the tricritical Ising model with both leading and subleading thermal perturbations. Moreover, further attention should be dedicated to the false vacuum decay in presence of unstable classical backgrounds, that we have studied in the specific case of the double sine–Gordon model. In fact, the semiclassical method is capable of providing interesting results about the dynamics of decay processes.

An opportune generalization of the semiclassical quantization technique has led us to the analytical study of finite–size effects in QFT. In fact, once the proper classical solutions are identified on the geometry of interest, one can implement on them the relativistically refined Goldstone and Jackiw's result and the DHN quantization method in order to estimate, respectively, the correlators and the spectrum. In particular, we have studied form factors and correlation functions for the SG and broken ϕ^4 theories on a twisted cylinder, and we have derived the scaling functions of the ground (and excited) states in few sectors of the SG model defined both on a cylinder and on a strip with Dirichlet boundary conditions. An interesting open problem is the systematic investigation of the finite–size spectrum, which consists in finding time–dependent classical solutions in the remaining topological sectors of the theory, and in applying to them the semiclassical quantization procedure. Furthermore, it would be useful to compare numerically the semiclassical results with the ones available from different techniques for the SG model in finite volume. This, in fact, would permit to test quantitatively the efficiency of the semiclassical approximation, as we have successfully done in the infinite volume case. A closely related subject is the study of two-dimensional QFT at finite temperature, which are known to represent the physical interpretation of the cylindrical geometry in which the compactified variable is Euclidean time, instead of space. A more profound understanding of the relation between finite-volume and finite-temperature pictures will give the opportunity to gain further insight in these both quantization schemes.

As a final remark, it is worth to emphasize again that the semiclassical method is equally suited to describe integrable and non–integrable models, if they admit kink–type solutions.

This feature, that we have fully exploited in the analysis of infinite–volume spectra, makes the analytical study of scaling functions in non–integrable theories a well stated problem, more complicated only from the technical point of view, but conceptually analogous to the procedure illustrated for the sine–Gordon model.

Acknowledgements

Bibliography

[1] G. Mussardo, V. Riva and G. Sotkov, Nucl. Phys. B 670 (2003) 464.

[2] G. Mussardo, V. Riva and G. Sotkov, Nucl. Phys. B 687 (2004) 189.

[3] G. Mussardo, V. Riva and G. Sotkov, Nucl. Phys. B 699 (2004) 545.

[4] G. Mussardo, V. Riva and G. Sotkov, *Semiclassical Energy Levels of Sine–Gordon Model on a Strip with Dirichlet Boundary Conditions*, hep-th/0406246, to appear in Nucl. Phys. B.

[5] A.M. Polyakov, JETP Lett. 12 (1970) 381.

[6] A.A. Belavin, A.M. Polyakov and A.B. Zamolodchikov, Nucl.Phys. B241 (1984) 333.

[7] P. Ginsparg, *"Applied Conformal Field Theory"*, in: *Fields, strings and critical phenomena*, Les Houches Lecture Notes 1988, eds. E. Brézin and J. Zinn-Justin.

[8] A.B. Zamolodchikov and Al.B. Zamolodchikov, Sov. Sci. Rev. A. Phys. 10 (1989) 269.

[9] P. Di Francesco, P. Mathieu and D. Sénéchal, *Conformal field theory*, Springer, New York (1997).

[10] *Finite–Size Scaling*, edited by J.L. Cardy, Amsterdam, North–Holland, 1988.

[11] H.W.J. Blote, J.L. Cardy and M.P. Nightingale, Phys. Rev. Lett. 56 (1986) 742;

J.L. Cardy, Nucl. Phys. B 240 (1984) 514; Nucl. Phys. B 270 (1986) 186; Nucl. Phys. B 275 (1986) 200; *Conformal invariance and statistical mechanics*, Les Houches 1988, North Holland, Amsterdam.

[12] I. Affleck, Phys. Rev. Lett. 56 (1986) 746.

[13] D. Friedan, Z. Qiu and S. Shenker, Phys. Rev. Lett. 52 (1984) 1575.

[14] A.B. Zamolodchikov, Adv. Studies in Pure Math. 19 (1989) 641.

[15] G. Mussardo, Phys. Rep. 218 (1992) 215, and references therein.

[16] A.B. Zamolodchikov and Al.B. Zamolodchikov, Ann. Phys. 120 (1979) 253.

[17] R.J. Eden, P.V. Landshoff, D.I. Olive and J.C. Polkinghorne, *The analytic S-matrix*, Cambridge University Press, 1966.

[18] M. Karowski, P. Weisz, Nucl. Phys. B 139 (1978) 445.

[19] V.P. Yurov and Al.B. Zamolodchikov, Int. J. Mod. Phys. A 6 (1991) 3419.

[20] F.A. Smirnov, *Form Factors in Completely Integrable Models of Quantum Field Theory* (World Scientific) 1992.

[21] V.P. Yurov and Al.B. Zamolodchikov, Int. J. Mod. Phys. A 6 (1991) 3419;
Al.B. Zamolodchikov, Nucl. Phys. B 358 (1991) 524;
J.L. Cardy and G. Mussardo, Nucl. Phys. B 410 (1993) 451;
G. Delfino and G. Mussardo, Phys. Lett. B 324 (1994) 40;
G. Delfino and G. Mussardo, Nucl. Phys. B 455 (1995) 724.

[22] A.B. Zamolodchikov, Sov. J. Nucl. Phys. 44 (1986) 529.

[23] R.F. Dashen, B. Hasslacher and A. Neveu, Phys. Rev. D 10 (1974) 4130; Phys. Rev. D 11 (1975) 3424.

[24] J. Goldstone and R. Jackiw, Phys.Rev.D 11 (1975) 1486.

[25] C.G. Callan and D.J. Gross, Nucl. Phys. B 93 (1975) 29.

[26] J.L. Gervais, A. Jevicki and B. Sakita, Phys. Rev. D 12 (1975) 1038;
J.L. Gervais and A. Jevicki, Nucl. Phys. B 110 (1976) 113.

[27] L.D. Faddeev and V.E. Korepin, Phys. Rept. 42 (1987) 1.

[28] R. Rajaraman, *Solitons and instantons*, Amsterdam, North Holland, 1982.

[29] Y.S. Tyupkin, V.A. Fateev and A.S. Shvarts, Sov. J. Nucl. Phys. 22 (1976) 321.

[30] G.B. Whitham, *Linear and non–linear waves*, John Wiley and Sons, New York, 1974.

[31] A.C. Scott, F.Y.F. Chu and D.W. McLaughlin, Proc. I.E.E.E. 61 (1973) 1443.

[32] T.H.R. Skyrme, Proc. Roy. Soc. Lond. A 247 (1958) 260;
Proc. Roy. Soc. Lond. A 260 (1961) 127;
Proc. Roy. Soc. Lond. A 262 (1961) 237.

[33] S. Coleman, Phys. Rev. D 11 (1975) 2088.

[34] G. Delfino, G. Mussardo and P. Simonetti, Nucl. Phys. B 473 (1996) 469.

[35] D.K. Campbell, J.F. Schonfeld and C.A. Wingate, Physica 9D (1983) 1.

[36] G. Delfino and G. Mussardo, Nucl. Phys. B 516 (1998) 675.

[37] D.K. Campbell, M. Peyrard and P. Sodano, Physica 19 D (1986) 165.

[38] C.A. Condat, R.A. Guyer and M.D. Miller, Phys. Rev. B 27 (1983) 474.

[39] J.A. Krumhansl and J.R. Schrieffer, Phys. Rev. B 11 (1975) 3535.

[40] R. Giachetti, P. Sodano, E. Sorace and V. Tognetti, Phys. Rev. B 30 (1984) 4014.

[41] R.K. Bullough, P.J. Caudrey and H.M. Gibbs, *Double Sine Gordon Model*, in *Solitons*, Topics in Current Physics, Vol. 17 (Springer, Berlin 1980).

[42] D. Controzzi and G. Mussardo, Phys. Rev. Lett. 92 (2004) 021601.

[43] F.D.M. Haldane, Phys. Lett. A 93 (1983), 464; Phys. Rev. Lett. 50 (1983) 1153; Journ. Appl. Phys. 57 (1985) 3359;

I. Affleck, Nucl. Phys. B 257 (1985) 397;

I. Affleck and F.D.M. Haldane, Phys. Rev. B 36 (1977) 5291.

[44] I. Affleck, *Quantum Theory Methods and Quantum Critical Phenomena*, in *Fields, Strings and Critical Phenomena*, Les Houches XLIX, 1988.

[45] I. Affleck, *Soliton Confinement and the Excitation Spectrum of Spin-Peierls Antiferromagnets*, in *Dynamical properties of unconventional magnetic systems*, NATO ASI series E 349, eds A. Skjeltorp and D. Sherrington, Kluwer Academic (1998); cond-mat/9705127.

[46] M. Fabrizio, A.O. Gogolin, A.A. Nersesian, Nucl. Phys. B 580 (2000) 647.

[47] Z. Bajnok, L. Palla, G. Takacs and F. Wagner, Nucl. Phys. B 601 (2001) 503.

[48] Z. Bajnok, L. Palla, G. Takacs and F. Wagner, Nucl. Phys. B 587 (2000) 585.

[49] J.D. Gibbon, N.C. Freeman and R.S. Johnson, Phys. Lett. A 65 (1978) 380.

[50] C.J. Goebel, Prog. Theor. Phys. Suppl. 86 (1986) 261.

[51] S. Coleman, Phys. Rev. D 15 (1977) 2929;

C.J. Callan and S. Coleman, Phys. Rev. D 16 (1977) 1762.

[52] J.S. Langer, Ann. Phys. 41 (1967) 108.

[53] Al.B. Zamolodchikov, Nucl. Phys. B 358 (1991) 497.

[54] S. Habib, A. Khare and A. Saxena, Phys. Rev. Lett.79 (1997) 3797; Physica D 123 (1998) 341.

[55] M. Lüscher, Comm. Math. Phys 104 (1986) 177.

[56] T.R. Klassen and E. Melzer, Nucl. Phys. B 362 (1991) 329.

[57] V.P. Yurov and Al.B. Zamolodchikov, Int. J. Mod. Phys. A 5 (1990) 3221.

[58] M. Lüscher and U. Wolff, Nucl. Phys. B 339 (1990) 222.

[59] M. Lüscher, *Selected topics in lattice field theory*, Les Houches 1988, North Holland, Amsterdam.

[60] Al.B. Zamolodchikov, Nucl.Phys. B 342 (1990) 695.

[61] T.R. Klassen and E. Melzer, Nucl. Phys. B 350 (1991) 635.

[62] C. Destri and H.J. de Vega, Phys. Rev. Lett. 69 (1992) 2313; Nucl. Phys. B 438 (1995) 413;

A. Klumper and P.A. Pearce, J. Stat. Phys. 64 (1991) 13.

[63] V.V. Bazhanov, S.L. Lukyanov, A.B. Zamolodchikov, Comm. Math. Phys. 177 (1996) 381; Comm. Math. Phys. 190 (1997) 247; Nucl. Phys. B 489 (1997) 487; Comm. Math. Phys. 200 (1999) 297.

[64] D. Fioravanti, A. Mariottini, E. Quattrini and F. Ravanini, Phys. Lett. B 390 (1997) 243.

G. Feverati, F. Ravanini and G. Takacs, Phys. Lett. B 430 (1998) 264; Nucl. Phys. B 540 (1999) 543;

D. Fioravanti and M. Rossi, JHEP 0308 (2003) 42.

[65] A. LeClair and G. Mussardo, Nucl. Phys. B 552 (1999) 624.

[66] H. Saleur, Nucl. Phys. B 567 (2000) 602;

G. Delfino, J. Phys. A 34 (2001) L161;

G. Mussardo, J. Phys. A 34 (2001) 7399.

[67] F. Smirnov, *Quasi-classical study of form factors in finite volume*, hep-th/9802132 in L. D. Faddeev's Seminar on Mathematical Physics, Amer. Math. Soc. Transl. (2), Vol. 201 (2000), 283.

[68] P. Fonseca and A. Zamolodchikov, J. Stat. Phys. 110 (2003) 527;

A.I. Bugrij, *The correlation function in two dimensional Ising model on the finite size lattice. I.*, hep-th/0011104; *Form factor representation of the correlation function of the two dimensional Ising model on a cylinder*, hep-th/0107117.

[69] V.E. Korepin and N.A. Slavnov, Int. J. Mod. Phys. B 13 (1999) 2933.

[70] K. Takayama and M. Oka, Nucl. Phys. A 551 (1993) 637.

[71] N.D. Birrel and P.C.W. Davies, *Quantum fields in curved space*, Cambridge University Press, Cambridge, (1982).

[72] G. Mussardo, V. Riva, G. Sotkov, in preparation.

[73] Al.B. Zamolodchikov, Int. J. Mod. Phys. A 10 (1995) 1125.

[74] D. Bernard and A. LeClair, Comm. Math. Phys. 142 (1991) 99.

[75] S. Ghoshal and A.B. Zamolodchikov, Int. J. Mod. Phys. A9 (1994) 3841, Erratum-ibid. A9 (1994) 4353.

[76] P. Mattsson and P. Dorey, J. Phys. A33 (2000) 9065.

[77] Z. Bajnok, L. Palla, G. Takacs and G.Z. Toth, Nucl. Phys. B 622 (2002) 548.

[78] H. Saleur, S. Skorik and N.P. Warner, Nucl. Phys. B 441 (1995) 421.

[79] E. Corrigan and G.W. Delius, J. Phys. A 32 (1999) 8601;

E. Corrigan and A. Taormina, J. Phys. A 33 (2000) 8739.

[80] M. Kormos and L. Palla, J. Phys. A35 (2002) 5471.

[81] A. LeClair, G. Mussardo, H. Saleur and S. Skorik, Nucl. Phys. B 453 (1995) 581.

[82] S. Skorik and H. Saleur, J. Phys. A 28 (1995) 6605.

[83] J.S. Caux, H. Saleur and F. Siano, Phys. Rev. Lett.88 (2002) 106402; Nucl. Phys. B 672 (2003) 411.

[84] T. Lee and C. Rim, Nucl. Phys. B 672 (2003) 487.

[85] C. Rim, *Boundary massive Sine-Gordon model at the free Fermi limit and RG flow of Casimir energy*, hep-th/0405162.

[86] C. Ahn and R.I. Nepomechie, Nucl. Phys. B 676 (2004) 637.

[87] C. Ahn, M. Bellacosa and F. Ravanini, Phys. Lett. B 595 (2004) 537.

[88] Z. Bajnok, L. Palla and G. Takacs, *(Semi)classical analysis of sine-Gordon theory on a strip*, hep-th/0406149.

[89] H. Saleur, *Lectures on nonperturbative field theory and quantum impurity problems*, Les Houches 1998, North Holland, Amsterdam, cond-mat/9812110.

[90] I.S. Gradshteyn and I.M. Ryzhik, *Table of integrals, series, and products*, Academic Press, New York (1980).

[91] E.T.Whittaker and G.N.Watson, *A course of modern analysis*, Cambridge, Cambridge University Press, 1927.

[92] H. Hancock, *Lectures on the theory of elliptic functions*, Dover, New York (1958).